

**STUDIES ON THE CATALYSIS BY
SULFATED MIXED OXIDES OF TIN WITH
SOME RARE EARTH ELEMENTS**

THESIS SUBMITTED TO THE
COCHIN UNIVERSITY OF SCIENCE AND TECHNOLOGY
IN PARTIAL FULFILMENT OF THE
REQUIREMENTS FOR THE DEGREE OF

DOCTOR OF PHILOSOPHY

IN

CHEMISTRY

IN THE FACULTY OF SCIENCE

BY

JYOTHI T. M.

DEPARTMENT OF APPLIED CHEMISTRY
COCHIN UNIVERSITY OF SCIENCE AND TECHNOLOGY
KOCHI - 682 022

JANUARY 1999

Dedicated to my loving parents

CERTIFICATE

This is to certify that the thesis herewith is an authentic record of research work carried out by Jyothi T.M under my supervision, in partial fulfillment of the requirements for the degree of Doctor of philosophy of Cochin University of Science and Technology, and further that no part thereof has been presented before for any other degree.



Dr.S .Sugunan
(Supervising teacher)
Professor in Physical Chemistry
Department of Applied Chemistry
Cochin University of Science and Technology
Kochi- 22

Kochi-22
13th January 1999

DECLARATION

I hereby declare that the work presented in this thesis entitled, “ Studies on the catalysis by sulfated mixed oxides of tin with some rare earth elements ”, is entirely original and was carried out by me independently under the supervision of Dr. S. Sugunan, Professor in Physical Chemistry, Department of Applied Chemistry, Cochin University of Science and Technology, Kochi-22, India, and has not been included in any other thesis submitted previously for the award of any degree.

Kochi-22
13th January 1999


JYOTHI. T.M

ACKNOWLEDGEMENTS

With great pleasure, I wish to express my deep sense of gratitude and obligation to my supervising guide, Prof. (Dr) S. Sugunan for his valuable guidance, research training, constant encouragement, inspiring discussions and valuable suggestions throughout this investigation.

I am equally indebted to Dr. B. S. Rao, Deputy director, National Chemical Laboratory, Pune, who helped me enormously with concrete suggestions, stimulating discussions and thought provoking comments during my stay at NCL, Pune. I will ever remain grateful to him for his sincere help.

I feel grateful to Prof. Mohammed Yusuff, Head of the Department of Applied Chemistry and former Head of the Department Prof. P. Madavan Pillai, for providing the necessary facilities for carrying out my work.

I am extremely thankful to Dr. A. V. Ramaswamy, Head, Catalysis Division, NCL, Pune and Dr. Paul Ratnaswamy, Director, NCL for permitting me to carry out a part of my research work in NCL.

I take this opportunity to thank all the teaching, administrative and technical staff of the Department of Applied Chemistry for their help during various occasions. I also extend my appreciation and thanks to scientific and supporting staff of Catalysis Division, NCL for their cooperation and help. I am also delighted to thank Dr. M. B. Talawar, HEMRL, Pune for his encouragement and love.

I must gratefully acknowledge Dr. P. A. Unnikrishnan, Mr. Binoy Jose, Mr. Rohit, Mr. Xavier, Ms. Rani Abraham, Mr. Suresh, Dr. H. S. Sony, Dr. Mirajkar, Dr. Bhelekar, Dr. Budhkar, Mr. Ramakrishnan, Dr. Gopinathan, Dr. (Mrs) Nalini Jacob, Mr. Kavedia, Ms. Violet Samuel, Dr. A. P. Singh, Dr. S. G. Hegde, Dr. Akashe, Dr. V. R. Chumbale, Dr. Shaikh, Mr. Rajagopal, Mr. Thomas Mathew, Mr. Sivasankar Mr. Kiran Rao, Mr. Prakash Bhosle, Ms. Ranjeet Ahedi and Dr. T. Raja for the help rendered by them whenever sought.

I should specially thank my labmates Dr. Anto Paul, Dr. C. R. Seenaa, Dr. Bindhu Jacob, Dr. Binsy Varghese, Prof. C. G. Ramankutty, Mr. Sreekumar, Ms. Renuka, Ms. Rehna and Ms. Suja for the warmth they have shown towards me and also for their encouragement and cooperation. I wish to place on record my sincere gratitude to Ms. Renuka for helping me a lot in completing the thesis.

Special regards to all my friends, teachers and family members for their love and affection which enabled me to pursue my goals wholeheartedly.

Financial assistance from U.G.C, New Delhi is greatly acknowledged.

Jyothi T.M

PREFACE

It is well known that upon proper treatment with sulfuric acid or ammonium sulfate, many metal oxides exhibit strong acidity. The sulfate modified ZrO_2 , Fe_2O_3 , SnO_2 , TiO_2 and zirconia containing mixed oxides have been found to be promising catalysts for the low temperature esterification, isomerisation, alkylation and cracking. The discovery of strong non-zeolitic solid was a breakthrough because of the simple method of preparation, high thermal stability and low reducibility.

A comparative account of the acid-base properties and catalytic activity of mixed oxides of tin with lanthanum and samarium and their sulfate modified analogues is presented in this thesis. Alcohol decomposition reaction is used to probe surface acid-base properties of the catalysts. Catalytic activity study comprises the oxidative dehydrogenation reactions of ethanol, cyclohexanol, cyclohexane and ethylbenzene and alkylation of phenol, anisole and aniline with methanol.

The general conclusions drawn from the study are summarised in the last chapter of the thesis. The development of new processes based on strong solid acid catalysts to replace HF and H_2SO_4 is needed for environmental as well as safety considerations. The addition of a second metal oxide component to sulfate modified oxides is very important as it enhances the thermal stability and catalytic activity and hence there is a plenty of scope for further research in this field.

CONTENTS

CHAPTER I	INTRODUCTION	
1.1	Heterogeneous catalysis	2
1.2	Metal oxides as catalysts	3
1.3	Acid-base properties and oxidation activity of SnO ₂ containing systems	5
1.4	Rare earth oxides as catalysts	8
1.5	Modified oxides	10
1.5a	Different types of sulfated oxides	12
1.5b	Effect of sulfate treatment on surface area and crystalline structure of the oxide	13
1.5c	Mechanism of sulfate adsorption	13
1.5d	Creation of strong Lewis and Bronsted acid sites	14
1.5e	Metal promoted sulfated oxides	14
1.6	Determination of acid-base properties; titration methods	15
1.7	Alcohol decomposition as a test reaction to probe acid-base properties	17
1.8	Oxidative dehydrogenation of ethanol, cyclohexanol, ethylbenzene and cyclohexane	18
1.9	Alkylation of phenol, anisole and aniline with methanol	20
1.10	Reduction of aromatics containing different reducible groups	21
1.11	Present work	21
1.12	Main objectives of the work	22
	REFERENCES	24
CHAPTER II	EXPERIMENTAL	
2.1	Introduction	31
2.2	Materials	31

2.3	Preparation of the catalysts	32
2.3a	Preparation of mixed oxides	32
2.3b	Preparation of sulfated oxides	33
2.4	Catalyst characterisation	33
2.4a	X-ray diffraction	33
2.4b	Infrared spectroscopy	34
2.4c	Thermal analysis	36
2.4d	Scanning electron microscopy	38
2.4e	Surface area measurements	38
2.4f	Pore volume measurements	39
2.4g	Determination of acidity and basicity by Hammett indicator method	40
2.5	Catalytic activity measurements	42
2.5a	Liquid phase reactions	42
2.5b	Gas phase reactions	43
	REFERENCES	45
	RESULTS AND DISCUSSION	
CHAPTER III	ACID-BASE PROPERTIES AND CATALYTIC ACTIVITY OF MIXED OXIDES OF TIN WITH LANTHANUM AND SAMARIUM	47
3.1	Physico-chemical characteristics	48
3.2	Alcohol decomposition as a test reaction	58
3.2.1	Decomposition of cyclohexanol	58
3.2.2	Decomposition of t-butanol	62
3.2.3	Decomposition of isopropanol	63
3.2.4	Decomposition of butanols as a probe reaction to investigate acid-base properties of oxide systems	66
3.3	Oxidative dehydrogenation reactions	76
3.3.1	Oxidative dehydrogenation of ethanol	76
3.3.2	Oxidative dehydrogenation of cyclohexanol	81

3.3.3	Oxidative dehydrogenation of ethylbenzene and cyclohexane	84
3.4	Alkylation of phenol, anisole and aniline	87
3.4.1	Alkylation of phenol with methanol	87
3.4.2	Alkylation of anisole with methanol	96
3.4.3	Alkylation of aniline with methanol	102
3.5	Transfer hydrogenation of nitrobenzene using isopropanol as a hydrogen donor	108
	REFERENCES	115
CHAPTER IV ACID-BASE PROPERTIES AND CATALYTIC ACTIVITY OF SULFATED MIXED OXIDES OF TIN WITH LANTHANUM AND SAMARIUM		
4.1	Physico-chemical characteristics	119
4.2	Decomposition of Alcohols	132
4.3	Oxidative dehydrogenation reactions	137
4.3.1	Oxidative dehydrogenation of ethanol	137
4.3.2	Oxidative dehydrogenation of ethylbenzene and cyclohexane	140
4.3.3	Oxidative dehydrogenation of cyclohexanol	142
4.3.4	Comparative study of the catalytic activity of SO_4^{2-} and STS82 in the dehydrogenation of cyclohexanol	144
4.3.5	Mechanism of oxidative dehydrogenation reactions	147
4.4	Alkylation of phenol, anisole and aniline	149
4.4.1	Alkylation of phenol with methanol	155
4.4.2	Alkylation of anisole with methanol	156
4.4.3	Alkylation of aniline with methanol	156
	REFERENCES	159
CHAPTER V SUMMARY AND CONCLUSIONS		
5.1	Summary	162
5.2	Conclusions	164

CHAPTER I

INTRODUCTION

1.1 HETEROGENEOUS CATALYSIS

It is well known that a catalyst affects the kinetics of a reaction, through the provision of an alternative reaction mechanism of lower activation energy, but cannot influence the thermodynamic constraints governing its equilibrium. A catalyst can be defined as a substance that increases the rate at which a chemical reaction approaches equilibrium, while not being consumed in the process. The name heterogeneous catalysis implies that the catalyst and reactants are in different phase. Most often reactants are in gaseous phase and catalyst is in solid phase. Use of an insoluble, nonvolatile solid as catalyst for fluid phase reactions has several advantages; loss of the catalyst is minimised, it does not significantly contaminate the reaction products, and it stays physically in place in the reaction chamber. The use of liquid phase catalysts presents serious problems. It is often difficult to separate the catalyst and the product stream, large amount of catalyst is usually required, and the catalyst waste is significant (particularly acids) causing an environmental hazard. Also the cost of process installation and maintenance is high since the liquid acids are highly corrosive. From the above discussion it is clear that heterogeneous catalysis has several advantages over the conventional homogenous catalysis including the easy separation of products from the reaction stream, design of continuous flow reactors, environmentally benign processes *etc.* to name a few. Although the general definition of a catalyst given above emphasizes the acceleration of approach of equilibrium, the selectivity of a catalyst is often more important than its overall activity. An unselective catalyst may accelerate undesirable reaction pathways. In recent years the studies on heterogeneous catalytic process have been expanded so much that even selective formation of desired products become possible. The surface acid base properties of a given catalyst

can be so tuned to get desired activity and selectivity. In many cases product selectivity depends on the strength, number and distribution of acid-base sites on catalyst surface. The important types of heterogeneous catalysts in use include, metals, metal oxides (single, mixed and supported oxides), zeolites, clays and supported heteropoly acids.

1.2 METAL OXIDES AS CATALYSTS

Most of the solid acid base catalysts used in various chemical transformations are based on inorganic oxides as single, mixed or supported oxides. In most cases these oxides are to be modified chemically or physically so as to get desired catalytic activity for a particular reaction. Oxides because of their ability to take part in the exchange of electrons, protons or oxide ions are used as catalysts in both redox and acid base catalysis [1]. The most important type of reactions catalysed by oxides are oxidation reactions. For many years they have been the subject of considerable interest because more than 50% of the production of the chemical industry obtained from catalytic processes are oxidation products. Historically the first catalytic process, introduced into industrial operation (even before the term '*catalysis*' was coined in scientific literature) was the oxidation of SO₂. Some of the important reactions which require metal oxides as catalysts are oxidation of cyclohexane to cyclohexanone, oxidative dehydrogenation of ethylbenzene to styrene, oxidation of methane to formaldehyde, oxidative dehydrodimerisation of CH₄ to form ethane and hydroquinone, oxidation of benzene to phenol and conversion of phenol to catechol and hydroquinone, oxidation of toluene to benzaldehyde, and complete oxidation of hydrocarbons and CO [2]. The generation of new acid sites on mixing oxides was first proposed by Thomas [3] and further developed by Tanabe and co-workers [4]. There seems to be a common view in these reports that the generation of new sites is associated with the charge imbalance at locally formed M₁-O-M₂ bonding where M₁ is

the host metal ion and M_2 is the doped or mixed metal ion. For a certain combination of the metal oxides the number, strength and type of acid and base sites, usually generated are affected by preparation methods. Common methods of preparation include kneading, [5] co-precipitation [6], cogelation [7], complexation method [8], combustion synthesis [9], freeze drying technique [10] and spray drying technique [10]. The method followed in the present study is co-precipitation method because of its numerous advantages and simplicity

Several processes can take place when two oxides are mixed together, consequently there are different explanations for synergy involved,

- (a). Formation of a new compound or a solid solution by reaction between two phases.
- (b). Contamination of the surface of one phase by element coming from the other, namely mutual contamination, such as SnO_2 by Sb or vice-versa.
- (c). Formation of a monolayer of one oxide over the other
- (d) Classical bifunctional catalysis.
- (e) Formation of mobile oxygen species and some chemical action of the latter

In the last two cases two possibilities appear,

- [i]. The mobile oxygen species produced from one phase react directly with reactants adsorbed on the other (spillover oxygen is being used as reactant).

&

- [ii]. The mobile oxygen species emitted from one phase migrates on to the surface of the other and by reacting with it improves the catalytic activity (spillover oxygen being used as a controlling species) – this is the remote control mechanism [11].

In metal oxides two possible states of activated oxygen can be recognized; highly reactive surface states of adsorbed oxygen and less active lattice incorporated oxygen species. Obviously the former species are usually

considered to be important ones involved in complete oxidation and latter are believed to participate in selective partial oxidation. In both types the relation between the catalytic activity and physico-chemical characteristics of metal oxides is understood to confirm the redox model with volcano-type relations [12]. The major advantage of the multicomponent oxide is that it is possible to tune oxygen sorption properties by meticulously choosing the required metal components so as to crystallize in a particular structural system. In such cases the reactivity of oxygen is strongly dependent on the kind of neighbouring metal cations as well as metal oxygen bond distance and bond strength.

According to Ai *et al* the correlation between the catalytic activity and acid-base properties can be explained by the strength of acid base interactions between the reacting molecules and catalyst surface [13]. In the case of oxidation of butadiene which is basic the catalytic activity of several Mo-Bi-P and V-Mo mixed oxides increased with the acid amount of the catalyst. According to the investigators the more acidic catalysts interact more strongly with basic butadiene and activate it more easily. The oxidation activity of acetic acid over Mo-Bi-P and Ti-V-P oxides was correlated with the base amounts.

1.3 ACID-BASE PROPERTIES AND OXIDATION ACTIVITY OF SnO₂ CONTAINING SYSTEMS

Tin oxides are active catalysts for oxidation and are also used as a component of oxidation catalysts. However reports on acidic and basic catalysis of the oxides are not abundant. Tin oxide is often used in the form of a mixed oxide. In the presence of SnO₂ alone a few reactions are known viz., the oxidation of CO [14], the reduction of NO_x [15], the oxidation of olefin [16], and isomerisation [17]. The IR spectra of adsorbed pyridine and ammonia revealed that SnO₂ exhibits weak Lewis acidity, but doesn't show Bronsted acidity even

in the presence of H₂O. Adsorption of organic molecules often gives rise to the oxidation of adsorbates. Methanol is chemisorbed to give methoxyl groups, but they are readily oxidised to a surface formate [18]. Acetone and acetaldehyde are adsorbed predominantly as acetates. Itoh *et al* showed that tin (IV) oxide evacuated above 673 K gave an ESR signal at g value equal to 1.9 which was assigned to Sn³⁺. The signal intensity varied with evacuation temp, showing maximum at 773 K. The intensity of signal decreased upon exposure to oxygen and a signal of O² appeared. On exposure to nitrobenzene anion radicals were formed and the signal at 1.9 disappeared. These facts indicate that the paramagnetic centers are electron donating sites and most of them are located on the surface of SnO₂. On exposure to oxygen or nitrobenzene the conductivity becomes almost zero, indicating that the thermal reduction of tin (IV) oxide occurs only on the surface layer, but not in the bulk of the solid [19].

Acidity of SnO₂:– The acidity of SnO₂ calcined at 773K was reported to be 0.133 mmol/g as determined by butyl amine titration using methyl red indicator (Pka=4.8). However, No acid sites stronger than H₀ ≤ 4.0 were detected [20].

The hydrous tin oxide efficiently catalysed the reduction of carboxylic acid with 2-propanol in the vapour phase at temperatures ranging from 300-330^oC, to give the corresponding alcohols. The reductive halogenation of alkyl halides also proceeded over this catalyst. In the case of oxides after reaction the peaks assigned as Sn (0) is observed together with those of Sn (IV) from XPS [21].

Fuller *et al* reported the reduction of nitrous oxide by CO over tin oxide. The reaction occurs principally by a redox mechanism involving CO chemisorption, CO₂ desorption via lattice oxygen abstraction, and reduction of the catalyst by N₂O, the last being the rate determining step [22]. SnO₂ is

active for the oxidation of CO at moderately low temperatures ($< 150^{\circ}\text{C}$). The darkening in colour of the catalyst during the partial deactivation to a steady state condition at low temp is indicative of an overall partial reduction of the catalyst [23]. Pure SnO_2 is impractical as an oxidation catalyst because of its low activity. However the mixed oxide systems with some other metal oxides are known to be very effective for certain selective oxidations [24]. There have already been several reports on partial oxidations using such SnO_2 containing binary catalysts as $\text{SnO}_2\text{-V}_2\text{O}_5$ [25], $\text{SnO}_2\text{-MoO}_3$ [26], $\text{SnO}_2\text{-P}_2\text{O}_5$ [27], $\text{SnO}_2\text{-Sb}_2\text{O}_5$ [28] and $\text{SnO}_2\text{-Bi}_2\text{O}_3$ [29]. Pure SnO_2 has a fair basicity, and introduction of a small amount of V_2O_5 (2-20%) to SnO_2 remarkably enhances its basicity. It can be stated that SnO_2 rich catalysts are basic and V_2O_5 rich catalysts are acidic [30]. Pt/SnO_2 and Pd/SnO_2 are interesting catalysts for CO oxidation because of the synergistic effects [23]. Bond *et al* suggested that the spillover of CO and atomised oxygen from metal site to the support SnO_2 is mainly responsible for the enhanced catalytic activity of Pd/SnO_2 system though the extent of spill over is faster than that of oxygen [31]. A conspicuous catalytic synergy was observed when methacrolein production and selectivity were considered. The origin of the observed synergy and other experimental observation is explained in a satisfactory manner by the existence of a remote control mechanism, *i.e.*, $\alpha\text{-Sb}_2\text{O}_4$ produces mobile oxygen species (spillover oxygen) which by floating on to the surface of SnO_2 , creates new selective sites on the surface of the latter and / or regenerates those which have become deactivated. Spill over oxygen produced by $\alpha\text{-Sb}_2\text{O}_4$ seems to control the selective catalytic sites on SnO_2 by inhibiting the transformation to reduced non-selective sites. It also inhibits the formation of carbonaceous deposits[32]. Catalytic properties of binary oxides containing bismuth or tin for the oxidation of propylene have been studied at $300\text{-}600^{\circ}\text{C}$. In the case of tin oxide, benzene formation is highly enhanced by the addition of basic oxides whereas acrolein formation is promoted by acidic oxides [33]. The acidic property of SnO_2 is greatly enhanced by incorporating sulfate ions into the oxide [34]. Tatke and

Rooney noted that temperature of 473K were required for the isomerisation of 1-butene over SnO₂, but the reaction proceeded smoothly over SnO₂ containing a small amount of sulfate [35] at lower temperature.

1.4 RARE EARTH OXIDES AS CATALYSTS

The use of rare earth oxides as promoters or supports in catalytic reactions has been grown extensively due to its interesting properties. It is reported that, following appropriate pretreatment, rare earth sesquioxides are active for a variety of reactions including ortho/para hydrogen conversion [35], deuterium exchange reactions [36] of hydrocarbons, H₂-D₂ equilibration [37], alcohol dehydration [38], olefin isomerisation [39], decomposition of N₂O and NO [40] and oxidation reactions of hydrogen [41], CO [42] and hydrocarbons [43].

The reactions for which basic sites of rare earth oxides are relevant include, hydrogenation of olefins, double bond migration of olefins, aldol condensation of ketones, and dehydration of alcohols. For the isomerisation and hydrogenation, the oxides of sesquioxide stoichiometry show activity while the oxides with metal cations of higher oxidation states are highly inactive. The situation is different in aldol condensation, the oxides with high oxidation state, CeO₂, Tb₄O₇ and Pr₆O₁₁ show considerable activity. The oxides with metal cations of oxidation state higher than +3 possess weak basic sites which are sufficient to catalyse the aldol condensaton but not strong enough to catalyse hydrogenation and isomerisation [44]. Rare earth oxides show characteristic selectivity in dehydration of alcohols. 2-Alcohols undergo dehydration to form 1-olefins. The formation of thermodynamically unstable 1-olefins contrasts with the formation of stable 2-olefins over acidic catalysts [45]. Rare earth oxides have been classified as solid base catalysts on the basis of ¹⁸O binding energy studies [46]. Rare earth oxides exhibit activity as oxidation catalysts

and have low work functions. Taking advantage of this property of these oxides, negative ions can be produced by negative surface ionisation [47].

Normand *et al* tested the influence of the support on the reactivity of Pd / rare earth oxide catalysts. Based on these results they classified oxides in to three,

- (a). oxides of the type Re_2O_3 which are unreducible.
- (b). CeO_2 where anion vacancies can be created extrinsically by reduction process and
- (c). Pr_6O_{11} and Tb_4O_7 where anion vacancies exist due to nonstoichiometric nature of the oxides [48].

It has been reported by several authors that a large part of the basic sites determined by the adsorption of acidic substances consists of surface lattice oxygen O^{2-} ions. Keulks and Wragg have reported that the active oxygen species available for oxidation is lattice oxygen O^{2-} ions [49]. The acidic sites contribute to the activation of electron donor type reactants such as olefins and are connected with oxidising sites [50]. The adsorption and mechanism of surface reactions of 2-propanol on ceria calcined at different temperature is known to change the surface species on the oxide and remove surface bound OH groups with Bronsted type acidity at high temperatures with the formation of new sites of Lewis acidity from metal cations [51]. According to the mechanism proposed for this reaction exposed couples of Ce^{4+} and O^{2-} ions are active sites. It is found that in the aldol addition of butyraldehyde catalysed by rare earth oxides (ZrO_2 and La_2O_3), active site is the the surface O^{2-} ion and rate determining step is the α -H abstraction [52]. Rare earth oxides can store the oxygen during the oxidative step of the exhaust cycle and remove it during the reductive step, thereby broadening the air to fuel ratio [53].

In an attempt to identify the active sites for hydrogen atom abstraction, in the oxidative coupling of methane the catalyst was quenched from 650 to – 196°C and the presence of superoxide ions were detected by the E.P.R Spectroscopy. These ions are believed to be formed by the reaction of O₂ either with thermally generated electron hole pairs or with surface peroxide ions [54].

Minachev *et al* suggested that catalytic activity of rare earth oxides depends on the binding energy of oxygen with the surface, in the oxidation of hydrogen and propylene [55]. Bakumenko *et al* explained the difference in catalytic activity of different rare earth oxides on the basis of the heat of formation of oxides [56]. Lazukin and co-workers found a good correlation between the activation energy of the oxidation of propylene and the electrical conductivity of rare earth oxides and concluded that the electron transfer from the reactant or the intermediate, to the catalyst surface takes place in the rate determining step [57]. Some of the authors suggested from the results that the catalytic activity of the lanthanide oxides depend on the electronic configuration of the inner 4f subshell [55]. Catalytic activity of rare earth oxides has recently been reviewed in a book by Tanabe [58].

1.5 MODIFIED OXIDES

It is well known that catalytic activity of a catalyst is greatly affected by the methods of catalyst preparation and the conditions of pretreatment. This is illustrated by the fact that the physical or chemical property of a catalyst varies with the method of preparation and that chemical species adsorbed on the surface affect the catalytic activity profoundly. In most cases these oxides are to be modified chemically or physically so as to get desired catalytic activity in a particular reaction [59]. For example, the addition of well dispersed weakly

basic rare earth oxides titrates the stronger acid sites of amorphous silica-alumina and lowers the acid strength to the level shown by halided alumina. So they can be used in place of halided alumina, which often loses activity due to the removal of halogen. Rare earth oxides are referred to as permanent inorganic basic titrants.

** They are weakly basic and they can gradually titrate the acid sites to the desired level.

** They are easily dispersible. The weakly basic oxide should spread as a monolayer on the silica-alumina surface (If the oxides agglomerates the acid sites would not be uniformly titrated)

** They are non-reducible.

In general acid-base properties of catalysts play significant roles not only in acid base catalysis but also in oxidation catalysis. Acidic or basic substances such as P_2O_5 or K salts are often added to industrial oxidation catalysts in order to improve catalytic performance [60]. These additives suppress undesirable side reactions over oxidation by adjusting the acid base properties of the catalyst surface.

In 1979 Arata and co-workers reported that zirconia upon proper treatment with sulfuric acid or ammonium sulfate exhibits extremely strong acidity after calcination in air at $550^{\circ}C$ and is capable of catalysing the isomerisation of butane to isobutane at room temperature [61]. In this connection the extremely high catalytic activity of ZrO_2 modified with sulfate anion (sulfated zirconia, SZ) in various reactions is quite interesting. In fact the effect of anions on the catalytic activity of metal oxides has been known for a long time. This catalytic performance is unique compared to typical solid acid catalysts, such as zeolites, which show no activity for the reaction at such low temperatures. Using Hammett indicators, Hino and Arata claimed that sulfated

zirconia is an acid 10^4 times stronger than 100% sulfuric acid [62]. Acids stronger than 100% sulfuric acid are referred to as superacids. The strength of an acid can be characterised by the so-called Hammett acidity function, $-H_0$. The greater the value of the function, the stronger the acid.

$-H_0$ for 100% $H_2SO_4 = 12$

$-H_0$ for Sulf. $ZrO_2 = 16$

The strong acidity and the exceptionally high activity of SZ made it attractive as a catalyst in isomeric hydrocarbon producing processes such as hydroisomerisation, hydrocracking, alkylation and oligomerisation. However, a number of issues regarding the strength of acid sites in SZ, the nature of active sites, the role of Lewis and Brønsted acid sites in catalysis and the role and state of platinum supported on SZ are still controversial. Several reviews on this remarkable catalyst are available in the literature [63]. Since the discovery of its strong activity, SZ has attracted much attention as a potential process catalyst. The main reason is associated with the increasing need for environmentally benign processes. Current technology uses HF or H_2SO_4 as catalysts which suffer many drawbacks such as high toxicity and extreme corrosivity in addition to risk of handling large amount of hazardous acids.

1.5a Different types of sulfated oxides

Metal oxides other than ZrO_2 , which show enhanced acidity on sulfation include Fe_2O_3 , TiO_2 [64], SnO_2 [65], Al_2O_3 [66], and HfO_2 [67]. In addition sulfation of binary mixed oxides such as ZrO_2 - TiO_2 , ZrO_2 - Al_2O_3 [68], ZrO_2 - NiO [69], ZrO_2 - V_2O_5 [70], ZrO_2 - SiO_2 [71], ZrO_2 - HfO_2 [72] and ZrO_2 - SnO_2 [73] are also reported in literature. In recent years the development of metal promoted sulfated oxides is receiving increasing interest due to their higher

activity and thermal stability. A remarkable catalyst formulation consisting of iron and manganese promoted SZ (abbreviated as SFMZ) has recently been reported [74]. Hsu *et al* claimed that SFMZ is three orders of magnitude more active than the unpromoted catalyst for the isomerisation of butane at low temperature.

1.5b Effect of sulfate treatment on surface area and crystalline structure of the oxide

As compared to pure metal oxides their sulfated analogues have a higher surface area after calcination at temperatures $> 500\text{ }^{\circ}\text{C}$ in air. The larger surface area is attributed to the retardation of crystallisation on sulfate treatment. In the case of zirconia, sulfation inhibits sintering and delays the transition of amorphous phase to crystalline material as it is obvious from the shift in exothermic peak of DTA curves [75].

1.5c Mechanism of sulfate adsorption

The mechanism of sulfate incorporation in the solid is an anionic exchange between the OH groups of the solid and HSO_4^- ions from solution [76]. The acidity induced by the sulfate anion is then controlled by the presence of OH groups on the original material, the number of which can be changed by the conditions of preparation and pretreatment. Superacidity is created by adsorbing sulfate ion on to amorphous metal oxides followed by calcination in air to convert it to the crystalline form. So the material should be in the hydroxide form, which can be dried carefully at $110\text{ }^{\circ}\text{C}$. Al_2O_3 is an exception to this rule.

1.5d Creation of strong Lewis and Bronsted acid sites

Sulfate species are themselves Lewis acids and by attracting electrons they generate Lewis acid sites on the oxide surface. In other words strong Lewis acid sites are created by the electron withdrawing inductive effect of S = O bonds of the complex formed by the interaction of oxide with sulfate anion [77]. The existence of covalent S = O bonds in sulfur complexes formed are necessary for superacidity generation or in other words, acidity generation is brought about by the oxidation of sulfur to its highest oxidation state +6.

1.5e Metal promoted sulfated oxides

The iron manganese modified SZ (SFMZ) catalysts first developed by Hsu *et al* have generated strong interest due to their exceptionally high activity toward butane isomerisation at low temperature. There is no significant difference in acid strength between SZ and SFMZ. Comparative studies of acidity of promoted and unpromoted SZ were independently carried out by Tabora and Davis [78], and Wan *et al* [79].

More recently it is found that Cr and Mn promoted SZ has activity comparable to SFMZ [80]. It is inspiring that the incorporation of transition metals may increase the superacidity and catalytic activity of sulfated zirconia, although the nature of such an enhancement is far from clear. Miao *et al* has recently reported that the catalytic activity of sulfated oxides of Cr-Zr, Fe-Cr-Zr and Fe-V-Zr is 2-3 times greater than that of the well known sulfated Fe-Mn-Zr [81].

1.6 DETERMINATION OF ACID-BASE PROPERTIES; TITRATION METHODS

The simplest and most widespread method of the acid strength determination for a solid catalyst involves a collaboration of suitable colour indicator adsorbed on its surface, as the acidity of a solid catalyst is manifested by the conversion of an adsorbed neutral base into its conjugated acid. When the indicator (B) reacts with a Bronsted acid (AH) to form corresponding conjugate acid BH^+ and base A^- , the acid strength is expressed by the Hammett acidity function in the following way,

$$H_0 = pK_a + \log B/BH^+$$

and in the case of the interaction with a Lewis acid site

$$H_0 = pK_a + \log B/AB,$$

where B is the concentration of the neutral base which reacted with Lewis acid or electron pair acceptor A.

The amount of acid on a solid is usually expressed as the number or mmol of acid sites per unit weight or unit surface area of the solid, and is obtained by measuring the amount of base which reacts with the solid acid. Each of a series of Hammett indicators in dilute benzene solution is added to separate samples of the dried solid suspended in benzene and the resulting colour is noted. If the colour is that of the acid form of the indicator, then the value of H_0 function of the surface is the same or lower than the pK_a of the conjugate acid of the indicator. Then lower the pK_a of the colour changing indicator is, the greater the acid strength of the solid. The use of various indicators with different pK_a values enable us to determine the amount of acid at various acid strengths by amine titration method. This method gives the sum

of the amounts of both Bronsted and Lewis acid sites, since both proton donors and electron acceptors on the surface will react with either the electron pair (N^-) of the indicator or that of amine ($\text{N}:$) to form coordination bond [82].

The basic strength of a solid surface is defined as the ability of the surface to convert an adsorbed neutral acid to its conjugate base, i.e. the ability of the surface to donate an electron pair to an adsorbed acid. For the reaction of an acid indicator BH with a solid base B,

$\text{BH} + \text{B} \leftrightarrow \text{B}^- + \text{BH}^+$, the basic strength H_0 of B is given by equation,

$\text{H}_0 = \text{pK}_a + \log \frac{\text{B}^-}{\text{BH}}$, where BH is the concentration of the acidic form of the indicator and B^- is the concentration of the basic form. The amount of basic sites at various basic strength can be obtained by titrating a solid base suspended in benzene with benzoic acid or trichloroacetic acid using an appropriate acidic indicator

Both acidic and basic property can be determined on a common H_0 scale, where the strength of basic sites is expressed by the H_0 of the conjugate acid sites. It was found that the strongest H_0 value of the acidic sites was approximately equal to the strongest H_0 value of the basic sites. The equal strongest H_0 was termed " $\text{H}_{0,\text{max}}$ " which is a practical parameter to represent acid-base properties of the solid surfaces. The acidity at an H_0 value shows the number of acid sites whose acid strength is equal to or less than the H_0 value and the basicity at an H_0 value shows the number of basic sites whose basic strength is equal to or greater than the H_0 value.

1.7 ALCOHOL DECOMPOSITION AS A TEST REACTION TO PROBE ACID – BASE PROPERTIES

Model reactions are recommended as the best method for characterising industrial acid catalysis. In the decomposition of alcohols over various metal oxides Ai *et al* defined the ratio of dehydrogenation rate to the dehydration rate as a measure of the basicity of the catalyst and the dehydration rate as a measure of the acidity. This conclusion is drawn from the fact that the dehydrogenation take place with the intervention of both acidic and basic sites through a concerted mechanism [83]. Gervasini *et al* have studied isopropanol decomposition as a test reaction for a number of metal oxide systems and classified them in scales of acid strength [84]. Not only the nature of sites on the catalyst surface but the structure of alcohol also determine the reaction mechanism. Stronger acid sites and more stable tertiary carbenium ions result in E₁ mechanism, whereas the E₂ mechanism consists of a one step concerted reaction which require the simultaneous involvement of both acid and basic sites. However the above mentioned mechanisms are rarely distinguishable and quite often an intermediate situation occur particularly with E₁ and E₂ pathways [85]. Dehydration is favoured over oxides with small, highly charged cations while dehydrogenation has been associated with large more polarisable cations such as alkaline earth ions [86]. It has been postulated that acidic OH groups are required for dehydration. Exposed cations may be needed for dehydrogenation and in some cases also for dehydration. As a measure of the base strength of metal oxides Davis suggested the alcohol conversion selectivity [87]. The amount of 1-alkene produced by water elimination was proposed to depend on the base strength. Thus studies on alcohol decomposition may be used to define some of the properties of certain surfaces and to elucidate the nature of the catalytic sites which are present.

Kibby and Hall conceived the dehydrogenation reaction over hydroxyapatite catalyst to be as follows. The alcoholic proton is discharged to the basic site and hydrogen atom at the alpha carbon is discharged to the acidic site. The transition state has a high electron density as can be deduced from the positive slope of the linear relation between the logarithms of reaction rate and Taft inductive factor for substitution at α -carbon. This is found to be consistent with the rate determining transfer of a hydride ion from an adsorbed alkoxide [88]

The selectivities of dehydration and dehydrogenation products may be determined by employing a series of alcohols. They provide a finger print of a catalyst which if properly related to its structure and chemistry can provide much useful information concerning the way in which it functions.

1.8 OXIDATIVE DEHYDROGENATION OF ETHANOL, CYCLOHEXANOL, ETHYLBENZENE AND CYCLOHEXANE

Dehydrogenation is a reaction in which hydrogen is eliminated from a molecule in the form of dihydrogen or its reacted form by a hydrogen acceptor such as oxygen. The first one is a case of simple dehydrogenation and the second one is known as oxidative dehydrogenation. In the case of oxidative dehydrogenation since the rate determining step is probably the elimination of a proton, the basicity of the catalyst plays an important role, besides the redox properties of the catalyst. So acid base properties of catalysts in general play a significant role not only in acid base catalysis but also in oxidation catalysis. The mechanisms in which acidity or basicity take part in oxidation catalysis may be classified into two categories, (i) activation of one or more of the reactants or products and intermediates and (ii) acceleration of one or more of the reaction paths involved in overall oxidation reactions.

However, very few studies have been attempted concerning the quantitative relationship between the basicity and catalytic activity. Acid - base properties of catalysts in general play significant roles not only in acid-base catalysis but also in oxidation catalysis. Acidic or basic substances such as P_2O_5 or K salts are added to industrial oxidation catalysts in order to improve catalytic performance [89]. These additives suppress side reactions and deep oxidation by adjusting the acid base properties of the catalysts surfaces. According to Ai *et al* the correlation between the catalytic activity and acid base properties of the catalyst can be explained by the strength of acid base interaction between reacting molecules (reactants or products) and catalyst surface [90]. In the case of oxidation of butadiene which is basic, the catalytic activity increases with the acid amount of the catalyst. According to the investigators the more acidic catalysts interact with basic butadiene and activate it more easily. Similarly the oxidation activity of acidic reactants such as acetic acid can be correlated with the base amounts.

Styrene is produced industrially by simple dehydrogenation of ethylbenzene using catalysts containing Fe oxides as the main component (Fe-Cr-K, Fe-Ce-Mo, Fe-Mg-K) or Ca-Ni phosphate in presence of steam. According to Lee *et al* the promoting effect of alkali metals were in the order $Cs > K > Na > Li$ and this order is the order of increasing basicity [91]. According to Tagawa *et al* the acid sites of H_0 between 1.5 and -5.6 are proven to be the active sites to adsorb ethylbenzene reversibly, whose oxidation on the other hand, occurs on the base sites of pK_a between 17.2 and 26.5 [92]. The absolute activities of all rare earth oxides are quite low in the dehydrogenation of ethyl benzene and appreciable reactant conversion does not occur below $450^{\circ}C$ [94]. In the dehydrogenation of cyclohexane good correlation between the rate of dehydrogenation and the acid amount was obtained by Chang *et al* [93]. McGough *et al* found that the lanthanide rare

earth oxides are uniformly active for the dehydrogenation of cyclohexane and that the catalytic activity is notably independent of crystal structure, paramagnetism and in the case of praseodymium, it is independent of the valence state, within experimental error. According to the authors, the activity of rare earth oxides is associated with bonding involving the outer 5s and 5p electrons and that bonding is localised to specific ions in the sense that it is relatively unaffected by defect structure and crystal field splitting arising from neighbouring ions [95]. Oxidative dehydrogenation of ethanol gives acetaldehyde and acetic acid as oxidation products along with small quantities of dehydration products. It is reported that higher content of antimony oxide (32%) in oxide mixture of two metallic units of Sn and Mo shows higher selectivity towards acetaldehyde and acetic acid \cong 67%. Sb_2O_4 brings about the increase of activity and selectivity due to spillover oxygen [96]. Vanadium containing catalysts are the most widely studied systems in the oxidation of ethanol. Nakagawa *et al* studied the promoting effect of V_2O_5 in the oxidation of ethanol and the promoting effect is attributed to the formation of amorphous or two dimensional vanadium oxide. According to the authors oxygen in the surface V=O species act as basic sites in ethanol dehydrogenation [97].

1.9 ALKYLATION OF PHENOL, ANISOLE AND ANILINE WITH METHANOL

The alkylation of phenol is a very important reaction industrially and alkyl phenols are used widely in a variety of applications such as antioxidants, herbicides, insecticides or polymers. Depending on the catalysts, reaction conditions, and alkylating agents prevailing ortho or para monoalkylated, 2,4 or 2,6 dialkylated and 2,4,6 trialkylated products are formed [98]. Alkylation of aniline is also an industrially important reaction, as alkylated products are vital precursors for bigger organic and drug molecular build ups [99]. Alkylation of aniline and phenol usually yield mono and dialkylated products both at the ring

and at the side chain depending on the acidity. Large number of metal oxides were reported for aniline [100] and phenol (101) alkylations. In most cases anisole is an abundant product. Isomerisation of anisole to cresols was considered as an interesting process to be possibly realised as an alkylation of phenol by anisole. The anisole conversion to cresols can be an intermolecular reaction with phenol or an intramolecular rearrangement.

1.10 REDUCTION OF AROMATICS CONTAINING DIFFERENT REDUCIBLE GROUPS

In practice hydrogenation reactions are performed with homogenous or heterogeneous catalysts employing molecular hydrogen or by transfer hydrogenation [102]. Transfer hydrogenation has distinct advantages over molecular hydrogen method. It requires only mild conditions, offer enhanced selectivity and closed pressure systems involving hazardous hydrogen gas can be avoided. Most common of the heterogeneous catalysts is Raney nickel and is used extensively with hydrazine hydrate or propan-2-ol [103]. But it does not show any chemoselectivity towards the functional groups and also it leads to the hydrogenolysis during the reduction of ketones. Recently Ni stabilised zirconia has been reported to show chemoselectivity in transfer hydrogenation using propan-2-ol [104]

1.11 PRESENT WORK

Metal oxide systems containing Sn and rare earths are widely used in many oxidation reactions. Catalyst systems based on SnO₂ are among the most efficient for olefin selective oxidation like isobutene to methacrolein. Rare

earth oxides like La_2O_3 , Sm_2O_3 and CeO_2 are employed in the oxidative coupling of methane and oxidation of butane.

In recent years numerous studies have been devoted to the preparation of sulfated oxides (e.g. ZrO_2) and to their characterisation and catalytic performance in various chemical reactions. In many cases, modification with sulfate anion generates strong acidity even stronger than 100% sulfuric acid and hence they are useful in reactions like isomerisation, low temperature esterification, alkylation and cracking.

Single oxides like ZrO_2 , SnO_2 , HfO_2 , Fe_2O_3 and Al_2O_3 generates strong acid sites upon sulfate treatment. Addition of another metal component enhances the activity of these oxides (metal promoted sulfated oxides) However reports on the acid-base and catalytic activity of systems based on sulfated tin oxide is very sparse. Since SnO_2 and Fe_2O_3 are useful as oxidation catalysts, their sulfated analogues can show enhanced activity in such reactions. Hence a study relating to the promoting effect of rare earth oxide and sulfate anion on the activity of SnO_2 will be interesting.

1.12 MAIN OBJECTIVES OF THE WORK

The main objectives of the present work are the following .--

* To prepare binary mixed oxides containing varying amount of Sn and rare earths (La and Sm) and modify them by sulfate treatment by different methods and also to investigate the physico-chemical characteristics of these oxides using instrumental techniques viz. XRD, EDX, TG-DTA, BET-SA, IR, SEM and pore volume measurements.

** To compare the acid base properties of mixed oxide systems and their sulfated analogues employing alcohol decomposition as a test reaction.

** Attempts concerning the possibility of employing sulfated oxides with redox properties in oxidation reactions is very limited. So another objective of the present work is to find out the effect of sulfate treatment on the catalytic activity of aforementioned systems in some oxidation reactions like oxidation of ethanol, cyclohexanol, ethylbenzene and cyclohexane.

** Anisole, which is a by-product in the alkylation of phenol, could be converted into more useful products like 2,6 xyleneol avoiding the formation of dealkylated product, phenol. Hence alkylation of anisole with methanol is carried out to produce 2,6 xyleneol selectively.

** To understand the effect of newly created strong acid sites in the alkylation of phenol, anisole and aniline with methanol.

** Another objective is to highlight the merits and demerits of sulfate treatment including deactivation studies.

REFERENCES

- 1 J. Haber, "*Perspectives in catalysis*", Blackwell scientific publications, 1992, 371
- 2 A. Bielanski, J. Haber, "*Oxygen in catalysis*", Dekker, New York, 1991, "*New developments in selective oxidations*", (Eds.) G. Centi, F. Trifiro, Elsevier, 1990; A. Bielanski, J. Haber, Catal. Rev. 19 (1979) 1, H. H. Kung, "*Transition metal oxides-surface chemistry and catalysis*" Elsevier, 1988
- 3 C. L. Thomas, Ind. Eng. Chem., 41 (1949) 2564.
- 4 K. Tanabe, T. Takeshita., in "*Advances in catalysis*", Academic press, New York, 17 (1967) 315.
- 5 A. K. Chetani, P. Day, "*Solid state chemistry techniques*", Oxford University press, 1987
- 6 P. Courty, C. Marcilly, in "*Preparation of catalysts*" Stud. Surf. Sci. Catal., 1 (1976) 119.
- 7 L. Hench, J. K. West, Chem. Rev., 90 (1990) 33.
- 8 C. N. R. Rao, J. Gopalakrishnan, Acc. Chem. Res., 20 (1987) 228
- 9 R. Gopichandran, K. C. Patil, Mater. Lett., 12 (1992) 437
- 10 D. W. Johnson, P. K. Gallagher, F. Schrey, W. W. Rhodes, Am. Ceram. Soc. Bull., 55 (1976) 520; A. A. Balandin, Advan. Catal. Academic press, New York, 10 (1958) 95.
- 11 L. T. Weng, N. Spitaels, B. Yasse, J. Ladriere, P. Ruiz, B. Delmon, J. Catal., 132 (1991) 319
- 12 M. J. Fuller, M. E. Warwick, J. Catal., 29, (1973) 441, E. W. Thorton, P. G. Harrison. J. Chem. Soc. Faraday Trans. 1, 71 (1975) 461.
- 13 M. J. Fuller, M. E. Warwick, J. Catal., 39 (1975) 412; F. Solymosi, J. Kiss, J. Chem. Soc. Chem. Commun., (1994) 509.

- 14 T Seiyama, M. Egashira, T Sakamoto, I. Aso, *J. Catal.*, 24 (1972) 76
- 15 C Chemball, H. F. Leach, I. R. Shannon, *J. Catal.*, 29 (1973) 99
- 16 T Seiyama, M. Egashira, T Sakamoto, I. Aso, *J. Catal.*, 24 (1972) 76
- 17 C Chemball, H. F. Leach, I. R. Shannon, *J. Catal.*, 29 (1973) 99
- 18 E. W. Thorton, P. G. Harrison, *J. Chem. Soc. Faraday Trans. 1*, 71 (1975) 2468
- 19 M. Itoh, H. Hattori, K. Tanabe, *J. Catal.*, 43 (1976) 192.
- 20 G. W. Wang, H. Hattori, K. Tanabe, *Bull. Chem. Soc. Jpn.*, 56 (1983) 2407
- 21 K. Takashi, M. Shibagaki, H. Kuno, H. Matsushita, *Bull. Chem. Soc. Jpn.*, 67 (1994) 1107
- 22 M. J. Fuller, M. C. Warwick, *J. Catal.*, 39 (1975) 412.
- 23 M. J. Fuller, M. C. Warwick, *J. Catal.*, 29 (1973) 441
- 24 D. J. Hucknall "*Selective oxidation of hydrocarbons*", Academic press, London, 1974
- 25 K. Kaneko, T. Koyama, H. Furukawa, S. Wada, *Nippon Kagaku Kaishi.*, 1105 (1974) 1111
- 26 J. Builen, *J. Catal.*, 10 (1968) 188.
- 27 Y. Marakami, M. Inagaki, K. Iwayama, H. Uchida, *Shokubai.*, 12 (1970) 89
- 28 K. Wakabayashi, Y. Kamiya, N. Ohta, *Bull. Chem. Soc. Jpn.*, 40 (1967) 2172; 41 (1968) 2776.
- 29 T. Seiyama, T. Uda, I. Mochida, M. Egashira, *J. Catal.*, 34 (1974) 29
- 30 M. Ai, *J. Catal.*, 40 (1975) 318.
- 31 G. C. Bond, M. J. Fuller, I. R. Molly, *Proc. 6th intern. Cong. on Catalysis*, 1 (1997) 356.
- 32 L. T. Weng, N. Spitaels, B. Yasse, J. Ladriere, P. Ruiz, B. Delmon, *J. Catal.*, 132 (1991) 319
- 33 T. Seiyama, M. Egashira, T. Sakamoto, I. Aso, *J. Catal.*, 24 (1972) 76.
- 34 D. G. Tatke, J. J. Rooney, *Chem. Commun.*, (1969) 612, G. W. Wang, H. Hattori, K. Tanabe, *Chem. Lett.*, (1983) 959
- 35 P. W. Selwood, *J. Catal.*, 22 (1971) 123.
- 36 K. M. Minachev, E. G. Vakk, R. V. Dmitrier, E. A. Nasedkin, *Izv. Akad. Nauk,*

- SSSR, Serkhim., 3 (1964) 421
- 37 D. R. Ashmead, D. D Eley, R. Rudham, J Catal., 3 (1964) 280
- 38 K. M. Minachev, "*Catalysis*", J W High Tower, North Holland, (1973) p 219
- 39 Y S. Kodakov, V K. Nosteror, K. M Minachev, Izu. Akad Nauk SSSR Serkhim, 9 (1975) 2012.
- 40 J. F Road, J Catal., 28 (1973) 428, E. R. S Winter, J Catal. 22, (1971) 158
- 41 J. F Road, R. E. Conrad, J Phys. Chem., 76 (1972) 2199
- 42 E. V Aratamonov and L. A. Sazonov, Kinet. Katal 8 (1967) 131
- 43 K. M. Minachev, D. A. Kondrat'ev, G. V Antoshin, Kinet. Katal., 8 (1967) 131, H. Hattori, J. Inoko, Y Murakami, J. Catal., 42 (1976) 60
- 44 H. Hattori, H. Kumai, K. Tanabe, G Zheng, Proc. 8th National Symp Catal. India, Sindri, (1987) p.243, K. Tanabe, M. Misono, Y Ono, H Hattori, "*New solid acids and bases*", Kodansha, Elsevier, New York, (1989) p-43
- 45 Y Wakano, T Lizuka, H. Hattori, K. Tanabe, J. Catal., 57 (1978).
- 46 H. Vinek, H. Nolle, M. Ebel, K. Schwarz, J. Chem. Soc. Faraday Trans. 1, 73 (1997) 734.
- 47 J. E. Delmire, J. Phys. Chem., 91 (1987) 2883.
- 48 F. Le. Normand, J. Harrauh, R. Breauoh, I. Hilaire, A. Kiennemann, J Phys.Chem., 95 (1991) 257
- 49 K. Tanabe, K Saito, J Catal., 32 (1974) 144
- 50 G. W Keulks, J. Catal., 19 (1971) 232.
- 51 M. I. Zaki, N. Shepard, J. Catal., 80 (1983) 114.
- 52 R. Zhang, H. Hattori, K. Tanabe, Bull Chem Soc Jpn., 62 (1989) 2070
- 53 Y F F Yao, J. Catal., 87 (1984) 152.
- 54 R. C. H. Lin, K. D Campell, J. X. Weng, J. H. Lunsford, J Phys. Chem., 90 (1986) 534
- 55 K. M. Minachev, Proc. Int. Congr. Catal., 5th (1973) 219
- 56 T T .Bakumenko, I. T Chachenokova, Kinet. Katal., 10 (1969) 796.
- 57 V I. Lazukin, K. M Khol'yavenko, M. Y Rabanik, A. I Khanik, Katal., 29 (1971).

58. K. Tanabe, M. Misono, Y. Ono, H. Hattori, "New solid acids and bases" Kodansha, Elsevier, New York, (1989) p-18, 265
59. K. Morikawa, T. Shirasaki, M. Okada, Adv. Catal., 20 (1969) 97
60. K. Tanabe, M. Misono, Y. Ono, H. Hattori, Stud. Surf. Sci. Catal., 51 (1989).
61. M. Hino, S. Kobayashi, K. Arata, J. Am. Chem. Soc., 101 (1979) 6439, J. Chem. Soc. Chem. Commun., 851 (1980).
62. G. A. Olah, G. K. S. Prakash, J. Sommer, "Superacids" John Wiley & Sons, New York, (1985).
63. A. Corma, Chem. Rev. 95 (1995) 559, X. Song, A. Sayari, CHEMTECH (August 1995) 27; K. Tanabe, H. Hattori, T. Yamaguchi, Crit. Rev. Surf. Chem., 1 (1990) 1
64. K. Tanabe, M. Misono, Y. Ono, H. Hattori, Stud. Surf. Sci. Catal., 51 (1989) 199
65. H. Matsushashi, M. Hino, K. Arata, Chem. Lett., (1988) 1027
66. K. Arata, M. Hino, Appl. Catal., 59 (1990) 197
67. K. Arata, M. Hino, React. Kinet. Catal. Lett., 25 (1984) 143.
68. S. Baba, Y. Shibata, T. K. Awamura, H. Takaoka, T. Kimura, K. Kousaka, Y. Minato, N. Yokoyama, K. Lida, T. Imai., EP 17478369 (1986).
69. J. R. Sohn, H. W. Kim, J. T. Kim, J. Mol. Catal., 41 (1987) 375.
70. J. R. Sohn, Y. I. Pae, M. Y. Park, S. G. Jo, React. Kinet. Catal. Lett., 55 (1995) 325
71. J. R. Sohn, H. J. Jang, J. Mol. Catal., 64 (1991) 349
72. M. Y. Wen, I. Wender, J. W. Tierney, Energy Fuels, 4 (1990) 372.
73. A. Patel, G. Coudurier, J. Viedrine, Abstr. Book 14th North Am. Meeting Catal. Soc., Snowbird, Utah, June (1995), p-A67
74. C. Y. Hsu, C. R. Heimbach, C. T. Armes, B. C. Gates, J. Chem. Soc. Chem. Commun., 1645 (1992); E. J. Hollstein, J. T. Wei, C. Y. Hsu, US Patent 4918041 (1990); 4956519 (1990).
75. X. Song, Ph.D. dissertation, University Laval, 1995; K. Arata, M. Hino, Mater. Chem. Phys., 26 (1990) 213, K. Arata, Trends Phys. Chem., 2 (1991) 1

76. T Lopez, J Navarrete, R. Gomez, Appl. Catal. Gen., 125 (1995) 217
77. D. A. Word, E. I. Ko, J Catal., 150 (1994) 18.
78. J. E. Tabora, R. J Davis, J. Chem. Soc. Faraday Trans. 1, 91 (1995) 1825
79. K. T Wan, C. B. Khouw, M. E. Davis, *Abstr. Book, 209th Am. Chem. Soc. National Meeting, part 1*, Pap No. COLL-186 (1995).
80. X. Song, K. R. Reddy, A. Sayari, J. Catal., 161 (1996).
81. C Miao, W Hua, J Chen, Z. Gao, Cat. Lett., 37 (1996) 187
82. K. Tanabe, "*Solid acids and bases, their catalytic properties*", Accademic press. New York, (1970); C. J. Walling, J. Am. Chem. Soc, 72 (1950) 1164, H A Bensi, J. Am. Chem. Soc., 78 (1956) 5490.
83. M. Ai, Bull. Chem. Soc. Jpn., 49 (1976) 1328; M. Ai, J. Catal., 40 (1975) 318, 40 (1975) 327
84. A. Gervasini, A. Auroux, J. Catal., 131 (1991) 190
85. C. L. Kibby, W K. Hall, J. Catal., 29 (1973) 144
86. A. Eucken, E. Wicke, Naturwissen Schatten., 32 (1994) 161.
87. B. H. Davis in "*Adsorption and catalysis on oxide surfaces*", (Eds.) M. Che, G C. Bond, Elsevier, Stud. Surf. Sci. Catal., 21 (1985) 309
88. C. L. Kibby, W K. Hall, J. Catal., 29 (1973) 144
89. K. Tanabe, M. Misono, Y Ono, H. Hattori, Stud. Surf. Sci. Catal., 51 (1989)
90. M. Ai, T Ikawa, J Catal., 40 (1975) 203, M. Ai, S. Suzuki, Nippon Kagaku Kaishi., (1973), 21
91. E. H. Lee, Catal. Rev., 8 (1973) 285.
92. T Tagawa, T Hattori, Y Murakami, J. Catal., 75 (1982) 66.
93. R. C Chang, I. Wang, J Catal., 107 (1987) 195
94. E. Sushina, T V Meshcheryakwa, Vestn. Mosk. Univ Khim., 11 (1970) 106
95. C. B. McGough, G. Houghton, J. Phys. Chem., 65 (1961) 1887
96. P. A. Avasarkar, V R. Chumbhale, A. Y Sonsile, "*Catalysis Modern trends*" N.M Gupta, D.K. Chakrabarty (Eds.) New Delhi p.284.
97. Y Nakagawa, T Ono, H. Miyata, Y Kubokawa, J. Chem. Soc. Faraday Trasns. 1, 79 (1983) 2929.

- 98 H. Fiege, Ulmann in W Gerhartz, Y S Yamamoto, F T Cambell, R. Pfeffertorn, J F Rounsaville (Eds.), "*Encyclopedia of Industrial Chemistry*" 5th edn., VCH Verlag, vol. 48, 1987, p.45.
- 99 S. Narayanan, V Durgakumari, A. Sudhakar Rao, Appl. Catal. A, 111 (1994) 133
100. S. Balsama, P Beltrame, P L Beltrame, Appl. Catal., 13 (1984) 161; E. Santacesaria, D. Grasso, D. Gelosa, S. Carra, Appl. Catal., 64 (1990) 83, J M Perera, A. Gonzalez, M. A. Burrell, Ind. Eng. Chem, 7 (1968) 259
- 101 V Durgakumari, S. Narayanan, L. Guzzi., Catal. Lett., 5 (1990) 377; E. Santacesaria, M. Diserio, P Ciambelli, D Gelosa, S Carra, Appl. Catal., 64 (1990) 101, Z. H. Fu, Y Ono, Catal. Lett., 21 (1993) 43
102. R. A. W Johnstone, A. H. Wilby, I. D Entwistle, Chem. Rev., 85 (1985) 129
103. M. J. Andrews, C. N. Pillai, Ind. J. Chem, Sect. B, 16 (1978) 465.
- 104 T T Upadhyya, S .P Katdare, D. P Sabde, V Ramaswamy, A. Sudalai J Chem. Soc. Chem. Commun., (1997) 1119

CHAPTER II

EXPERIMENTAL

2.1 INTRODUCTION

Heterogeneous catalysis deals with the transformations of molecules at the interface between a solid (catalyst) and the gaseous or liquid phase carrying these molecules. This transformations involves a series of phenomena, the understanding and the control of which requires the study of,

- (a). How the catalyst is constituted in the bulk and at its surface and what transformation it undergoes (chemical reactions, exchange of atoms between surface and bulk, sintering *etc.*).
- (b) How the gaseous or liquid phase is modified (composition, kinetics *etc.*) and
- (c). The nature of the interface (adsorbed species and bonds between these species and the catalyst surface) *etc*

It is known that the activity of a catalyst is greatly influenced by the method of catalyst preparation and the conditions of pretreatment. This is illustrated by the fact that the physical or chemical structure of a catalyst varies with the method of preparation and that chemical species adsorbed on the surface affect the catalyst activity profoundly [1]. The development of powerful investigation methods (essentially physico-chemical phenomena) for the characterisation of catalysts has been a major advance in recent years.

2.2 MATERIALS

All the catalysts were prepared from corresponding metal salts. Samarium chloride (99.9%) and lanthanum chloride (99.9%) were obtained from Indian rare earths Ltd, Udyogamandal, Kerala and tin (II) chloride (98%) from

Ranbaxy India Ltd. All other chemicals were purified before experiments by standard procedures reported earlier [2].

2.3 PREPARATION OF THE CATALYSTS

2.2a Preparation of the mixed oxides

The mixed oxides were prepared from their corresponding mixed hydroxide precursors. The co-precipitation method [3] was employed for the preparation of mixed hydroxides. Required quantities of Sn (IV) solution and rare earth chloride solutions were mixed, diluted with water and boiled for 10 minutes. To this solution 1 l aq. NH_3 was added slowly with constant stirring to complete the precipitation. The pH of the final solution was in the range 8.5-9.5. The solution was boiled for 5 minutes more and allowed to stand overnight. This precipitate was washed several times with deionised water by decantation method until the precipitate was free from chloride ions. It was filtered, dried at 110°C for 6 hours and finally calcined at 500°C in air for 3 hours. These oxides were then sieved to get particles of 100-200 microns mesh size. The mixed oxides of the following compositions were prepared.

SnO_2 80% La_2O_3 20%-----TL82

SnO_2 80% Sm_2O_3 20%-----TS82

SnO_2 50% La_2O_3 50%-----TL55

SnO_2 50% Sm_2O_3 50%-----TS55

SnO_2 20% La_2O_3 80%-----TL28

SnO_2 20% Sm_2O_3 80%-----TS28

Sn (IV) salt solution was prepared from Sn(II) chloride by oxidation with conc. HNO_3 . Sn (II) chloride was taken in a china dish and conc. HNO_3 was added dropwise until a pasty material is formed. It was then dissolved in minimum amount of aqua-regia on a sand bath to get Sn (IV) solution. It was then diluted with distilled water.

2.2b Preparation of Sulfated oxides

Sulfated oxides were prepared [4,5,6] by the following three different methods.

(i). In the first method the mixed metal hydroxide was dried at 110 °C for 6 hours followed by another temperature treatment at 300 °C for 3 hours. 10 g of this material was immersed in 150 ml of 0.5 M (NH₄)₂SO₄ solution for 3hrs and then filtered without washing and dried at 110 °C for 6 hours.

(ii). In the second method the catalyst precursor was the mixed metal hydroxide itself which was dried at 90-100 °C for 2 hours. 10 g of this material was immersed in 0.5 M (NH₄)₂SO₄ solution for 3 hours and then filtered without washing and dried at 110 °C for 6 hours.

(iii). In the third method 10 g of tin hydroxide dried at 90-100 °C for 2 hours was immersed in 3 M H₂SO₄ for 3 hours and finally evaporated to dryness very carefully on a waterbath. It was then dried at 110 °C for 3 hours. The sulfate modified SnO₂ so obtained was then impregnated with rare earth nitrate solution. The material was dried at 110 °C for 6 hours to get rare earth modified sulfated tin oxide.

All the catalysts were calcined at 550 °C for 3 hours, sieved to a particle size of 100-200 microns and were kept in glass ampoules.

2.4 CATALYST CHARACTERISATION

All the catalysts were characterised by different physico-chemical techniques viz., XRD, surface area measurements (BET), pore volume measurements, thermal analysis (TG-DTA), IR spectroscopy (DRS), energy dispersive X-ray analysis, scanning electron microscopy, and acidity-basicity measurements by Hammett indicator method.

2.4a X-ray Diffraction

XRD is one of the most widely used and versatile techniques for the qualitative and quantitative analysis of solid phases and can provide useful information about the particle size of specific components. Other uses include the identification of the structure of the substance, its allotropic transformation, transition to different phases, purity of the substance, lattice constants and presence of foreign atoms in the crystal lattice of an active component. The principle of XRD is based on the interaction of X-ray with the periodic structure of a polycrystalline material which act as a diffraction grating. In this technique a fixed wavelength is chosen for the incident radiation and Bragg peaks are measured by observing the intensity of the scattered radiation as a function of scattering angle of 2θ , the interplanar distances or d-spacings are calculated from the values of the peaks observed from the Bragg equation,

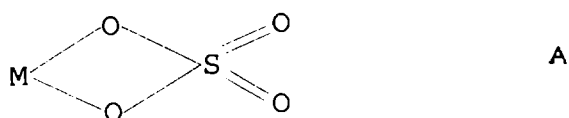
$$n\lambda = 2d\sin\theta, \text{ where 'n' is the order of reflection.}$$

The X-ray patterns of the samples were recorded using Ni filtered Cu $K\alpha$ radiation ($\lambda = 1.5404\text{\AA}$). Silicon was used as an internal standard to calibrate X-ray line patterns.

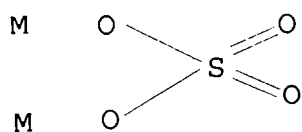
2.4b Infrared spectroscopy

The infrared spectrum is obtained when a molecule produces a change in dipole moment due to vibration. It can provide valuable information about the basic characteristics of the molecule, namely the nature of atoms, their spatial arrangement and their chemical linkage forces. IR spectroscopy has been extensively used for identifying various functional groups on the catalyst itself, as well as for identifying the adsorbed species and reaction intermediates on the catalyst surface. It can also be used to determine the surface acidity of catalysts employing suitable probe molecules.

In the case of sulfated oxides, a strong absorption at around 1380 cm^{-1} has been reported by many authors [7,8,9]. By comparison with the XPS results they postulated that a strong absorption at 1380 cm^{-1} is typical of the highest oxidation state of sulfur (S^{+6}) in $S=O$ bonds [10]. A free sulfite ion SO_3^{2-} shows two absorption bands at 1010 cm^{-1} (ν_3) and 961 cm^{-1} (ν_1). In the case of sulfates, free sulfate ion and SO_4^{2-} in metal sulfates such as $NiSO_4$, both of which belong to the same point group, T_d give absorption bands at 1105 and $1140\text{-}1090\text{ cm}^{-1}$ respectively. When sulfate ion binds to metal ion through one of its oxygen, a unidentate complex is formed with C_{3v} symmetry, and three absorption bands are noticed at $1147\text{-}1117$ (ν_3), $1044\text{-}1032$ (ν_3) and 970 cm^{-1} which are attributed to the asymmetric and symmetric vibrations of $S=O$ group and to the vibration of $S-O$ group respectively [11]. If sulfate co-ordinates to one or two metal ions through two of its oxygen, a chelating (A) or a bridged (B) bidentate complex is formed.



A



B

Sulphate: (A) Chelate bidentate
(B) Bridged bidentate

A chelating bidentate complex (A) has four absorptions at 1240-1230 (ν_3), 1125-1090 (ν_3), 1035-995 (ν_3) and 960-940 cm^{-1} (ν_1), which are assigned to the asymmetric and symmetric stretching frequencies of the S=O and S-O bonds. The bridged bidentate complex (B) also has four bands at 1195-1160 (ν_3), 1110-1105 (ν_3), 1035-1030 (ν_3), and 990-960 cm^{-1} (ν_1). The highest ν_3 frequency in the chelating bidentate complexes is higher than that in the case of bridged bidentates [12]. Organic sulfates and molecular H_2SO_4 belong to the same point group C_{2v} , show four absorptions at 1440-1350, 1230-1150, 960-1000 and around 910 cm^{-1} . The characteristics of these species are the remarkably high S=O stretching frequencies (asymmetric at 1440-1350 cm^{-1} and symmetric at 1230-1150 cm^{-1}) well above those of inorganic sulfate complexes.

The IR spectra were recorded using a FTIR spectrometer (Perkin Elmer Series1600) in the range of 400-1700 cm^{-1} using nujol mull techniques. 20 mg of the sample was taken mullled with nujol to form a homogenous mixture and was applied to KBr plates to record the spectrum. In some cases material was pelletised with KBr and spectra were taken. Diffuse reflectance spectra (DRS) were taken by supporting the pure sample on a sample holder

2.4c Thermal analysis

Thermography has found wide importance in different fields of science. In chemistry it is used to determine phase composition, hydration, polymerisation, solvent retention, purity, melting, decomposition etc. The most commonly used thermal methods are thermogravimetry(TG) and differential thermal analysis(DTA). In TG the weight of a substance heated at a controlled rate is

recorded as a function of time or temperature. The information that can be obtained from the TG curve is as follows.

- i. The curved portions in the graph indicate weight losses.
- ii. Weight loss can be used to determine the composition of a compound.
- iii. If there is no weight loss at a particular temperature it can throw light on its thermal stability
- iv It can also give information about the procedural decomposition temperature (the lowest temperature at which cumulative mass change attains a magnitude which the thermobalance can easily read out).

DTA is a technique in which the temperature difference between the sample and a thermally inert reference substance is continuously recorded as a function of furnace temperature or time. The measurement of changes in heat content is carried out by heating the two materials at elevated temperatures at a predetermined rate. The thermal effects may be either endothermic or exothermic and are caused by physical phenomenon such as fusion, crystalline structure inversions, boiling, vapourisation, sublimation and others. Some enthalpic effects are also caused by chemical reactions such as dissociation or decomposition, oxidation, reduction, combination and displacement etc. In this manner endo and exothermal bands and peaks appearing on the thermograms give informations regarding the detection of enthalpy changes. It has been found that most of the above transitions or reactions produce endothermic heat effects. Only a few such as oxidation, some decomposition reactions, certain crystalline inversions give exothermic heat effects.

Simultaneous TG-DTA analysis of the samples were performed on a automatic derivatograph (SETARAM TG-DTA92). The thermograms of the samples were recorded under the following conditions., weight of the sample-

30mg, heating rate-10 K/minute, atmosphere-air flow. α -Alumina was used as the reference material.

2.4d Scanning electron Microscopy

This technique allows essentially the imaging of the topography of a solid surface by use of back scattered or secondary electrons, with a good resolution of about 5nm. In the SEM a fine probe of electrons is scanned over the specimen surface using deflection coils.

Interaction between the primary beam and the specimen produces various signals(back scattered electrons, secondary electrons, X-ray etc.) which may be utilized to form an image. The appropriate signal is detected, amplified, and displayed on a cathode ray tube screened synchronously with the beam. The incorporation of wavelength or energy dispersive X-ray detectors with the SEM provides a powerful analytical facility.

In the present study the morphology and crystal size of the samples were investigated using a Scanning Electron Microscope (Stereoscan 440 Cambridge,UK).

2.4e Surface area measurements

Omnisorb 100 CX (supplied by COULTER Corporation, USA) unit was used for the measurement of N_2 adsorption to determine surface areas. The samples were activated at 673K for 2 hours in high vacuum (10^{-6} Torr). Then the weight of the sample was noted and it is then cooled to 94K using liquid N_2 . After this sample was allowed to adsorb nitrogen gas and the BET surface area was calculated.

The general form of BET equation can be written as follows.

$$1/V_{ads}(p_0-p) = 1/V_M S + [C-1/V_M S] p/p_0 \text{ where,}$$

V_{ads} = volume of the gas adsorbed at pressure p ,

p_0 = saturated vapour pressure

V_m = volume of the gas adsorbed for monolayer coverage

C = BET constant

By plotting the left side of the above equation against p/p_0 , a straight line is obtained with a slope of $C-1/V_m C$ and an intercept of $1/V_m C$. The BET surface area is calculated using the following formula,

$$S_{BET} = X_M \cdot N \cdot A_m \cdot 10^{-20}$$

where N is the avagadro number, A_m is the cross sectional area of the adsorbate molecule and X_M is the number of moles of N_2 adsorbed.

2.4f Pore volume measurements

According to Dubinin [13] pores can be classified according to their diameter, as micropores ($<20 \text{ \AA}$), mesopores ($20-200 \text{ \AA}$) and macropores ($>200 \text{ \AA}$). The adsorption behaviour of a solid is largely determined by the number, shape and size of the pores. In the present study Mercury porosimeter is used for determining pore size distribution of the catalysts. A wetting liquid like water or alcohol will enter into a capillary on its own because of the hydrostatic pressure difference. For a non-wetting liquid like mercury, sufficient pressure will have to be applied to force it into the capillary. The relation between the pore radius(r_p) and the radius of the meniscus (r_s) is obtained by,

$$r_p = -r_s \cos\theta \quad (1)$$

$$\Delta p = \frac{2\gamma}{r_s} \quad (2)$$

expressing in r_p

$$\Delta p = \frac{2\gamma \cos\theta}{r_p} \quad (3), \text{ where } \theta \text{ is the contact angle of mercury and solid.}$$

The above equation allows to calculate the pressure that will be needed to force mercury into pores of radius, r_p . In this instrument, the solid sample is immersed in a reservoir of mercury, the upper part of which ends in a narrow capillary. The upper part of mercury is in contact with a conducting wire just touching the mercury surface. As pressure is applied, the wire loses contact with mercury cutting of the electrical circuit. The wire is then lowered by a micrometer arrangement till the contact is made. The difference in volume in the capillary is the volume of the pore occupied by mercury under pressure.

Measurements of specific surface area and pore size distributions of the catalysts were carried out using Quantachrome, Autoscan-92 porosimetry (USA) by taking 300-400mg of sample. Accurate data acquisition was made as the instrument is connected through a computer

2.4g Determination of acidity and basicity by Hammett indicator method

The indicators used for determining the acidity and basicity are summarised in tables 2.1 and 2.2. Two drops of 0.1 % solution of the indicator in benzene was added to 0.1 g of solid suspended in 5ml dry benzene and allowed to stand for five minutes. The acidity at various acid strength of the solid was measured by titrating with a 0.1 N solution of n-butyl amine in benzene. In all cases titration was continued until a permanent colour change is obtained. It took about 10 hours for each titration. At the end point the basic colour of the indicator appeared [14].

Table 2.1 Basic indicators used for the measurement of acid strength

Indicator	colour		pKa*
	Base form	Acid form	
Methyl red	yellow	red	+4.8
Dimethyl yellow	yellow	red	+3.3
Crystal violet	blue	yellow	+0.8
Dicinnamalacetone	yellow	red	-3.0
Anthraquinone	colourless	yellow	-8.2
p-Nitrotoluene	colourless	yellow	-11.35 ^a
2,4-Dinitrotoluene	colourless	yellow	-13.75 ^a

* pKa of the conjugate acid, BH⁺ of indicator, B, (pK_{BH⁺}) ^aThe acid strength corresponding to the indicator is higher than that of 100 percent H₂SO₄.

Similarly the basicity was measured by titrating 0.1 g of solid suspended in 5 ml of benzene with 0.1 N solution of trichloroacetic acid in benzene using appropriate indicators. At the end point the colour of the indicator on the surface were the same as the colors which appeared by adsorption of respective indicators on the acid sites. The colour of the benzene solution was the basic colour at the end point, and it turned acidic colour by adding an excess of acid

Table 2.2 Indicators used for the measurement of basic properties

Indicators	Colour		pKa*
	Acid form	Base form	
Dimethyl yellow	yellow	red	+3.3
Methyl red	yellow	red	+4.8
Bromothymolblue	yellow	green	+7.2
2,4-Dinitroaniline	yellow	violet	+15.0

*pKa of indicator, BH, (=pK_{BH})

2.5 CATALYTIC ACTIVITY MEASUREMENTS

2.5a Liquid phase reactions

All the liquid phase reactions were (reduction of nitro compounds, ketones and unsaturated compounds) carried out batchwise in a 100 ml round bottom flask fitted with a reflux condenser with continuous stirring. In a typical run 50 mg of catalyst was dispersed in a solution containing 500 mg (4.06 mmoles) of nitrobenzene, 25 mg KOH (4.46 mmoles) pellets and 10 ml isopropanol. The mixture was vigorously stirred and heated under reflux for 3 hours in an oil bath. After the completion of the reaction (monitored by TLC), catalyst was filtered off, washed with isopropanol and excess distilled water was added to get an emulsion. Then it was extracted with dichloromethane and excess solvent was removed by rotary evaporation. The products were analysed in a gas chromatograph (Shimadzu GC 15A), fitted with an SE30 column (non-polar silicon fluid) and FID detector. In some cases products were isolated by column chromatography and identity of products established by IR, ¹H, NMR, GC-MS (Shimadzu, QP 2000A). Conversions are given in terms of total amount of reactant converted.

2.5b Gas phase reactions

All the vapour phase reactions were carried out in a vertical flow-type reactor consisting of 2.2 cm I.D and 30 cm length, kept in a cylindrical furnace mounted vertically. The catalyst (2.5-3 grams as pellets) was loaded in the middle of the reactor and packed with glass beads. The temperature was measured by a thermocouple placed in the middle of the catalyst bed. Before each experiment catalyst was activated in a current of dry air at 500 °C for 6 hours and then brought to the reaction temperature in presence of nitrogen flow. The reactant feed was introduced at the top of the reactor by means of an infusion pump (SAGE, USA) in the absence of any carrier gas. After the reaction, products were cooled using ice cooled water in a condenser connected to the reactor and collected at the bottom in a sample tube for analysis. The mass balance was noted each time. The products were analysed in a gas chromatograph (GC 15-A) fitted with FID and TCD. The gas products were collected using an ORSAT apparatus. The analysis was further confirmed by GC-MS and GC-FTIR. After each experiment the same catalyst was reactivated at 500°C in dry air for subsequent runs. A schematic diagram of the reactor set up used in the present study is shown.

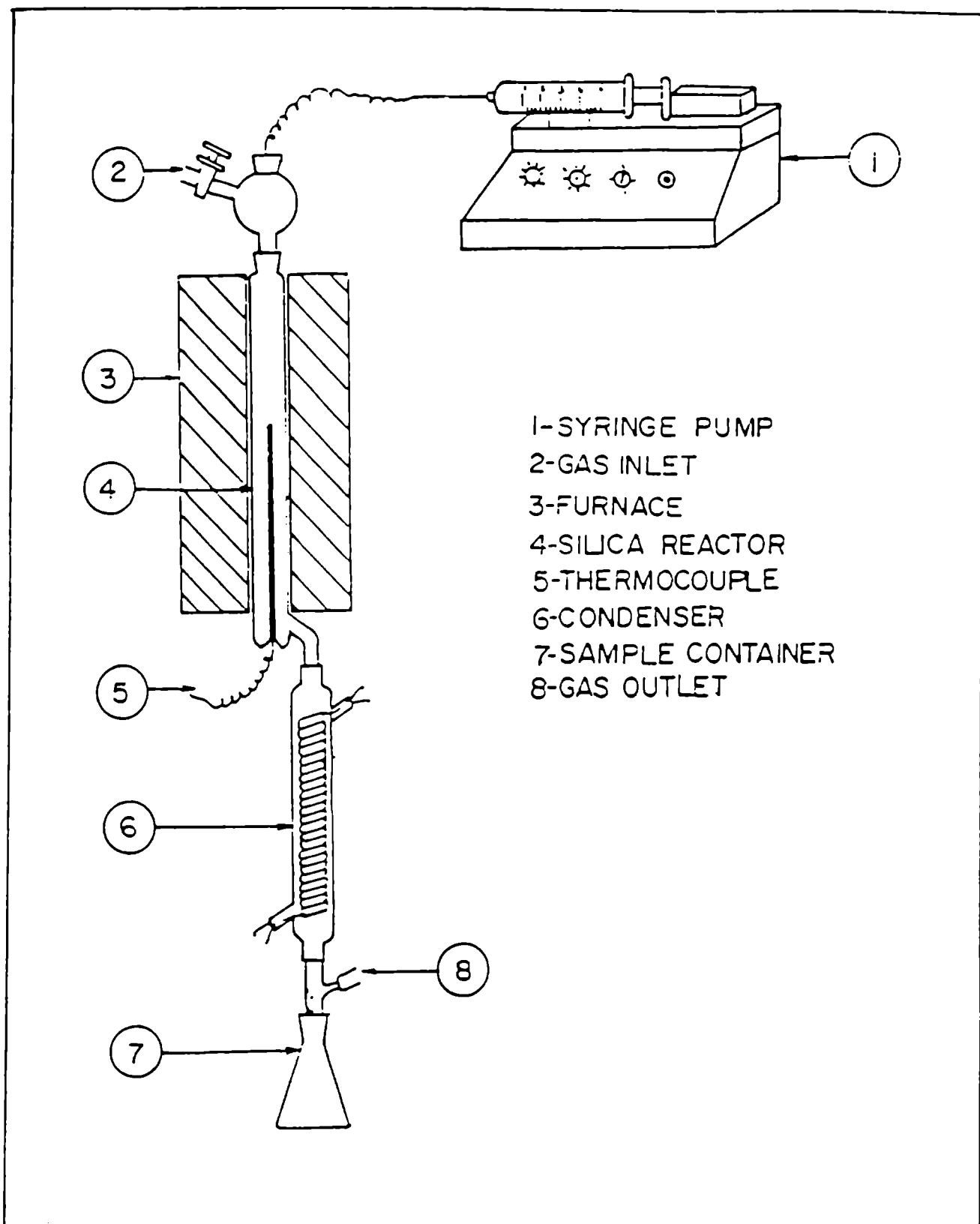


Fig. Reactor Set-up for Reactions carried out at atmospheric pressure.

REFERENCES

- 1 K. Morikawa, T Shirasaki, M. Okada, *Adv Catal.*, 20 (1969) 97; R. J Peglar, F H. Hambleton, J. H. Hockey, *J Catal.*, 20 (1971) 309
- 2 D D Perrin, W L. F Armarego, D R. Perrin, in "*Purification of laboratory chemicals*", 2nd edition Pergamon press, 1980.
- 3 P Courty, C Marcilly, in "*Preperation of catalysts*" *Stud. Surf. Sci. Catal* 1 (1976) 119
- 4 H. Matsuhashi, M. Hino, K. Arata, *Chem. Lett.*, (1988) 1027
- 5 H. Matsuhashi, M. Hino, K. Arata, *Appl. Catal.*, 59 (1990) 205
- 6 M Hino. S. Kobayashi, K. Arata, *J Am. Chem. Soc.*, 101 (1979) 6439; M Hino, K. Arata, *J. Chem. Soc. Chem Commun.*, (1980) 851, M. S. Scurrrell, *Appl. Catal.*, 34 (1987) 109; M. Hino, K. Arata, *Catal. Lett.*, 30 (1995) 25
- 7 K. Nakamoto, "*Infrared and Raman spectra of inorganic and co-ordination compounds*", 3rd edition, Wiley, New York, (1978) 241
- 8 T Jin, *Inorg. Chem.* 23 (1984) 4376.
- 9 R. L. Parfitt, R. S. C. Smart, *J. Chem. Soc. Faraday Trans. I*, 73 (1977) 796
10. J R. Sohn, H. W Kim, M. Y Park, E. H. Park, J. T Kim, S. E. Park, *Appl. Catal. A General.*, 128 (1995) 127; D A. Ward, E. I. Ko, *J. Catal.*, 150 (1994) 18.
- 11 N. B. Colthup, *J. Opt. Soc. Am.*, 40 (1950) 397
12. R. A. Maruis, J. M. Fresio, *J Chem. Phys.*, 27 (1957) 564
- 13 M. M. Dubinin, *Chem. Rev.*, 60 (1960) 235.
- 14 K. Tanabe, M. Misono, Y Ono, H. Hattori, "*New solid acids and bases, their catalytic properties*" (Eds) B. Delmon, J. T Yates, Elsevier, *Stud. Surf. Sci. Catal.*, 51 (1989).

RESULTS AND DISCUSSION

CHAPTER III

ACID-BASE PROPERTIES AND CATALYTIC ACTIVITY OF MIXED OXIDES OF TIN WITH LANTHANUM AND SAMARIUM

3.1 PHYSICO-CHEMICAL CHARACTERISTICS

Energy dispersive X-ray analysis is used to determine the chemical composition of all the mixed oxides prepared. The metal oxide percentage and metal percentage are given in Table 3 1

Table 3.1 EDX analysis of metal oxide samples*

Composition		TS82	TS55	TS28	TL82	TL55	TL28
Atom %	Sn	76.18	47.63	16.11	78.22	46.90	21.83
	Sm	23.82	52.37	83.89			
	La				21.78	53.10	78.47
Oxide %	SnO ₂	76.05	44.27	14.34	78.11	45.68	17.83
	Sm ₂ O ₃	23.95	55.73	85.66			
	La ₂ O ₃				21.89	54.32	82.17

*All the samples were calcined at 500 °C in air

X-ray diffraction patterns of Sn-Sm and Sn-La mixed oxide systems calcined at 500 °C for 6 hours are shown in Figure 3 1(a) and 3 1(b). It can be noted that the intensity of diffraction peaks decreases after the addition of Sm₂O₃ or La₂O₃ (10 mol%) to SnO₂ system. So the addition of a second oxide hinder the crystallisation of SnO₂ phase by preventing the aggregation of the smaller particles. Similar observation was reported when TiO₂ is added to ZrO₂ [1]. TS82 sample shows cassiterite as the prominent phase, no reflections due to Sm₂O₃ or La₂O₃ are detected. This means that La₂O₃ or Sm₂O₃ is well dispersed on the SnO₂ support material. The specific surface areas of these samples (TS82 and TL82) are higher (102.7 and 105.7 m²/g) compared to other systems. TS55 and TL55 shows the co-existence of both SnO₂ and rare earth oxide phases. However, no compound formation is observed at 500 °C,

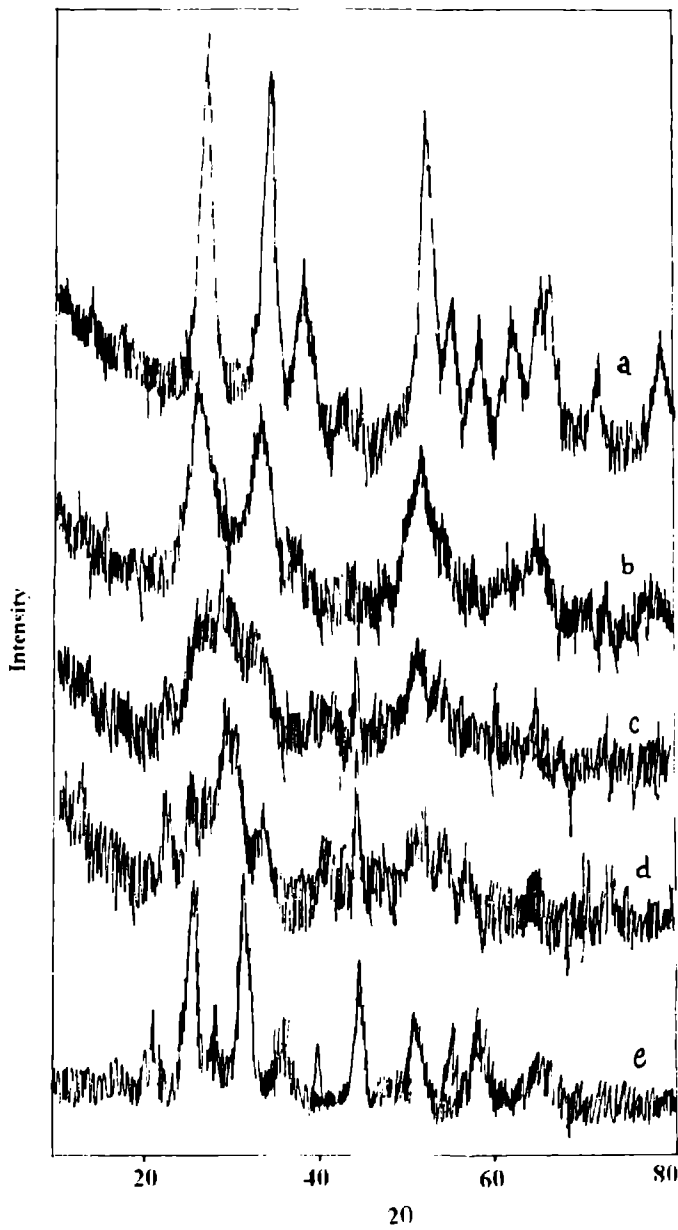


Fig. 3 1(a). X-ray diffraction patterns of of SnO₂^a, TL82^b, TL55^c, TL28^d and La₂O₃^e calcined in air at 500 °C

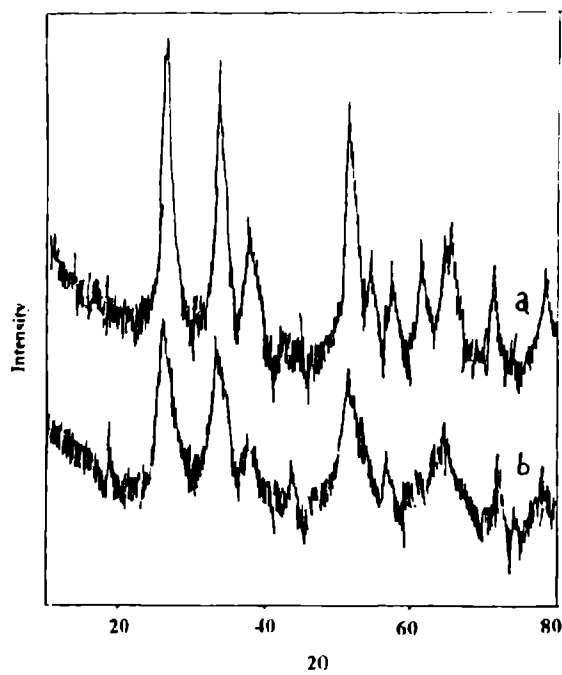


Fig. 3 1(b) X-ray diffraction patterns of SnO₂^a and TS82^b calcined in air at 500 °C

which is the temperature at which the material is calcined. Similarly TS28 and TL28 also show both SnO₂ and rare earth oxide phases.

The BET surface areas determined by N₂ adsorption are in the order TS82 > TS55 > TS28 and TL82 > TL55 > TL28. The higher surface area of TS82 and TL82 samples may be due to the presence of small amount of Sm₂O₃ or La₂O₃, which prevent the aggregation of SnO₂ particles. As more and more rare earth oxide is added to SnO₂, agglomeration takes place and this may be the reason for the lower surface area of other systems. The BET surface area of all the samples are presented in Table 3.3. No micropores are detected in any case except TS28 and TL28, where very small amount of micropores are detected.

Pore volume of all the catalysts are also given in Table 3.3. Pore volume increases in the order TL82 > TL55 > TL28 and TS82 > TS55 > TS28. The catalysts TL82 and TS82 contain only few number of pores with radius > 30 Å. Almost all the pores are in the region 20-30 Å. No pores are detected below 20 Å. So they can be considered as mesoporous materials (pore radius 20-200 Å) in which most of the pores are of almost uniform size and radius [2]. Compared to TS82 and TL82, other systems TS55 and TL55 contain more number of pores with radius > 30 Å. Some pores are detected in the macroporous region also (>200). In the case of TL28 and TS28 pore radius ranges from 30 to 1000 Å or more. A large number of pores with radius > 30 Å are detected. So a notable variation in the pore volume and pore size distribution is observed, as the composition of the catalyst changes. TS82 and TL82 are catalysts in which pores are of uniform size, while in the extreme cases, TS28 and TL28 pores are not of uniform size. The pore volume distribution curves are shown in Figure 3.2.

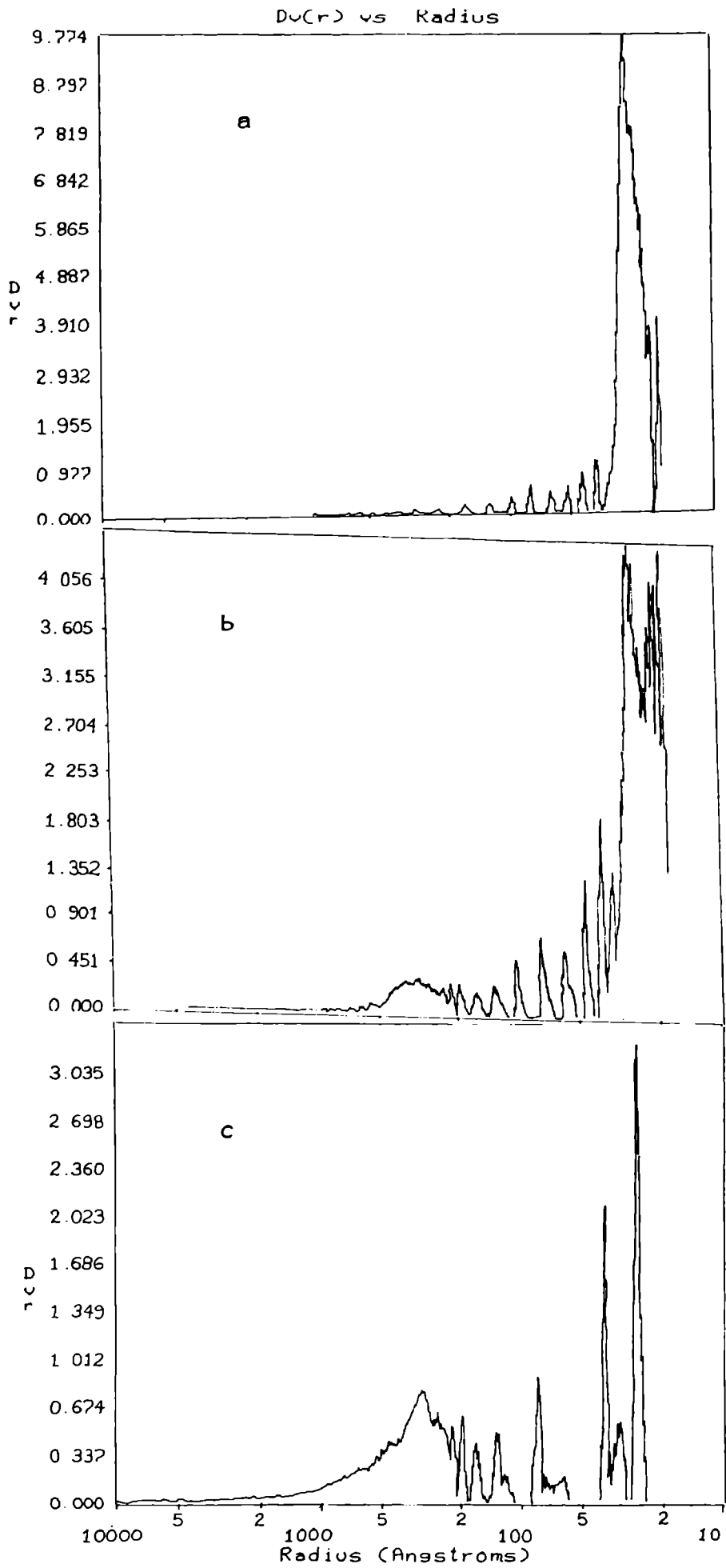


Fig. 3.2 Pore volume distribution curves of TL82^a, TL55^b and TL28^c calcined in air at 500 °C

Only one distinct weight loss has been seen, from 37 to 275 °C (7.35 %) in the case of TS82. Another gradual and slow weight loss is observed from 276 to 586 °C (2.41 %). The weight loss of the catalyst below 150 °C is due to the desorption of adsorbed water. The weight loss from 150-500 °C may be due to the evolution of structural water and also due to the dehydroxylation of the catalyst [3]. Above 400 °C the catalyst loses structural water due to excessive dehydration. Three distinct weight losses are observed in the case of TS28, one at 32-260 °C (4.04 %), another at 263-445 °C and one more at 402-518 °C (2.6 %). These weight losses are in accordance with the one reported in the case of lanthanum hydroxide [4,5], since in TS28 or TL28 percentage of rare earth component is more. In the case of La(OH)₃, an initial small weight loss at 100-200 °C is due to the removal of adsorbed water or water of crystallisation, the first true stage of La(OH)₃ occurs in the range 250-350 °C and results in the formation of a well defined hexagonal LaOOH intermediate.



Subsequent dehydration of oxyhydroxide to La₂O₃ occurs at 350-420 °C and is completed at 420 °C. The final broad peak showing weight loss at 450-800 °C is due to the decomposition of a surface layer of unidentate carbonate species existing on the oxide as a result of interaction of the highly basic lanthanum hydroxide precursor with atmospheric carbon dioxide during preparation and handling [6].

In the case of TS55 also three characteristic weight losses are seen similar to that of TS28 system. If we examine the DTA of TS55 an exothermic peak can be seen around 850 °C, which may be due to the formation of a new compound or a phase change. Same type of exotherm is obtained in the case of TS28 also but not very distinct as in the case of TS55. However no exotherm

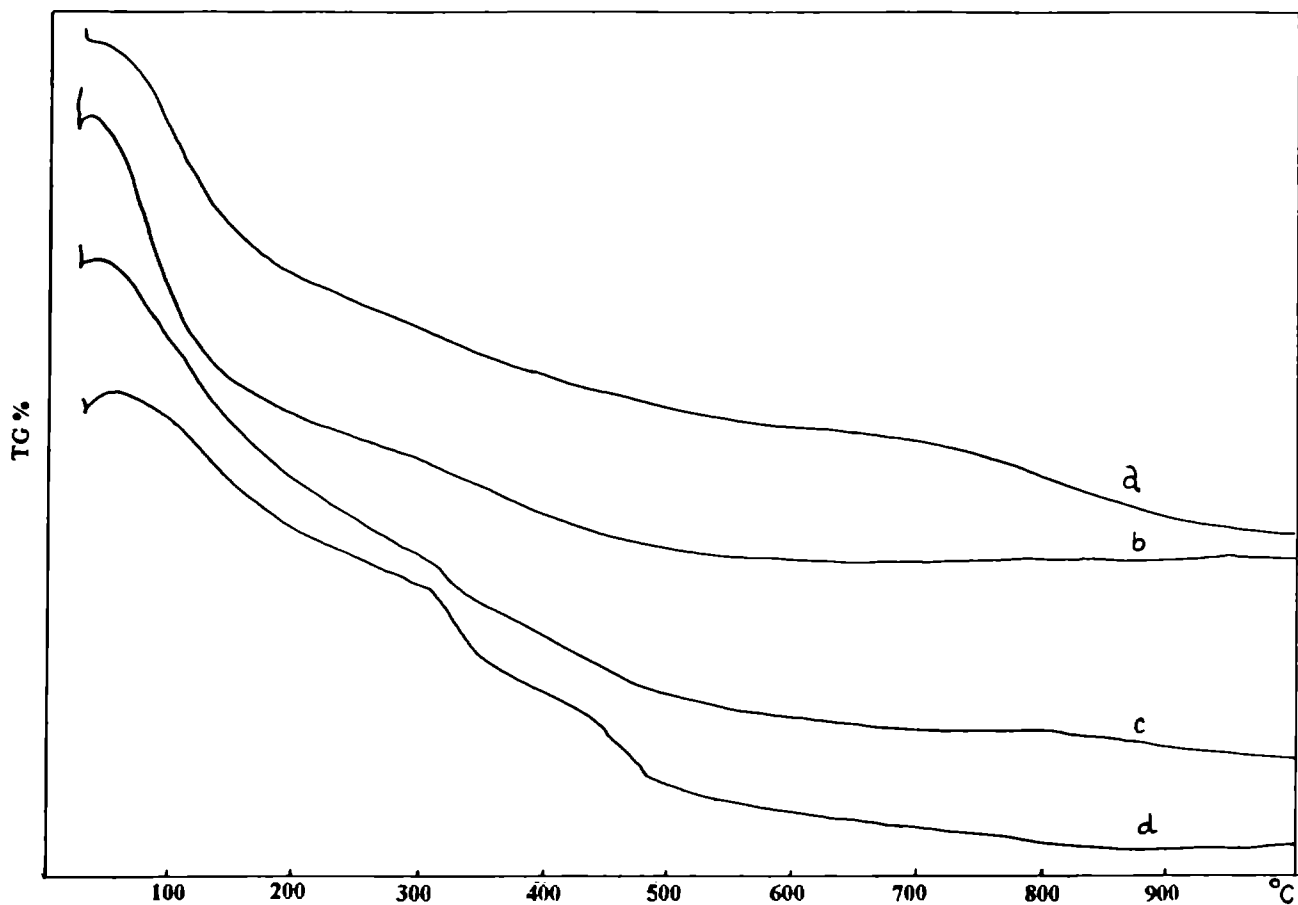


Fig. 3.3(a) TG curves of SnO₂^a, TS82^b, TS55^c and TS28^d

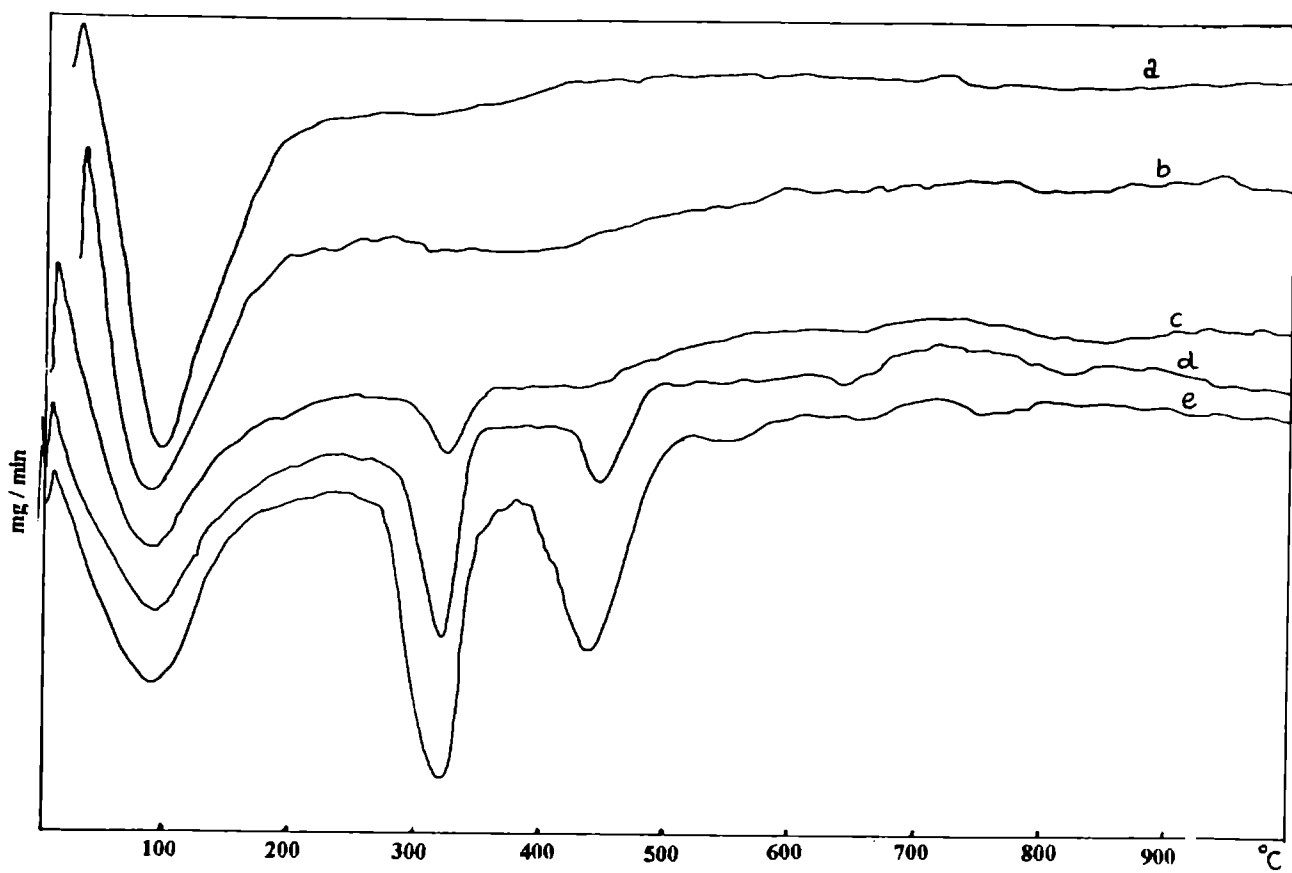


Fig.3.3(b) DTG curves of SnO₂^a, TS82^b, TS55^c, TS28^d and Sm₂O₃^e

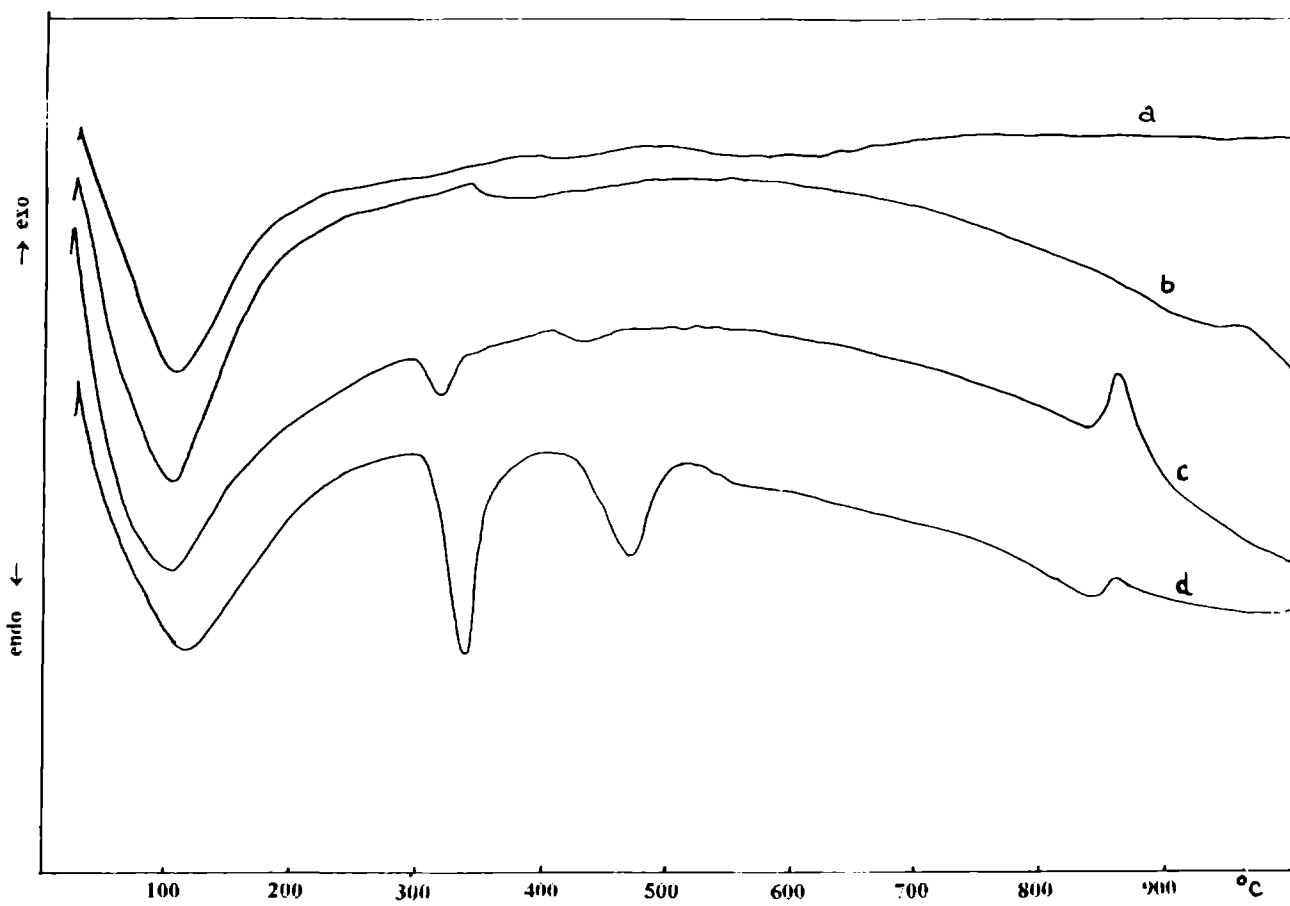


Fig.3.3(c) DTA curves of SnO₂^a, TS82^b, TS55^c and TS28^d

could be detected in the case of TS82. The TG-DTA curves are shown in Figures 3.3(a), 3.3(b) and 3.3(c).

The IR spectra of TS82, TS55 and TL82 catalysts are shown in Figure 3.4 (a) and 3.4 (b). Bands in the region $400\text{-}550\text{ cm}^{-1}$ are representative of the metal oxygen absorptions [7,8] McDewitt and Davidson have obtained the IR lattice vibrational spectra in the region $700\text{-}500\text{ cm}^{-1}$ of eight cubic rare earth oxides [9] Oxides are usually non-absorbing above 1000 cm^{-1} but most show a strong band and some weaker one in the $900\text{-}300\text{ cm}^{-1}$ region. Other lattice vibrational modes occur below this region. A band near 1645 cm^{-1} could be due to bending vibrational modes of OH, if the hydrogen of OH belong to the molecularly adsorbed water [10]. Other bands in the region $1200\text{-}1600\text{ cm}^{-1}$ are believed to be associated with surface bicarbonate species [8].

The basicity at various pKa values using different Hammett indicators are summarised in Table 3.2. The oxides under study responded only to bromothymol blue (pKa 7.2), methyl red (pKa 4.8) and dimethyl yellow (pKa 3.3). All the catalysts except TS55 gave basic colour change [11]. It can be seen that basicity of the catalysts are in the order $\text{TS82} > \text{TS28} > \text{TS55}$ and $\text{TL82} > \text{TL28} > \text{TL55}$ at an activation temperature of $500\text{ }^{\circ}\text{C}$.

The acid-base strength curves intersect at a point on the abscissa where acidity = basicity = 0, known as $H_{0,\text{max}}$ [11,12]. A catalyst with a large $H_{0,\text{max}}$ value has strong basic sites and weak acid sites and if $H_{0,\text{max}}$ is small it has strong acid sites and weak basic sites. We found that TS55 has a $H_{0,\text{max}}$ value of 4.6 at $500\text{ }^{\circ}\text{C}$ and 6.3 at $700\text{ }^{\circ}\text{C}$. This means that basicity increases with increase in activation temperature from 500 to $700\text{ }^{\circ}\text{C}$. We could not determine the $H_{0,\text{max}}$ value of TS82, TL82, TL55 and TL28 since these oxides were purely basic at activation temperatures of 300 , 500 and $700\text{ }^{\circ}\text{C}$. $H_{0,\text{max}}$ of TS28 catalyst is 6.4 at $700\text{ }^{\circ}\text{C}$.

Table 3.2 Basicity and acidity of catalysts activated at 500 °C

Catalysts	Basicity mmol/g			Acidity mmol/g		
	pKa \geq 7.2	pKa \geq 4.8	pKa \geq 3.3	pKa \leq 7.2	pKa \leq 4.8	pKa \leq 3.3
TS82	0.064	0.139	0.178	---		
TS55	---		0.102	0.015	0.015	
TS28	0.038	0.076	0.127	---		
TL82	0.076	0.203	0.165	---		
TL55	0.051	0.114	0.139	---		
TL28	0.038	0.063	0.152	---		
SnO ₂	---		0.108	0.104	0.076	
La ₂ O ₃	0.400	0.870	1.420	---		
Sm ₂ O ₃	0.560	0.660	0.980	---		

Table 3.3 Physico-chemical properties of the catalysts

Catalysts*	Surface area m ² /g	Pore volume cm ³ /g	XRD phase detected	Basicity mmol/g
TS82	102.70	0.315	SnO ₂	0.178
TS55	69.05	0.447	mixed	0.102
TS28	31.59	0.691	mixed	0.127
TL82	105.70	0.283	SnO ₂	0.165
TL55	55.63	0.416	mixed	0.139
TL28	26.42	0.719	mixed	0.152

*Catalysts calcined at 500 °C in air

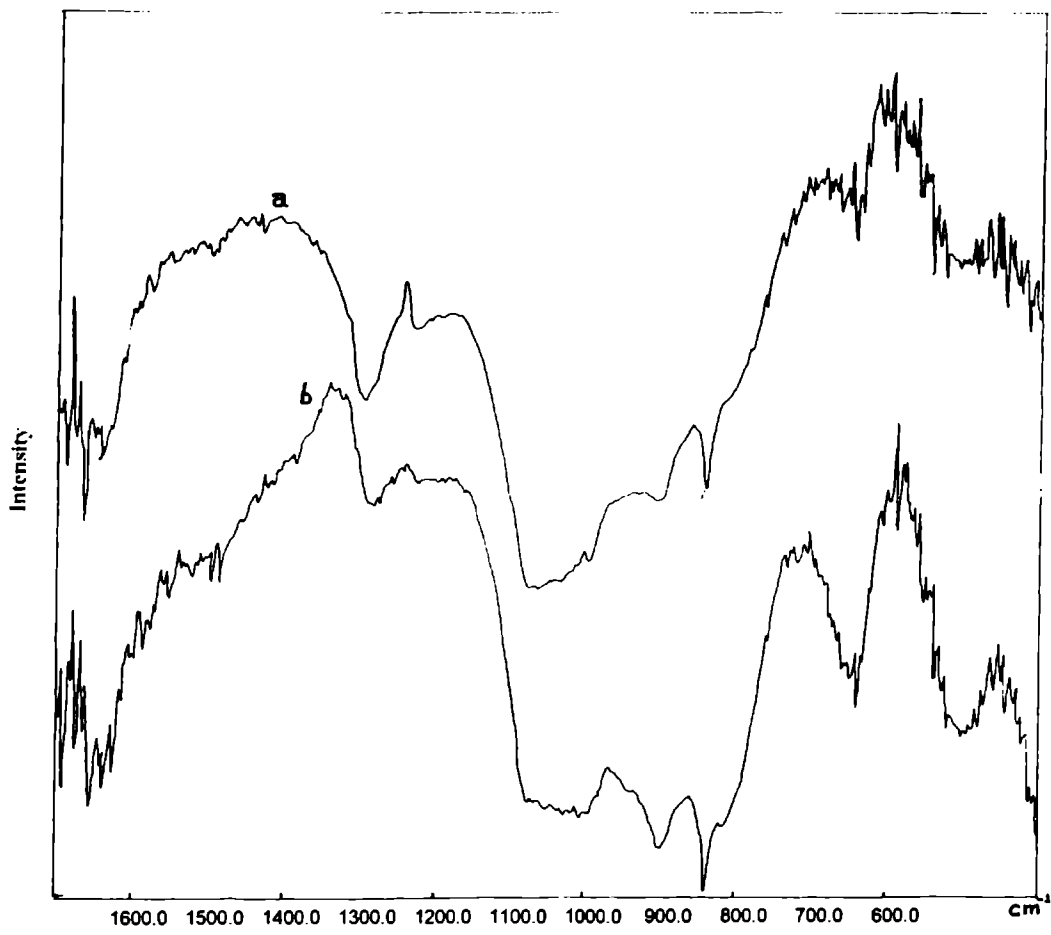


Fig.3 4(a) FTIR spectra of TL82^a and TL55^b

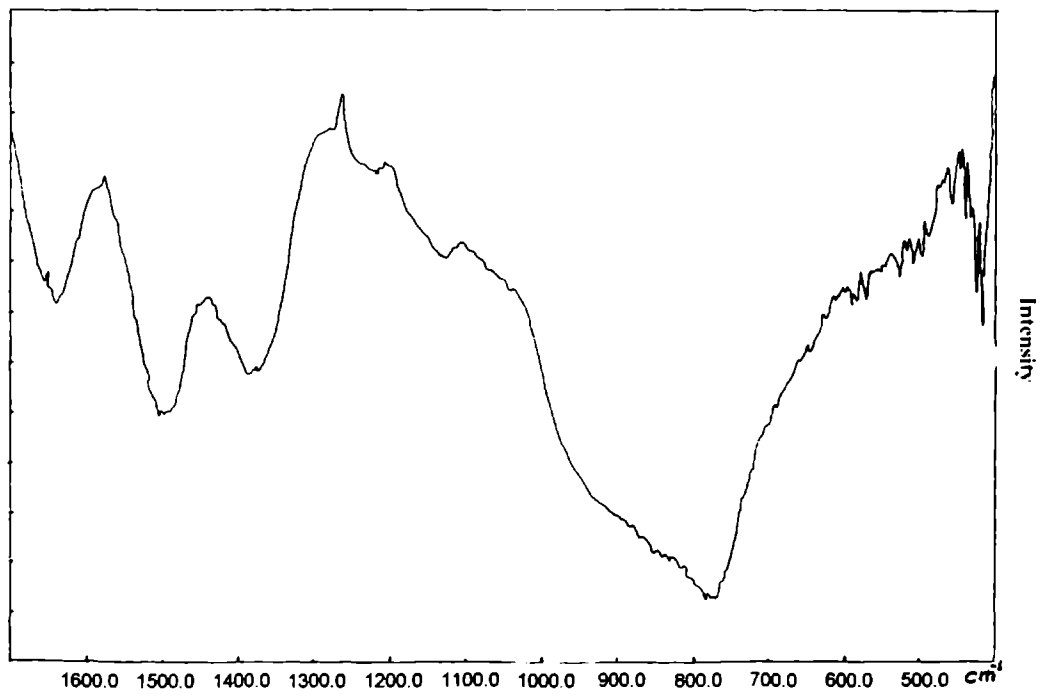


Fig.3.4(b) FTIR spectra of TS82

3.2 ALCOHOL DECOMPOSITION AS A TEST REACTION

3.2.1 Decomposition of Cyclohexanol

Both dehydration and dehydrogenation proceeds over the mixed oxide systems under study. Dehydrogenation is the main reaction. Selectivity towards dehydration and dehydrogenation are summarised in Table 3.4. Selectivity towards dehydration products are in the order TS55 > TS28 > TS82 and TL55 > TL28 > TL82. Only traces of methyl cyclopentenes are detected, indicating that acid sites strong enough to isomerise cyclohexene formed, are not present. Pines and Pillai have reported the formation of methyl cyclopentene over highly acidic aluminas [13]. Compared to isopropanol and *t*-butanol dehydration cyclohexanol requires stronger acid sites. According to Bezouhnia *et al* Bronsted acid sites are responsible for the dehydration of cyclohexanol to cyclohexene [14]. They also postulated the following hydrogen abstraction scheme for cyclohexanol dehydrogenation (Fig. 3.5)

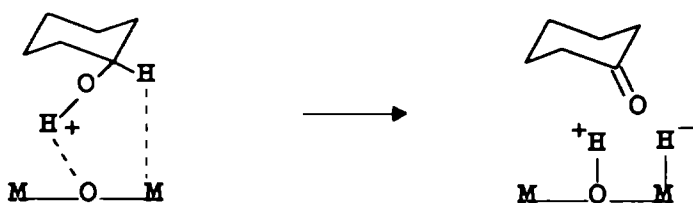


Fig 3.5 Mechanism of dehydrogenation of cyclohexanol

Table 3.4 Decomposition of cyclohexanol over different binary oxides

Catalysts	Conversion %	^a Conv to C=C %	^b Conv to C=O %	Sel. of C=C %	Sel of C=O %
TS82	48.16	12.45	35.71	25.86	74.14
TS55	58.12	26.96	31.16	46.40	53.60
TS28	45.80	19.60	26.20	42.80	57.20
TL82	45.03	10.24	34.79	22.75	77.24
TL55	54.75	22.29	32.46	40.72	59.78
TL28	47.47	17.09	30.38	36.02	63.98

Reaction conditions: Reaction temp. 350 °C, Feed rate 4 ml/h, TOS 2 h, Catalyst weight 2.7 g, Calcination temp. 500 °C.

^aConversion to C=C: Conversion to dehydration products which is calculated as follows,

Conversion to dehydration products = Total cyclohexanol conversion × selectivity of dehydration products./ 100

^bConversion to dehydrogenation products (C=O) = Total cyclohexanol conversion × selectivity of dehydrogenation products./ 100

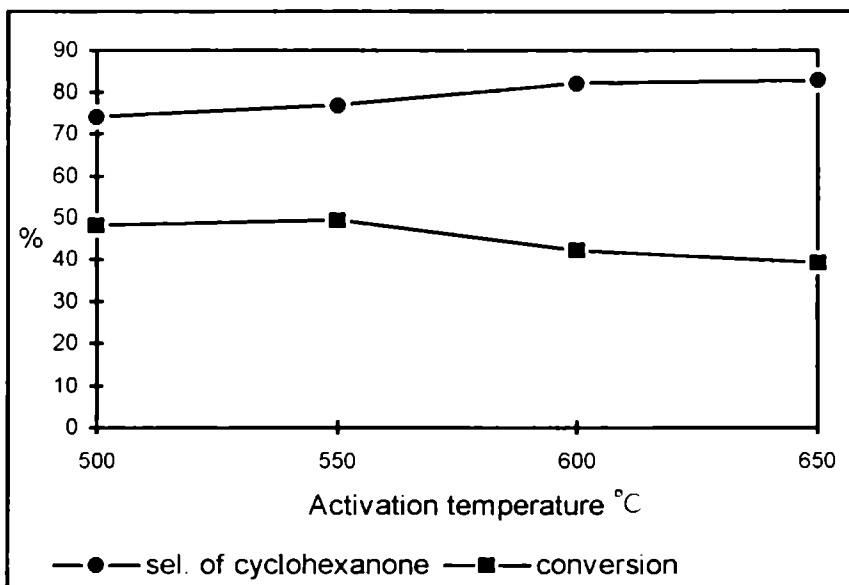


Fig. 3.6 Effect of activation temperature of the catalyst on the selectivity of cyclohexanone.

Reaction conditions. Reaction temp 350 °C, Feed rate 4 ml/h, TOS 2 h, Catalyst (TS82) weight 2.7 g.

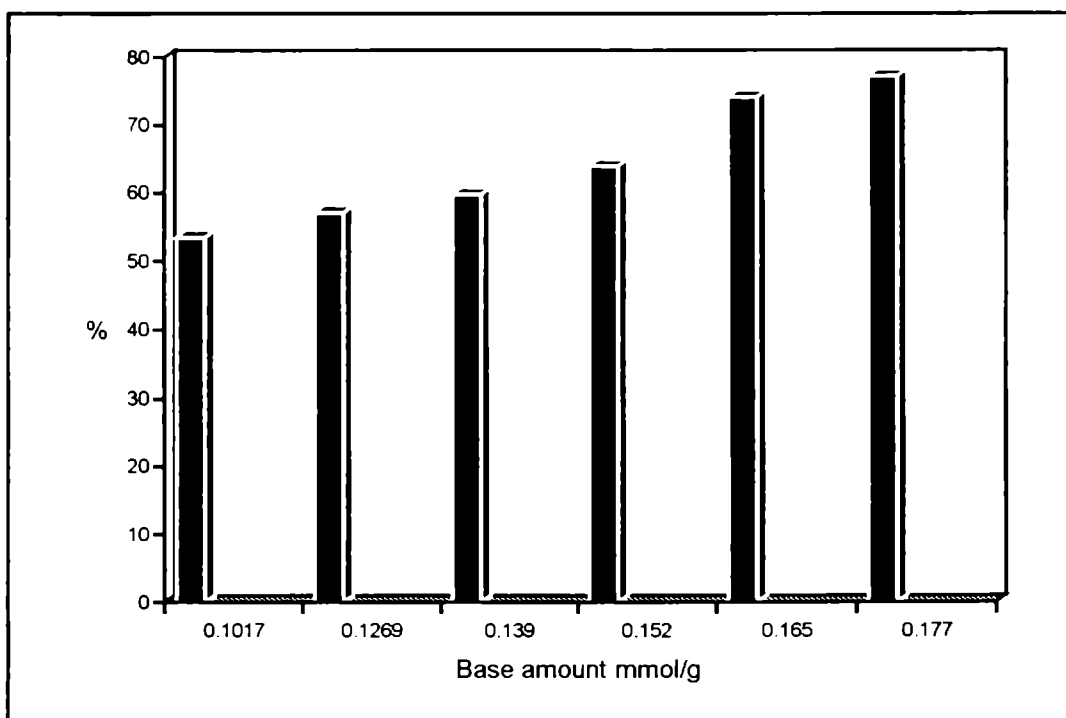


Fig. 3 7 Effect of base amount on the selectivity of cyclohexanone

Reaction temp 350 °C, Feed rate: 4 ml/h, TOS 2 h, Catalyst weight 2.7 g,
Calcination temp. 500 °C

note: base amount is determined by Hammett indicator method and catalysts are arranged in the increasing order of their basicity.

In the mechanism of dehydrogenation of cyclohexanol to cyclohexanone the metal cation is acting as a Lewis acid site. According to the authors the basic sites originating from the oxygen in oxide lattice is responsible for dehydrogenation. We activated the catalyst to different temperatures prior to the reaction and found an increase in cyclohexanone selectivity (Fig.3 6) with increase in activation temperature. This may be due to the formation of O^{2-} ions at higher temperatures. As determined by Hammett indicator method basicity increases slightly by activation, from 500 to

650 °C and then decreases. Correlation of basicity determined by Hammett indicator method and selectivity of cyclohexanone is demonstrated in Fig 3 7. As the base amount increases cyclohexanone selectivity also increases. High activity in the formation of cyclohexanone is probably due to the presence of stronger basic centres. The lower yield of cyclohexanone in the case of TS55 and TL55 compared to other catalysts indicate the absence of strong basic centres though weak or medium strength basic centres may be present. So the formation of cyclohexene and cyclohexanone indicates the presence of weak and / or medium strength acidic centres and medium and / or strong basic centres respectively. Thus the test reaction of cyclohexanol indicates the presence of acidic and basic centres of probably different strengths as the composition of the catalyst is varied. Based on the above results catalysts can be arranged in the increasing order of their basicity as TS55 < TS28 < TS82 and TL55 < TL28 < TL82 and their acidity follows the reverse order.

3.2.2 Decomposition of *t*-butanol

t-Butanol can undergo only dehydration reaction without any other side reactions like dehydrogenation. So it is useful for comparing the acidity of a set of catalyst systems [15]. Reaction is carried out at 200 °C at a feed rate of 6 ml/h. From the results obtained it is clear that the acidity of tin-samarium oxide and tin-lanthanum oxide systems are in the order TS82 < TS28 < TS55 and TL82 < TL28 < TL55. Isobutene is the main product with small amounts of other products like 1-butene and 2-butene. So the isobutene formed cannot undergo further isomerisation reaction, which must be due to the scarcity of stronger acid sites [16,17].

Table 3.5 Dehydration of *t*-butanol over different catalysts

Catalyst	Conversion %
TS82	44.22
TS55	63.89
TS28	60.12
TL82	43.86
TL55	59.46
TL28	51.43

Reaction conditions: Reaction temp. 200 °C, Catalyst weight 2.7 g, Feed rate: 6 ml/h, Activation temp. 500 °C, TOS 3 h.

3.2.3 Decomposition of Isopropanol

Dehydration is the main reaction over all the oxide systems studied at 250 °C. In most cases selectivity of dehydration product propene is about 98-99%. Linear dependence of temperature on the conversion of isopropanol as well as on the propene selectivity is shown in Figure 3.8. No ether was detected at any of the selected temperatures. But at higher feed rates propene selectivity decreases producing more and more acetone and small amounts of ether. It can be seen that catalytic activity increases with increase in surface area of the systems, which is in the order TS82 > TS55 > TS28 and TL82 > TL55 > TL28. If we compare the product selectivity towards dehydration and

dehydrogenation it is obvious that there is not much difference if go from one system to another. In the case of TL series comparison is possible, where we get maximum propene selectivity in the case of TL55. So on the basis of propene selectivity alone the increasing order of acidity is $TL82 < TL28 < TL55$. The ratio of dehydrogenation activity to the dehydration activity which is a measure of the basicity of a system [18] matches well with the those obtained by Hammett indicator method, so the basicity of the systems are in the order $TL82 > TL28 > TL55$ and $TS82 > TS28 > TS55$. The higher dehydrogenation activity of (partial oxidation) of systems containing more amount of SnO_2 indicate that the redox properties are predominating over the acid base properties. The dehydrogenating activity is in general attributed to the redox properties as well as to the acid base properties in the decomposition of alcohols [19]. The product inhibition studies with H_2O and H_2 were also carried out. It is found that dehydrogenation activity is favoured by the introduction of water alongwith the feed, however conversion of alcohol is decreased. When the reaction is conducted in the presence of controlled flow of hydrogen, the dehydrogenation is almost completely suppressed giving only dehydration products propene and water. Poisoning of the catalyst with pyridine prior to the experiment resulted in a considerable decrease in conversion to about 5%. Furthermore, after the poisoning of the catalyst with ammonia vapours even traces of propene is not detected. Pyridine adsorbs predominantly on Lewis acid sites and ammonia on both Lewis and Bronsted acid sites.

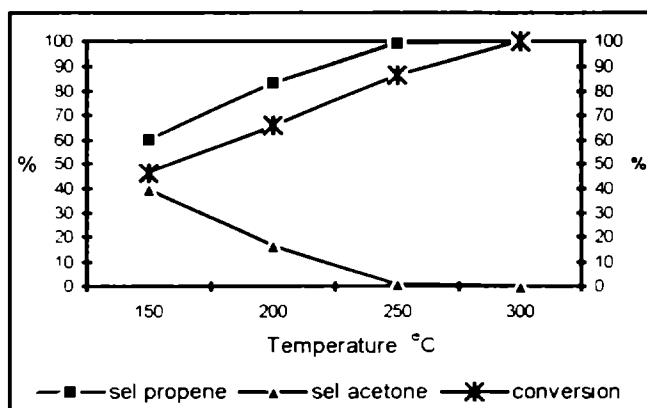


Fig.3.8 Effect of temperature on the selectivity of propene and acetone
 Reaction conditions. Activation temp. 500 °C, Feed rate 4 ml/h, TOS 3 h,
 Catalyst TS82 (2.7 g).

Table 3.6 Decomposition of isopropanol over different catalysts

Catalyst	Sel c=c	Sel. c=o	Conv to propene	Conv to acetone	v_a^* $\times 10^{-6}$	v_b^* $\times 10^{-8}$	v_b/v_a $\times 10^{-3}$	Conv %
TS82	99.29	0.71	85.74	0.61	4.46	3.10	6.90	86.36
TS55	99.62	0.38	80.60	0.30	6.24	2.32	3.70	80.91
TS28	99.42	0.58	79.24	0.46	13.40	7.79	5.80	79.71
TL82	96.49	3.51	69.78	2.53	3.53	12.80	36.00	72.32
TL55	99.28	0.72	62.86	0.45	6.04	4.32	7.10	63.32
TL28	97.01	2.79	59.56	1.83	12.10	37.00	30.50	61.40

v_a Dehydration rate

v_b Dehydrogenation rate

* Rate in mol/h g catalyst = Fractional conversion \times feed rate in mol/h / weight of the catalyst in g.

Reaction conditions: Activation temperature 500 °C, Reaction temperature 250 °C, Feed rate 4 ml/h, TOS 3 h.

3.2.4 Decomposition of butanols as a probe reaction to investigate acid-base properties of oxide systems

The following types of mechanisms, are possible in the catalytic dehydration of alcohols, where A and B stand for acidic and basic centers of catalysts respectively [20,21].

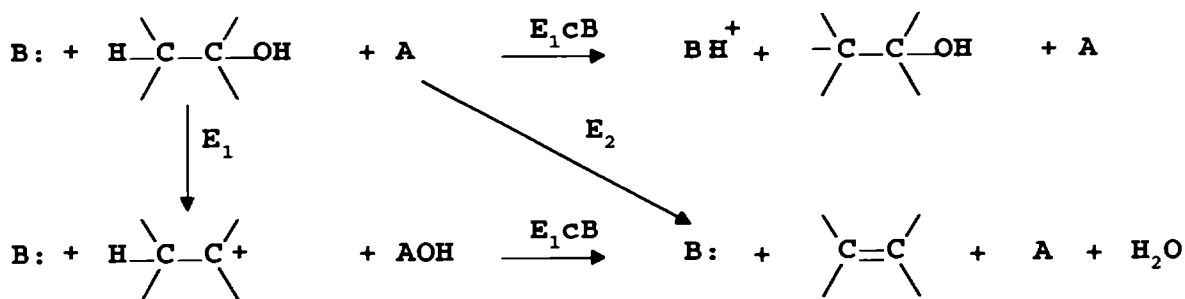


Fig. 3 9 Mechanism of alcohol decomposition

The first step of dehydration is the formation of a carbanion in the case of E₁cB mechanism. This mechanism occurs with strongly basic catalysts such as La₂O₃, ThO₂ and alkaline earth oxides [22]. In E₁ type mechanism the first step is the formation of carbenium ion by abstraction of an OH group. Strongly acidic catalysts like alumino-silicate dehydrate via this mechanism [23]. The acidic centers may be either B or L type. In E₂ type mechanism, the elimination of a proton and a hydroxyl group from alcohols are concerted without the formation of ionic intermediates. Alumina is a typical E₂ oxide [24].

The product distribution is one of the most important clues in arriving at a possible mechanism of the reaction. With E₁ mechanism, isomerisation takes place in the carbenium ion stage. Thus the formation of 2-butene from 1-

butanol is indicative of the E_1 mechanism. High selectivity for 1-butene (Hoffmann orientation) from 2-butanol is indicative of E_1cB , whereas E_1 and E_2 give mainly 2-butene (Saytzeff orientation). Noller and Thomke [25] recommended the use of deuterated reactants or catalysts and give the following criteria for the three mechanisms.

(i). With the E_1cB mechanism, exchange is found in both the alcohol and the olefins, but only in beta positions, indicating that the carbanion undergoes reconversion to the alcohol

(ii). With the E_1 mechanism exchange in all positions of the olefins is observed, but no exchange at all in the alcohol (this indicate that the carbenium ion formed is not reconverted into alcohol).

(iii). With E_2 mechanism, exchange doesn't occur, both alcohols and olefins retaining their original isotope composition. The mechanism of dehydration may differ from alcohol to alcohol, even if the same catalyst is used. Most of the examined alcohols showed E_1 on BPO_4 , E_2 (sometimes mingled with E_1) on $Ca_3(PO_4)_2$ and E_1cB on Sm_2O_3 . There are two exceptions, dehydration of ethanol over BPO_4 and 2-methyl 2-propanol over Sm_2O_3 , both proceed with E_2 mechanism [26].

The reaction of isobutanol over these oxides show that both dehydration and dehydrogenation take place, the extent of which depends on the acid-base properties of the catalysts. Isobutene is the major product, alongwith some amount of butenes which must be formed by the isomerisation of isobutene. The selectivity of dehydration products is in the order $TS55 > TS28 > TS82$ and $TL55 > TL28 > TL82$. Moreover the selectivity of isomerisation products also follow the same order. Isomerisation reaction requires stronger acid sites and hence the formation of 1-butene and 2-butene indicate the presence of some stronger acid sites. The dehydrogenation activity follows the reverse order. The results are summarised in Table 3.7. The ratio of dehydrogenation rate to dehydration rate which is a measure of the basicity,

correlates well with what is obtained by Hammett indicator method. As the temperature is increased the selectivity of the aldehyde is decreased whereas the selectivity of butenes is increased, since as the temperature increases the contribution of ionic structures increases. An increase in feed rate increases the selectivity of dehydrogenating product as expected. Addition of water alongwith the feed also enhanced the dehydrogenation selectivity. When the reaction is carried out separately over SnO₂ and La₂O₃, isobutene 60% and aldehyde 35% are formed in the case of SnO₂ and isobutene 78% and aldehyde 20% are formed in the case of La₂O₃. A slow and steady deactivation is observed in the case TS82 and TL82 with time on stream which indicate the participation of redox centers in the dehydrogenation reaction. The colour of the catalyst after the reaction turned gray which suggest the reduction of Sn⁴⁺ species during redox cycle [27].

Reactions of *t*-butanol, 2-butanol, 1-butanol also are conducted. *t*-Butanol dehydrated to isobutene with small amounts of butenes. 2-Butanol dehydrated mainly to 2-butene (Saytzeff elimination) with small amounts of 1-butene and a considerable amount of dehydrogenated product (18%) is also formed. Dehydration of 1-butanol afforded 1-butene as the major product alongwith 2-butene and isobutene. These observations suggest that dehydration occur via Saytzeff elimination and hence the mechanism can be either E₁ or E₂ type. Since dehydration products requiring isomerisation are formed in very less quantities, the dehydration over these systems is proposed to be mainly E₂ type probably mixed with some E₁. In the case of TS82 only small quantities of isomerisation products are formed, whereas in the case of TS55 and TS28 the yield of isomerisation products are comparatively greater and hence the contribution of an E₁ type mechanism cannot be excluded.

Table 3.7 (a) Decomposition of isobutanol over different catalysts

Catalyst	Sel.C=C %	Sel.C=O %	Conversion %
TS82	70.66	29.34	63.61
TS55	83.14	16.86	60.67
TS28	78.81	21.19	44.83
TL82	69.16	30.84	62.81
TL55	81.86	18.14	56.18
TL28	75.61	24.39	49.80

Table 3.7 (b) Contd.

Catalyst	Conv to C=C	Conv to C=O	Sel. 1-butene	Sel. 2-butene	v_a $\times 10^{-6}$	v_b $\times 10^{-7}$	v_b/v_a
TS82	44.94	18.67	2.09	2.16	2.09	8.68	0.41
TS55	50.44	10.23	9.40	7.80	3.40	7.07	0.20
TS28	35.33	9.50	9.55	7.65	5.34	14.3	0.26
TL82	43.43	19.38	1.81	2.01	1.96	8.76	0.45
TL55	45.98	10.20	9.21	7.64	3.90	8.76	0.22
TL28	37.65	12.15	9.18	7.38	6.80	21.9	0.32

v_a . Dehydration rate v_b . Dehydrogenation rate

Reaction conditions: Activation temp. 500 °C, Reaction temp 300 °C, Feed rate 4 ml/h, TOS 3 h, Catalyst weight 2.7 g.

In the case of catalyst having more number of acid sites (and also stronger sites) the mechanism is E_1 type and literature survey shows that catalyst having very weak acid sites and very strong basic sites dehydrate alcohol via E_1cB mechanism. So it is expected that catalysts having acidic and basic sites with intermediate strength can dehydrate alcohol via E_2 route. Moreover in the case of oxides where dehydrogenation products are also formed, the most viable mechanism of dehydration will be one involving both acid and base sites simultaneously *i.e.*, E_2 mechanism.

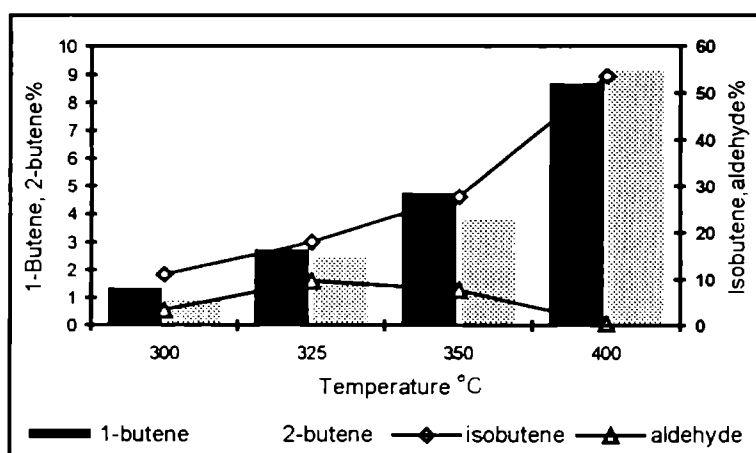


Fig.3 10 Effect of temperature on the product distribution

Reaction conditions: Activation temp. 500 °C, Feed rate 4 ml/h, TOS 3 h, Catalyst weight 2.7 g (TS82).

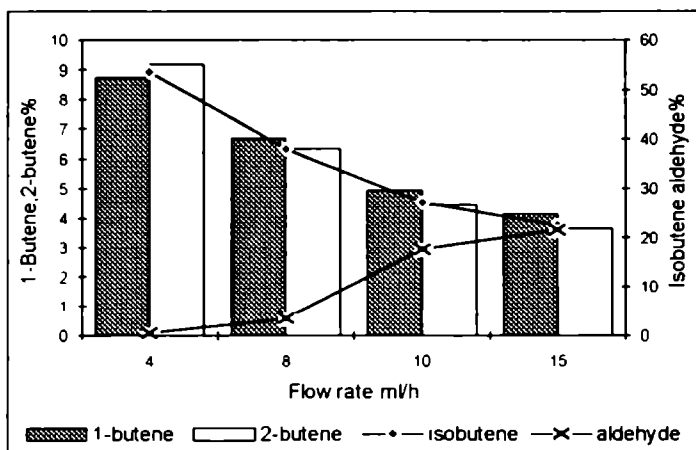


Fig. 3.11 Effect of feed rate on the product distribution

Reaction conditions: Activation temp. 500 °C, Reaction temp. 300 °C, TOS 3 h, Catalyst weight 2.7 g (TS82).

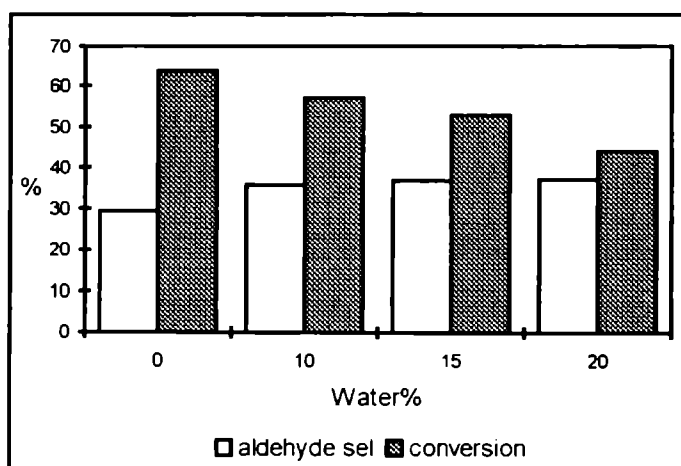


Fig 3 12 Effect of water on the selectivity of aldehyde

Reaction conditions: Reaction temp. 300 °C, Feed rate 4 ml/h, TOS 3 h, Catalyst weight 2.7 g (TS82).

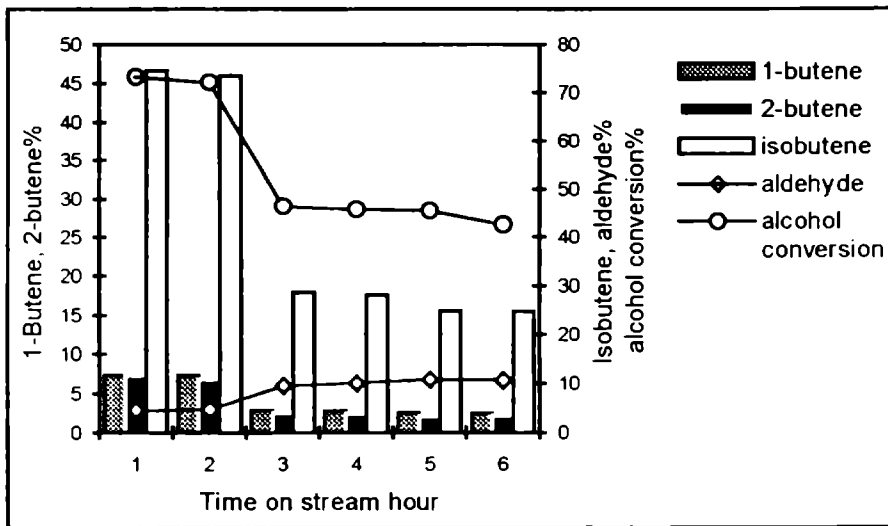


Fig 3 13 Effect of time on stream on the product distribution and conversion
 Reaction conditions: Reaction temp. 300 °C, Catalyst TL82 (2.7 g), Feed rate 4 ml/h

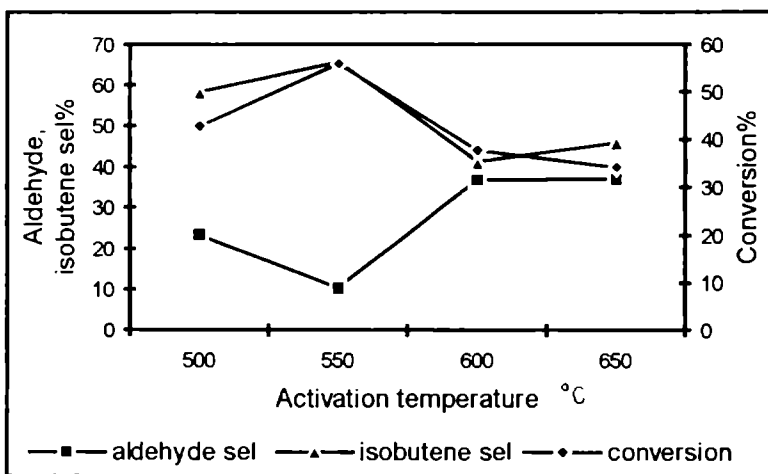


Fig 3 14 Effect of activation temperature on the selectivity of products
 Reaction temp 300 °C, Catalyst TL82 (2.7 g), Feed rate 4 ml/h

The conversion of four alcohols are in the order *t*-butanol (100%) > 2-butanol (55.03%) > isobutanol (52.93%) > 1-butanol (31.79%) at 350°C. Branching of alcohol molecule promotes olefin formation and enhances the reactivity, this reactivity increases in the order of primary, secondary and tertiary alcohols [28].

In the present study the order of reactivity of ethanol, n-butanol and isopropanol are compared. The high reactivity of IPA is due to the effect of the substituted methyl group attached to the α -carbon atom. n-Butanol is more reactive than ethanol because of the longer chain of the alkyl group. The activation energy for dehydration follow the sequence given below in the case of zeolites [29].

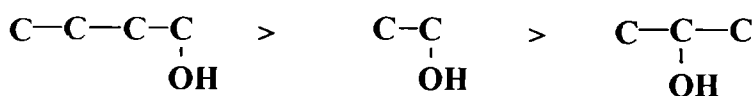


Fig. 3.15 The order of activation energy for alcohol dehydration.

This order shows that activation energy increases with alkyl chain length in primary alcohols but decreases with branched alcohol. The sequence of decrease in activation energy corresponds to decreasing acid strength of the hydrogen atom on the beta carbon atom. The lower the acidity, the higher the energy required for H atom abstraction. However when the acidic sites on the catalyst are strong enough to give complete abstraction of OH groups, the abstraction of hydrogen atoms from the beta carbon becomes the rate determining step in the formation of activated complex.

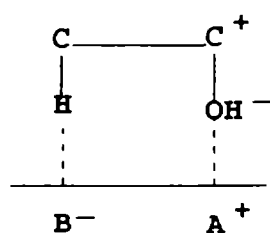


Fig. 3 16. Transition state for the dehydration of alcohol.

It is found that the dehydration of most reactive alcohol requires the least activation energy [30]. In the catalytic dehydration of aliphatic alcohols the alcohol chain length therefore affects both the abstraction of the OH group from the alpha carbon atom and the hydrogen from the beta carbon atom. The alkyl chain length exerts an inductive effect on the OH group increasing the electronegativity of the latter [31]. This increase in electron density favours strong interaction between the OH group and the acidic sites on the catalyst surface. We have already seen that the alcohol dehydration via E_1 mechanism produces an intermediate carbenium ion; the E_2 mechanism involves the simultaneous abstraction of the hydrogen atom from the beta position by the basic site and the OH group from the alpha carbon by the acid paired sites. The inductive effect on the OH group probably shifts the reaction mechanism from E_2 to E_1 in the dehydration of longer chain alcohols.

Comparison of the dehydration of ethanol, IPA and n-butanol

The activity of these alcohols are in the order IPA > ethanol > n-butanol. We have already showed that these catalysts contain only weak acid sites. So the possibility of E_1 mechanism is less, even in the case of n-butanol which is a long chain alcohol whose alkyl chain inductive effect is to be taken into account. However acid strength of beta hydrogens are in the order ethanol > n-butanol. So the abstraction of beta hydrogen atom must be important, in the case of these oxide systems.

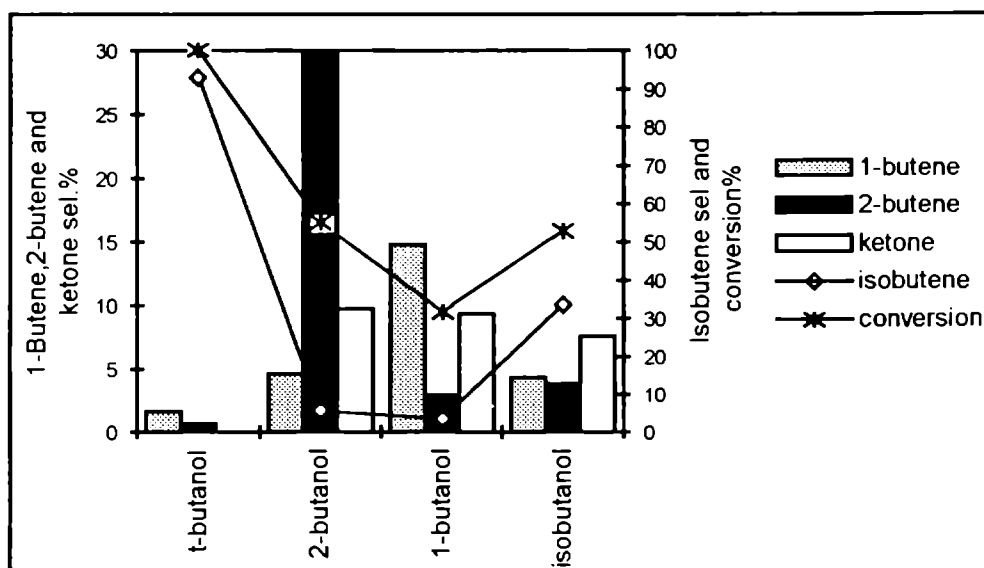


Fig 3.17 Effect of alcohol structure on the selectivity of products
 Reaction temp 300 °C, Catalyst TL82 (2.7 g), Feed rate 4 ml/h

Had the mechanism been E_1 in the case of n-butanol, it would have given more conversion than ethanol under similar experimental conditions. Also n-butanol dehydration produced little isomerisation products. Here three things are to be considered (i). inductive effect of the alkyl chain length which polarises OH group (ii). The acidity of beta hydrogen atom and (iii) the strength of acid base sites on the catalyst surface. So a consideration of all these factors can give an idea about the reaction mechanism. Presence of strong acid sites on the catalyst surface and a favourable inductive effect of the alkyl chain length can always shift the mechanism towards E_1 . In the present systems, we found that little isomerisation products are formed even in the case of n-butanol, where the inductive effect of alkyl chain length must play some role. This may be because the acid sites are weak and hence not strong enough

to immediately generate carbenium ion. Again if the basic sites present are very strong we expect more Hoffmann elimination products. So these catalyst systems contain probably more number of medium and weak basic sites and weaker acid sites. Also in such cases it is expected that dehydration is accompanied by dehydrogenation.

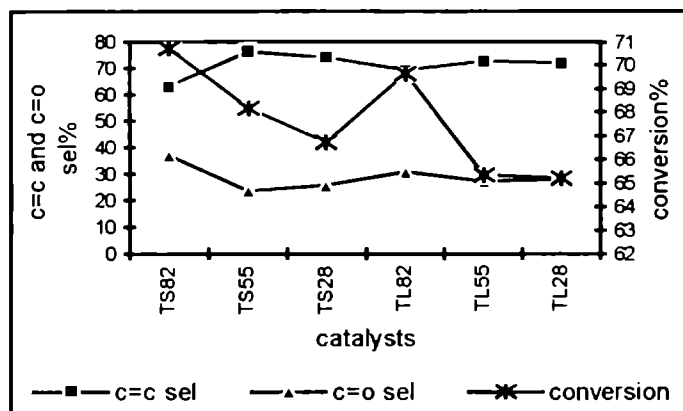


Fig. 3 18 Decomposition of ethanol over different catalysts
Reaction temp. 400 °C, Feed rate 4 ml/h, Catalyst weight 2.7 g

3.3 OXIDATIVE DEHYDROGENATION REACTIONS

3.3.1 Oxidative dehydrogenation of ethanol

In the oxidative dehydrogenation of ethanol, acetaldehyde, ethane and small amounts of carbon oxides and acetic acid are formed. The acetic acid is formed by the oxidation of acetaldehyde. The effect of temperature on product selectivity is presented in Figure 3 19. At lower temperature acetaldehyde selectivity is less, which increases with increase in temperature. But even at 450°C ethylene is the major product. So at higher ethanol conversions the undesirable dehydration predominates. Out of the four catalyst systems investigated the aldehyde selectivity follows the order TL82 > TS82 > TS55 >

TS28 (Fig. 3.20). This means that aldehyde selectivity decreases as the SnO_2 content decreases, with a concomitant increase in the selectivity of carbon oxides. SnO_2 containing systems are well known for their partial oxidation activity and rare earth oxides are considered as complete oxidation catalysts. This may be the reason why carbon oxide selectivity is increasing with increase in rare earth oxide content.

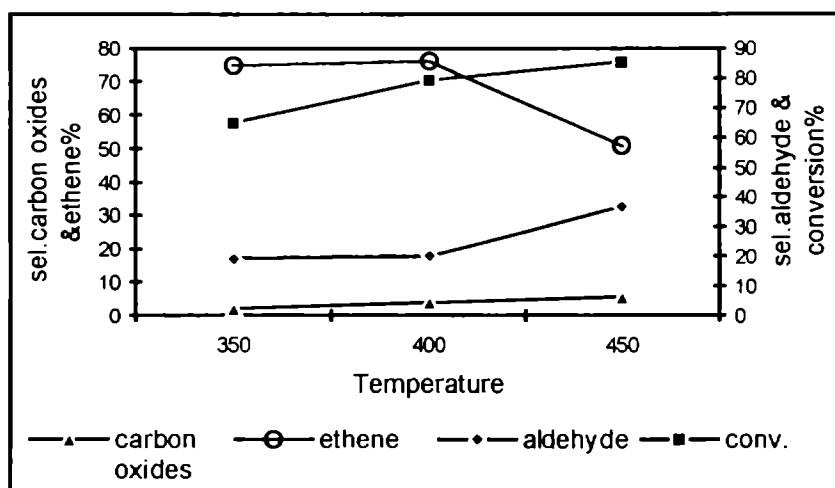


Figure 3.19 Effect of temperature on the product selectivity and conversion of ethanol

* Air was passed over the catalyst through a ethanol saturator maintained at 20°C.

Reaction conditions: Activation temp. 500 °C, Feed rate 4 ml/h, TOS 2 h, Catalyst (TL82) weight 2.7 g.

The effect of feed rate on the product selectivity is studied at 400 °C and 450 °C (fig 3.21). At 400 °C aldehyde selectivity increased tremendously from 19.80 % at a feed rate of 4 ml/h to 55.7 % at 10 ml/h. Similarly at 450 °C, aldehyde selectivity increased from 36.78 to 76.43 % when the feed rate is varied from 4 ml/h to 10 ml/h. The catalytic activity is tested for about 8

hours and it is found that aldehyde selectivity dropped considerably after 6 hours (Fig 3.22). The conversion also is affected during the same period. After 8 hours period catalyst turned slightly gray in colour. However its activity is regenerated after the calcination in air at the same temperature for about 24 hours. This is probably due to the reduction of Sn^{4+} sites during the redox cycle. The effect of catalyst activation temperature is shown in Table 3.8.

Aldehyde selectivity increases with rise in temperature and reaches a maximum at $650\text{ }^{\circ}\text{C}$ and then decreases. The activity of present systems are compared with that of single oxide components SnO_2 and La_2O_3 . It can be seen that SnO_2 shows better aldehyde selectivity but conversion is low. La_2O_3 produces a large amount of carbon oxides alongwith acetaldehyde (Table 3.9). The conversion to aldehyde is greater in the case of TL82, which follows the order $\text{TL82} > \text{SnO}_2 > \text{La}_2\text{O}_3$. This shows that mixed oxide is a better catalyst compared to their single oxide analogues.

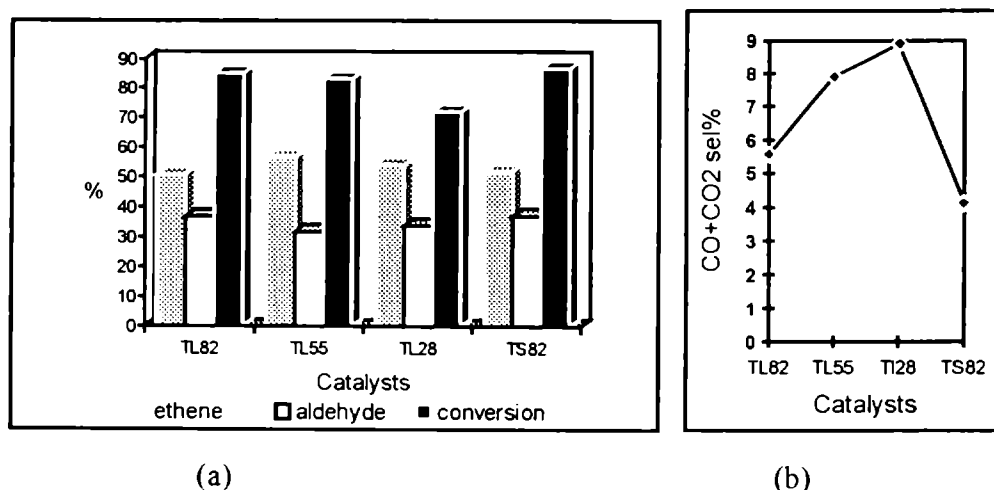
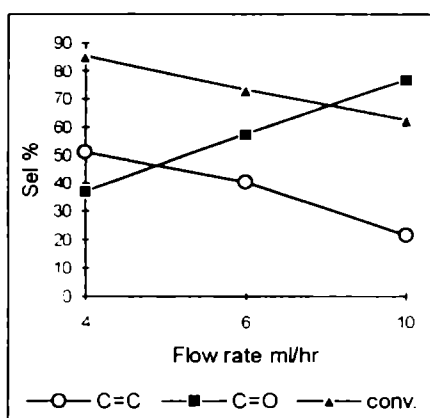
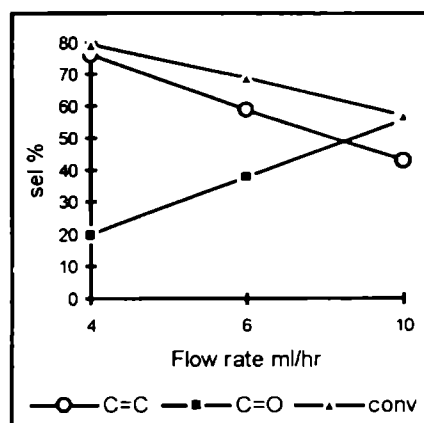


Figure 3.20: Effect of catalyst composition on the selectivity of products and conversion of ethanol

Reaction conditions: Activation temp. $500\text{ }^{\circ}\text{C}$, Reaction temp. $400\text{ }^{\circ}\text{C}$, Feed rate 4 ml/h , TOS 2 h , Catalyst (TL82) weight 2.7



(a)



(b)

Figure 3.21 Effect of feed rate on the product selectivity and ethanol conversion at (a) 400 °C and (b) 450 °C

Reaction conditions: Activation temp 500 °C, TOS 2 h, Catalyst (TL82) weight 2.7 g.

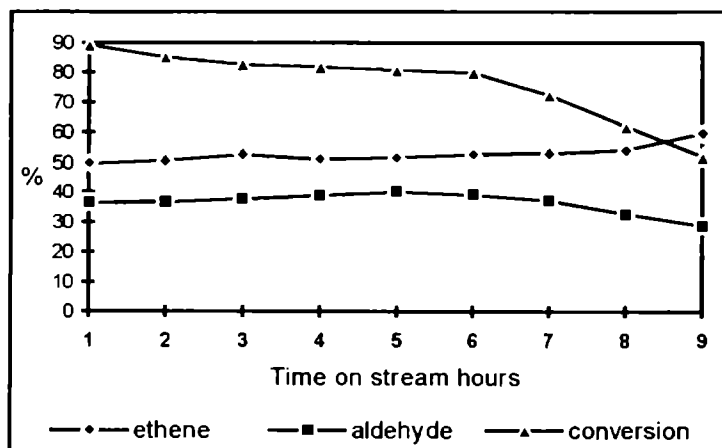


Figure 3.22 Effect of time on stream on the conversion of ethanol

Reaction conditions: Activation temp. 500 °C, Reaction temp. 450 °C, Feed rate 4 ml/h, Catalyst (TL82) weight 2.7 g.

Table 3.8 Effect of catalyst activation temperature on the product selectivity and ethanol conversion

Selectivity %	500 °C	600 °C	650 °C	700 °C
Carbon oxides	5.57	5.38	5.21	5.28
Ethene	50.70	47.8	45.81	45.21
Aldehyde	36.78	42.86	46.89	47.10
Conversion %	85.20	83.8	72.16	66.8

Reaction conditions: Reaction temp. 450 °C, Feed rate 4 ml/h, Catalyst (TL82) weight 2.7 g.

Table 3.9 Comparative study of TL82, SnO₂ and La₂O₃ in the oxidative dehydrogenation of ethanol

Selectivity %	TL82	SnO ₂	La ₂ O ₃
Carbon oxides	5.57	19.86	28.18
Ethene	50.70	5.18	18.02
Aldehyde	36.78	73.96	53.80
Conversion (%)	85.20	32.80	23.60
Conversion to aldehyde (%)	31.33	24.25	12.69

Reaction conditions: Activation temp. 500 °C, Reaction temp. 450 °C, Feed rate 4 ml/h, Catalyst weight 2.7 g.

3.3.2 Oxidative dehydrogenation of cyclohexanol

The effect of temperature on the conversion and product selectivity is presented in Fig.3.23. The product selectivity is not much influenced by temperature, even though conversion of cyclohexanol increased with increase in temperature. All the catalysts showed very good selectivity > 90 % towards cyclohexanone. In this case also TS82 and TL82 gave better cyclohexanone yield. The selectivity of cyclohexanone is in the order TL82 > TL28 > TL55. We have already found that the basicity of these catalysts also follows the same order. This means that not only the redox properties of the catalysts, their acid-base properties also influence the product selectivity in the oxidative dehydrogenation reaction of cyclohexanol. Furthermore the selectivity of cyclohexanone is more in the case of present systems than in the case of individual oxides SnO₂ and La₂O₃. So the combination of these components increases notably the activity and selectivity towards dehydrogenation product. The effect of water on the product selectivity is investigated over TL82 at 350 °C. Conversion of cyclohexanone is decreased after introducing more and more water (Table 3.11). The selectivity of cyclohexanone increases slightly from 90.1 to 96.3 %. Water is the by product of dehydration reaction and so it is expected that addition of water can suppress this side reaction and enhance the selectivity of dehydrogenation product. The selectivity of cyclohexanone increased slightly by changing the calcination temperature (Table 3.12), but conversion is affected badly due to the decrease in surface area at higher temperature. The effect of feed rate on the selectivity of cyclohexanone is shown in Table 3.13. The dehydrogenation activity increased slightly as the feed rate is increased.

Table 3.10 Effect of catalyst composition on the selectivity of cyclohexanone and cyclohexene

Selectivity %	TL82	TL55	TL28	TS82
Cyclohexene	6.20	8.80	7.90	6.30
Cyclohexanone	93.60	90.80	91.60	93.10
Conversion (%)	52.10	50.80	42.18	53.61

Reaction conditions. Activation temp. 500 °C, Reaction temp. 350 °C, Feed rate 4 ml/h, Catalyst weight 2.7 g.

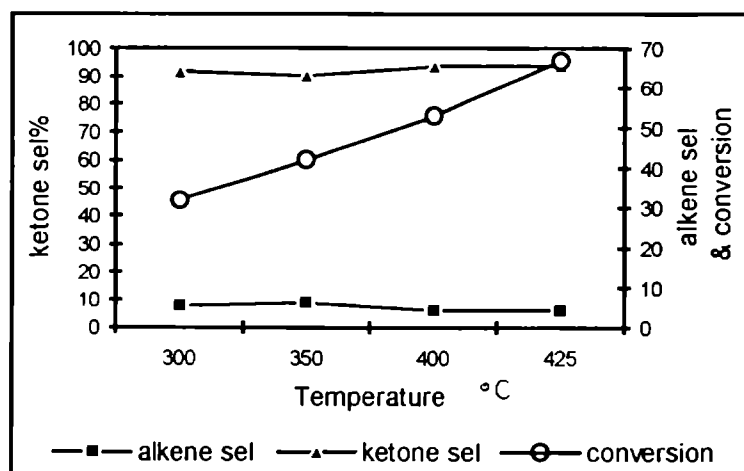


Figure 3.23 Effect of temperature on the product selectivity and cyclohexanol conversion

Reaction conditions: Activation temp. 500 °C, Feed rate 4 ml/h, Catalyst (TL82) weight 2.7 g.

Table 3.11 Effect of water on the product selectivity and conversion of cyclohexanol

Selectivity %	Water in the alcohol feed				
	0 %	5%	10%	15%	20%
Cyclohexene	8.90	6.40	5.90	3.80	3.70
Cyclohexanone	90.10	93.60	94.10	96.20	96.30
Conversion (%)	42.03	45.80	45.60	40.16	35.02

Reaction conditions: Activation temp. 500 °C, Feed rate 4 ml/h, Catalyst (TL82) weight 2.7 g.

Table 3.12 Effect of catalyst activation temperature

Selectivity %	500 °C	600 °C	650 °C	700 °C
Cyclohexene	8.90	5.20	3.10	3.00
Cyclohexanone	90.10	94.80	96.90	97.00
Conversion (%)	42.03	48.86	39.16	28.06

Reaction conditions: Activation temp. 500 °C, Feed rate 4 ml/h, Catalyst (TL82) weight 2.7 g.

Table 3.13 Effect of feed rate on the product selectivity and conversion of cyclohexanol

Selectivity %	4 ml/h	6 ml/h	10 ml/h
Cyclohexene	8.90	7.80	5.60
Cyclohexanone	90.10	92.02	94.40
Conversion (%)	42.03	37.18	32.20

3.3.3 Oxidative dehydrogenation of ethyl benzene and cyclohexane

The oxidative dehydrogenation of ethyl benzene and cyclohexane are studied at 425 °C in the presence of air. In the absence of air conversion is very low and moreover benzene and styrene are formed in almost equal amounts. In the presence of air styrene is the main product. The same type of observations are made in the case of cyclohexane also. Out of the four catalyst systems studied TS82 showed better conversion and styrene yield. Conversion of ethyl benzene follows the order TS82 > TS55 > TS28. Considerable amount of carbon oxides are formed in the case of TS28 by the complete oxidation of ethylbenzene. Single oxides SnO₂ and La₂O₃ showed poor yield. According to Tagawa *et al* the acid sites of H₀ between 1.5 and -5.6 are proven to be the active sites to adsorb ethyl benzene reversibly, whose oxidation on the otherhand occurs on the basic sites of pK_a between 17.2 and 26.5 [35]. The tendency to have maximum activity suggests the co-operative effect of the acid base properties of the catalysts which varies with catalyst composition. However, in the present systems no acid sites or basic sites in the aforementioned ranges are observed. So it must be noted that apart from the acid base properties of catalysts, their redox properties also influence the catalytic activity to a greater extent. In this reaction, the catalytic activity

increases as a function of SnO₂ content. Hence Sn⁴⁺ sites may be the active sites in the oxidative dehydrogenation reaction. The addition of rare earth oxide increases the surface area and amorphous nature of the catalysts. These factors also may contribute towards increase in catalytic activity. Moreover the oxygen in the rare earth oxide lattice are highly mobile.

Table 3.14 Effect of catalyst composition on the selectivity of styrene

Product	TS82	TS55	TS28	TL82	SnO ₂	La ₂ O ₃
distribution %						
Benzene	4.49	5.40	1.19	3.75	0.31	0.18
Ethylbenzene	70.41	81.95	85.95	72.12	94.40	96.10
Styrene	23.68	9.42	5.00	22.82	4.90	3.10
Carbon oxides	1.42	3.23	7.86	1.31	0.39	0.72
Conversion (%)	29.59	18.05	14.05	27.88	5.60	3.90

Reaction conditions: Activation temp. 500 °C, Reaction temp. 450 °C Feed rate 4 ml/h, Catalyst weight 2.7 g.

Table 3.15 Reaction in the absence of air

Product distribution %	Absence of air	Presence of air
Benzene	3.38	4.49
Ethylbenzene	92.31	70.41
Styrene	3.23	23.08
Carbon oxides	1.08	1.42
Conversion (%)	7.69	29.59

Reaction conditions: Activation temp. 500 °C, Reaction temp. 450 °C, Feed rate 4 ml/h, Catalyst (TS82) weight 2.7 g.

Table 3.16 Oxidative dehydrogenation of cyclohexane over TL82

Product distribution %	Absence of air	Presence of air
Benzene	0.66	4.80
Cyclohexene	3.83	14.20
Cyclohexane	95.13	78.50
Others	0.38	2.50
Conversion (%)	4.87	21.50

Reaction conditions: Activation temp. 500 °C, Reaction temp. 450 °C, Feed rate 4 ml/h, Catalyst (TL82) weight 2.7 g.

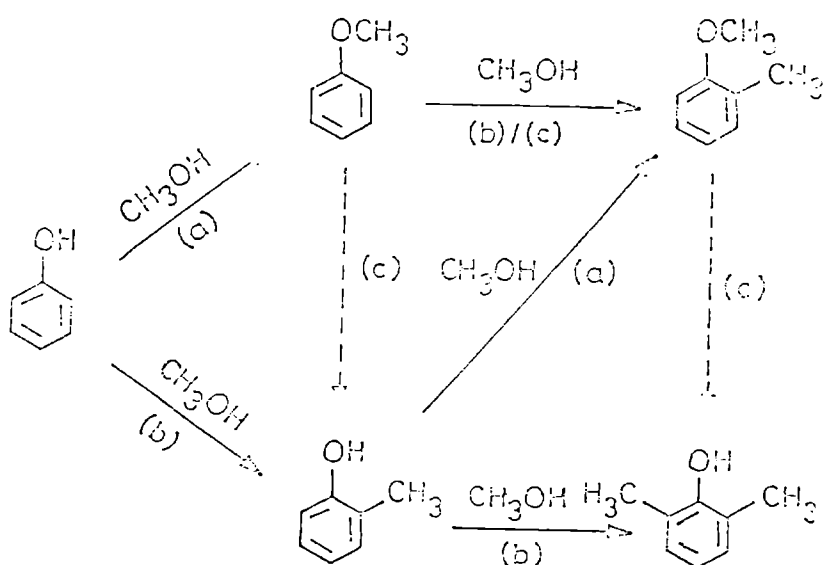
3.4 ALKYLATION OF PHENOL, ANISOLE AND ANILINE WITH METHANOL

3.4.1 Alkylation of Phenol with methanol

Conversion and selectivities of different products in the alkylation of phenol with methanol over Sn-La and Sn-Sm binary mixed oxides of varying composition are shown in Table 3 17. It can be seen that all the catalysts give very little O-alkylated products and hence the C-alkylation takes place predominantly over these catalyst systems. The selectivity of o-cresol and 2,6-xyleneol, which are the main products varies with the catalyst composition. Maximum 2,6-xyleneol selectivity is observed in the case of TS55 and TL55 catalysts. Moreover some amount of trimethyl phenols are also formed over these catalysts. In the case of TS82 and TL82 o-cresol is the main product, whereas TS28 and TL28 afforded o-cresol and 2,6-xyleneol in nearly equal amounts. The conversion of phenol over these two catalysts is lesser, which is due to lower surface area of these samples. It is well known that the selectivity of products depends on the acid-base properties of the catalysts [36]. Oxide catalysts are reported to be more selective for the synthesis of 2,6-xyleneol and o-cresol [37].

At low temperatures (250 °C) anisole and o-cresol are formed at a phenol conversion of only 2.64%, anisole being the main product (selectivity 85.64%). It is reported that the activation energy of O-alkylation is lower than that of C-alkylation [38]. As the temperature is increased o-cresol selectivity is decreased while the selectivity of 2,6-xyleneol is enhanced, alongwith small amounts of trimethyl phenol. In the temperature range 300-425 °C, the

selectivity of anisole remained practically constant. There can be two important pathways for the formation of 2,6-xylenol and o-cresol. First one is through the formation of anisole formed initially, which further react with methanol to give 2,6-xylenol via methylanisole isomerisation. Second one is direct C-alkylation in which o-cresol formed initially react again with one mole of methanol to give 2,6-xylenol.



(a) O-alkylation (b) C-alkylation (c) Inter molecular reaction

Fig. 3.24. Pathways of phenol alkylation.

The surface acid base properties of the catalysts determine the reaction mechanism and reaction pathway. It is reported that acidic catalysts such as silica-alumina or condensed phosphoric acid promote the O-alkylation reactions giving phenyl ethers while basic catalysts such as MgO or ZnO-Fe₂O₃ promote the direct alkylation giving o-cresol without passing through the phenyl ether intermediate [39,40]. The ortho selectivity of the catalysts (formation of o-cresol, 2,6-xylenol, 2-methylanisole) can be attributed to the nature of adsorption of phenol over the catalyst surface. As described by Tanabe, the phenolate ion is adsorbed such that the ortho position is very near to the catalyst surface in the case of basic catalysts such as MgO, hence the ortho position can be methylated. However the interaction of acidic catalysts are different which influence the electron current around the benzene ring such that the aromatic ring lie parallel to the catalyst surface.

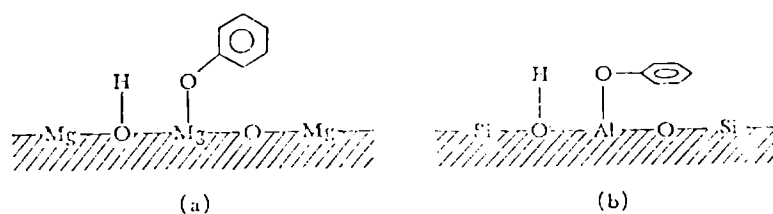


Fig. 3.25. Adsorption of phenol on (a) MgO and (b) Al₂O₃.

So the methylation can take place at all possible positions. This is actually observed in the case of acidic catalysts. It has been found that catalysts with strong acid sites favour O-alkylation while weak acid sites or strong basic sites favour C-alkylation [42]. In the present case to understand the mechanism by which the alkylation takes place we carried out the following experiments. We found that at 350 °C o-cresol and 2,6-xylenol are the main products. If the reaction proceeds via anisole intermediate at low phenol conversions, anisole must be formed. So we increased the feed rate (decreased the contact time) step by step. But even at low contact time (higher feed rate) only a small amount of anisole is formed. The selectivity of anisole remained constant with increase in phenol conversion, while the yield of o-cresol reached a maximum, then decreased with consequent increase in the yield of 2,6-xylenol. These results indicate that the o-cresol undergo secondary reactions to give 2,6-xylenol and trimethyl phenol to a greater extent. From these results it is concluded that the formation of anisole does not occur appreciably over these catalysts, and hence the alkylation of phenol over these catalysts proceeds through direct C-alkylation without the intervention of anisole as the intermediate. When a mixture of o-cresol and methanol in 1:7 molar ratio was passed over these catalysts a large amount of 2,6-xylenol is formed.

When a mixture of anisole and methanol were passed over these catalysts 2,6-xylenol 80.52 %, cresol 8.59 %, phenol 9.2 % and TMP 1.43 % are formed at a conversion of 27.21 %. This means that the conversion of anisole to 2,6-xylenol is possible over these catalysts. When 2-methylanisole alone was passed over these catalysts at the same temperature and it can be seen that 2,6-xylenol is the main product alongwith small amounts of cresol and TMP. This supports the above mechanism for the formation of 2,6-xylenol from anisole.

We tried to correlate the acid base properties of the catalysts with dehydration and dehydrogenation activity employing cyclohexanol decomposition as a test reaction. The selectivity of cyclohexene is found to be in the order TL55 > TL28 > TL82 and TS55 > TS28 > TS82. So TS55 and TL55 systems are more acidic and TS82 and TL82 systems are least acidic. Now the product selectivity in the alkylation of phenol with methanol can be easily correlated with the acid base properties of the catalysts. The higher selectivity of secondary alkylated product, 2,6-xyleneol in the case of TS55 and TL55 must be due to its higher acidity. Whereas over less acidic systems TS82 and TL82 o-cresol is the main product. In the decomposition of cyclohexanol, dehydrogenation was the main reaction. However, in the reaction of isopropanol and isobutanol selectivity of dehydration products was high. Only weak acid sites are required for the dehydration of isopropanol and isobutanol. Stronger acid sites are needed for the dehydration of cyclohexanol. Qualitatively it can be concluded that most of the acid sites present on these catalysts are weak acid sites. From titration methods it is found that comparatively strong basic sites are also present on these systems. These observations are supported by the observation of Benzouhanava *et al* that the weak acid sites or strong basic sites favour C-alkylation [43]. Moreover Tilmat-Muy *et al* and Marzaenski *et al* claimed that weak acid sites favour C-alkylation [44,45].

Table 3.18 Effect of catalyst composition in the alkylation of phenol with methanol.

Product distribution (wt%)	TS82	TS55	TS28	TL82	TL55	TL28
Anisole	0.15	0.31	0.18	0.15	0.30	0.17
Phenol	23.86	23.21	40.00	24.69	24.39	43.82
o-Cresol	45.61	22.74	29.96	43.25	26.97	26.75
2,6-Xylenol	27.64	41.79	27.26	29.14	41.84	26.57
TMP*	2.70	9.05	1.43	2.45	6.50	1.58
Others	0.04	2.90	1.17	0.32	nil	1.11
Conversion	76.14	76.79	60	75.31	75.61	56.18
Sel.C-alkylation	99.81	99.60	99.70	99.80	99.60	99.67
Sel.o-cresol	59.90	29.61	49.93	57.42	35.66	47.61
Sel. 2,6-xylenol	36.30	54.42	45.43	38.69	55.33	47.29

* Trimethylphenol

Calcination temp. 500 °C, Reaction temp. 350 °C, Molar ratio (Phenol methanol) 1:6, Feed rate 4 ml/h, TOS 1 h, Catalyst. 3 g.

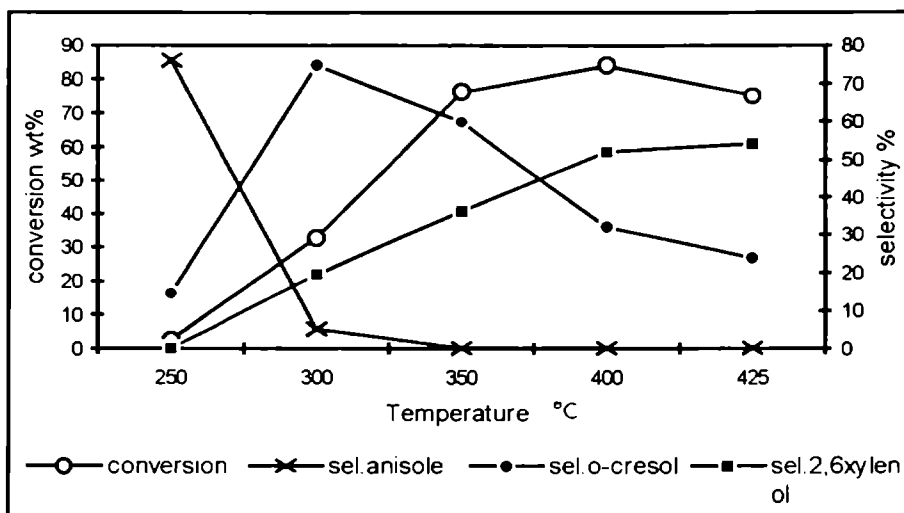


Figure 3.26 Effect of temperature in the alkylation of phenol with methanol
 Calcination temp. 500 °C, Molar ratio (Phenol : methanol) 1:6, Feed rate. 4 ml/h, Catalyst (TS82) 3 g.

Table 3.19 Effect of Feed rate on the selectivity of products in the alkylation of phenol with methanol.

Product	4 ml/h	6 ml/h	8 ml/h	10 ml/h
distribution %				
Anisole	0.14	0.19	0.20	0.21
Phenol	23.86	38.69	49.23	69.90
o-Cresol	45.61	43.44	39.14	24.20
2,6-Xylenol	27.64	16.74	10.88	5.69
TMP	2.70	0.91	0.21	nil
Conversion	76.14	61.31	49.23	30.1
Sel.C-alkylation	99.81	99.76	99.60	99.31
Sel.o-cresol	59.90	70.85	79.50	80.39
Sel.2,6-xylenol	36.30	27.30	22.10	18.90

Calcination temp. 500 °C, Reaction temp. 350 °C, Molar ratio (Phenol methanol) 1:6, TOS 1 h, Catalyst TS82 3 g

Table 3.20 Self reactions of anisole, methylanisole and alkylation of anisole and o-cresol with methanol

Product distribution wt%	Anisole	Anisole+ methanol	oCresol+ methanol	Methyl anisole
Anisole	90.61	72.79	nil	nil
Phenol	6.50	1.02	nil	nil
methylanisole	nil	1.50	2.70	42.50
Cresol	3.19	2.34	4.89	2.80
2,6-Xylenol	0.30	21.91	88.28	53.20
TMP	nil	0.39	4.11	1.20
Conversion wt%	9.39	27.21	95.20	57.50
Sel.phenol	67.07	9.20	nil	nil
Sel.cresol	33.97	8.59	nil	4.86
Sel.2,6-xylenol	3.19	80.52	92.93	92.52

Calcination temp. 500 °C, Reaction temp. 350 °C, Molar ratio (anisole/o-cresol methanol) 1:6 TOS. 1 h, Catalyst TS82. 3 g.

3.4.2 Alkylation of anisole with methanol

In order to choose an optimum feed mix, the alkylation reactions were carried out at 380 °C taking several anisole to methanol molar ratios. In the figure the selectivity of products and conversion are plotted against molar ratios (Figure 3.28). We have selected a molar ratio of 1:6 for further study as the conversion and selectivity were better

The product distribution and selectivity to 2,6-xyleneol over Sn-La and Sn-Sm binary mixed oxides of different compositions are presented in Table 3.20. It can be seen that 2,6-xyleneol is the main product in all cases (> 80%). Selectivity of products is not much influenced by catalyst composition. In all cases the amount of dealkylated product, phenol is very less. The lower activity in the case of TL28 and TS28 catalysts is attributed to their low surface area. We compared the activity of the present catalyst systems with two acidic catalysts H-beta zeolite and silica-alumina and a basic catalyst, Mg-Al hydrotalcite. The results are summarised in Table 3.21. All these catalysts gave poor selectivity to 2,6-xyleneol under same experimental conditions. Mg-Al hydrotalcite afforded 2,6-xyleneol with a selectivity of 58.4%, along with other products like methylanisole and o-cresol [46]. However, the dealkylation is very less in this case compared to silica-alumina and H-beta zeolite. Dealkylation must be due to the presence of strong acid sites present in these catalysts.

The effect of temperature on the conversion and selectivity of 2,6-xyleneol was studied in the temperature range 350-420 °C. Anisole conversion increased with temperature and also an increase in the selectivity of 2,6-xyleneol is observed. Moreover the selectivity of methylanisole decreases with increase in temperature and are not detected above 380 °C. This suggests that

the methylanisole as soon as it is formed is isomerised to xylenol. To understand the mechanism in detail, we conducted the reaction of methylanisole alone at different temperature and contact time. As the temperature increases the conversion to xylenol increases. Conversion to 2,6-xylenol is further increased by increasing the contact time of the feed. If the reaction takes place via the isomerisation of methylanisole the effect of feed rate will give an idea about the mechanism of the reaction. When we changed the feed rate from 4 ml/h to 10 ml/h (Figure 3.29), it is found that the selectivity of methylanisole increases with increase in feed rate with a concomitant decrease in the selectivity of 2,6-xylenol. As expected the conversion of methylanisole dropped down at higher feed rates. Based on the above results the alkylation of anisole to 2,6-xylenol takes place in two steps, (i). Formation of methylanisole and (ii) Isomerisation of methylanisole to 2,6-xylenol.

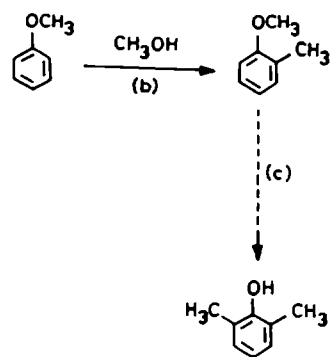


Fig. 3.27 Pathway of anisole alkylation.

Table 3.20: Alkylation of anisole with methanol over Sn-La and Sn-Sm mixed oxides

Product	TS82	TS55	TS28	TL82	TL55	TL28
distribution %						
Anisole	45.6	43.2	52.8	46.1	44.8	53.8
Phenol	1.2	1.3	1.2	1.1	1.4	1.2
methylanisole	2.30	2.31	1.10	2.09	0.80	1.30
o-Cresol	2.90	3.80	3.90	3.60	3.70	3.80
2,6-Xylenol	44.80	46.38	40.10	44.61	45.80	39.80
TMP	2.20	3.01	0.90	2.50	3.50	0.70
Conversion %	54.40	56.80	47.20	53.90	55.20	46.1
Sel.xylenol %	82.35	81.65	84.95	82.76	82.97	86.33

Calcination temp. 500 °C, Reaction temp. 380 °C Molar ratio (Anisole methanol) 1:6, TOS 1 h, Catalyst TS82. 3 g.

Table 3.21 Alkylation of anisole with methanol over H-BETA zeolite, Silica-alumina, Mg-Al hydrotalcite

Product distribution %	H-Beta zeolite	Silica-alumina	Mg-Al hydrotalcite
Anisole	12.88	9.81	33.46
Phenol	37.96	40.80	2.80
methylanisole	4.80	4.10	10.91
Cresols	16.80	12.80	13.96
Xylenols	14.90	18.90	38.87
Poly alkylates	1.80	10.31	nil
Others	10.86	3.28	nil
conversion wt%	87.12	90.19	66.54
sel.xylenols	17.10	20.95	58.41

Calcination temp. 500 °C, Reaction temp. 380 °C Molar ratio (Anisole:methanol) 1:6, TOS 1 h, Catalyst 3 g

Table 3.21 Alkylation of anisole with methanol- Effect of temperature on the product distribution

Product	350 °C	380 °C	400 °C	420 °C
distributions %				
Anisole	56.80	43.20	34.80	16.38
Phenol	0.20	1.30	2.60	2.61
Me-anisole	9.82	2.31	nil	nil
Cresol	3.61	3.80	3.71	3.52
Xylenol	27.61	46.38	53.79	70.29
TMP	1.80	3.01	5.10	7.20
Conversion %	43.20	56.80	65.20	83.62
Sel.xylenol %	63.91	81.65	82.5	84.05

Calcination temp. 500 °C, Molar ratio (Anisole : methanol) 1:6, Feed rate 4 ml/h, TOS 1 h, Catalyst TS82. 3 g.

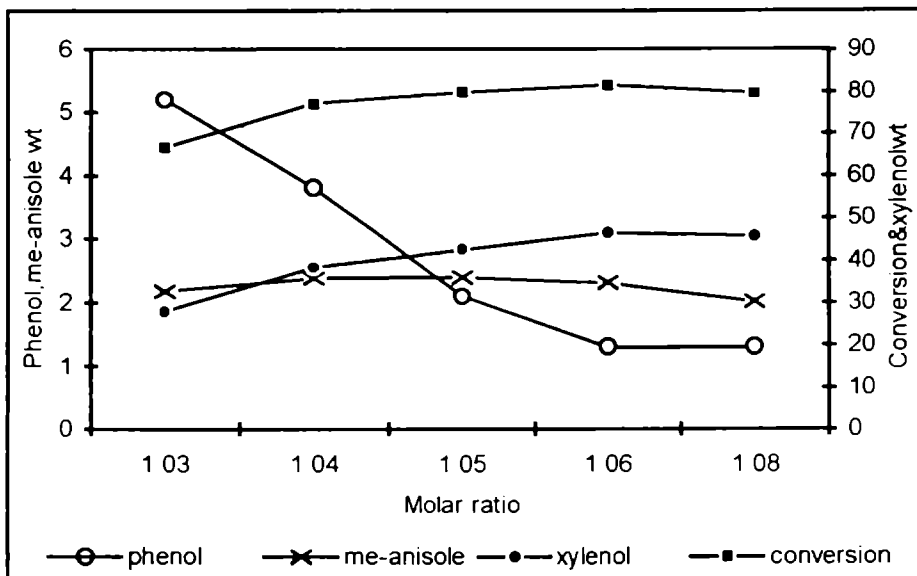


Figure 3.28 Effect of anisole-methanol molar ratio on product distribution
 Calcination temp. 500 °C, Reaction temp. 380 °C, Feed rate 4 ml/h, TOS 1 h,
 Catalyst TS82. 3 g

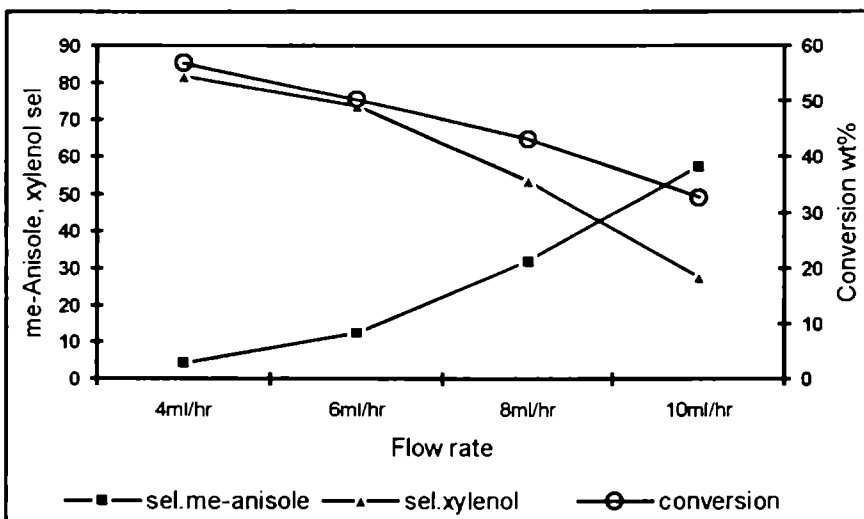


Figure 3.29 Effect of feed rate on the selectivity of methylanisole and xylenol
 Calcination temp. 500 °C, Reaction temp. 380 °C, Molar ratio (Anisole-methanol) 1:6, TOS 1 h, Catalyst TS82. 3 g

3.4.3 Alkylation of aniline with methanol

3.4.3 (a) Effect of aniline-methanol molar ratio:---

The optimum feed mix molar ratio is selected by carrying out the reactions by taking aniline-methanol premixed in various mole ratios at 350 °C. From the product analysis only two products are detected N-methylaniline (NMA) and N,N-dimethylaniline (NNDMA), in which N-methyl aniline selectivity is greater than 95%. Selectivity of products and aniline conversion are plotted against various aniline-methanol molar ratios in Figure 3.30. Aniline-methanol molar ratio of 1:7 is chosen for further study (conversion 62.3%).

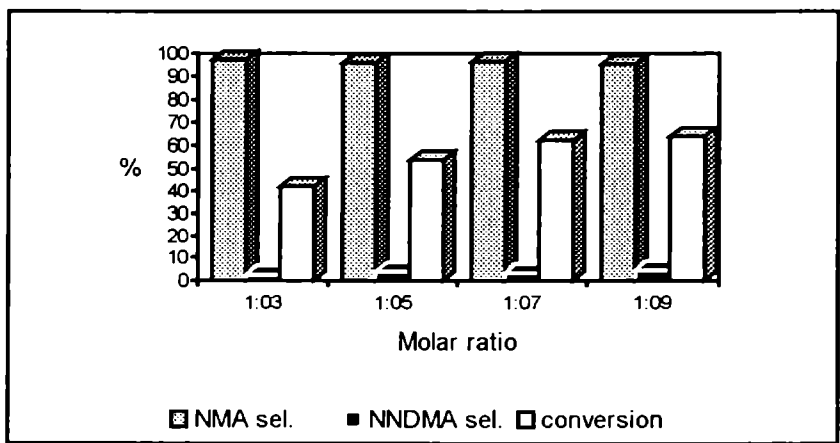


Figure 3.30: Effect of molar ratio on the product selectivity and conversion of aniline

Calcination temp. 500 °C, Reaction temp. 350 °C, Feed rate 4 ml/h, TOS 1 h, Catalyst TS82. 3 g.

NMA. N-methylaniline and NNDMA. N,N-dimethylaniline.

3.4.3 (b) Effect of temperature:---

The effect of temperature on the selectivity of products and aniline conversion is investigated in the temperature range 300-400 °C employing 1:7 aniline methanol as the feed and TS82 as catalyst at a feed rate of 4 ml/h (Fig. 3.31). It can be seen that maximum NMA selectivity is obtained at 350 °C and as the temperature increases more NNDMA is formed. Conversion of aniline increases as the temperature is increased from 300-400 °C. However, at 400 °C no other products are detected.

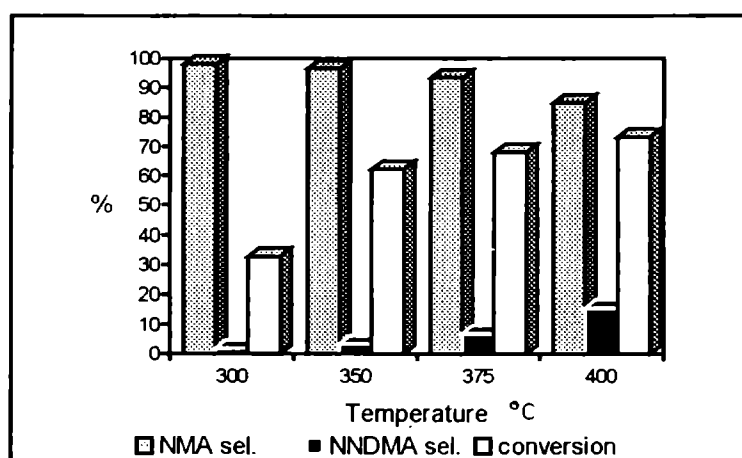


Figure 3.31 Effect of temperature on the selectivity of products

Calcination temp. 500 °C, Reaction temp. 350 °C, Molar ratio (Aniline methanol) 1:7, Feed rate 4 ml/h, TOS 1 h, Catalyst TS82. 3 g.

3.4.3 (c) Effect of feed rate:---

To investigate the effect of contact time on the selectivity of products and conversion of aniline, a mixture of aniline and methanol in the molar ratio 1:7, was passed at different feed rates over TS82 at 350 °C (Fig. 3.32). At a feed

rate of 10 ml/h, 99.6% NMA selectivity is obtained (aniline conversion 29.6%)
 At higher feed rates contact time is low and hence subsequent alkylation of NMA is difficult. The conversion of aniline decreases as expected at higher feed rates.

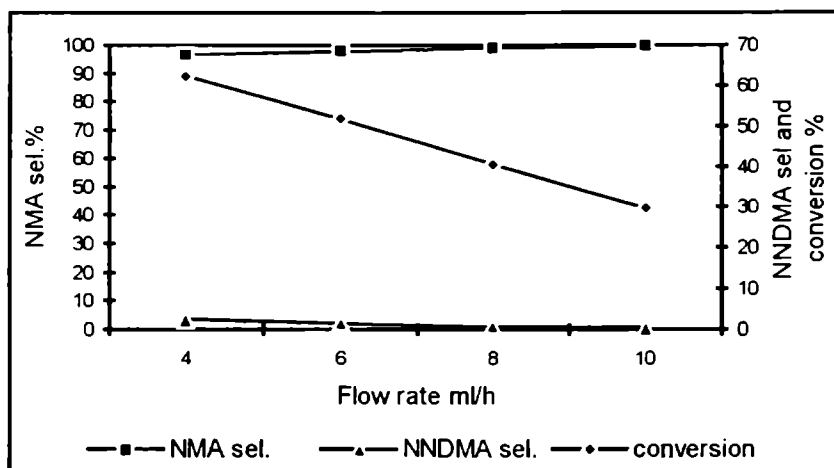


Figure 3.32 Effect of feed rate on the selectivity of products

Calcination temp. 500 °C, Reaction temp. 350 °C, Molar ratio (Aniline methanol) 1:7, TOS 1 h, Catalyst TS82. 3 g.

3.4.3(d) Effect of catalyst composition on the selectivity of products:---

The product selectivity and aniline conversion as a function of catalyst composition is presented in the Figure 3.33. The selectivity of NMA decreases in the order TL82>TL28>TL55 and TS82 > TS28 > TS55. In the case of TS55 and TL55 an appreciable amount of dialkylated product is formed. The maximum NMA selectivity is found in the case of TL82. The lower aniline conversion in the case of TL28 and TS28 must be due to their low surface area. The selectivity of products (NMA and NNDMA) can be correlated with the dehydration or dehydrogenating activity in the decomposition of cyclohexanol (Fig.3.36). The selectivity of dehydrogenation products are in the

order TL82 > TL28 > TL55 which correlates with the NNDMA selectivity TS55 and TL55 systems which are more acidic give more NNDMA. This can be accounted by the presence of relatively stronger acid sites, which might be necessary for the consecutive methylation of aniline in the formation of N,N-dimethylaniline. As the basicity increases NNDMA selectivity decreases with a concomitant increase in the selectivity of NMA. The mechanism of aniline methylation is shown in Figure 3.37, which involves simultaneous participation of both acid and basic sites [47]. However, the overall basicity must be determining the product selectivity. The higher selectivity of NMA may be due to the fact that the removal of hydrogen from N-methylaniline and approach of methyl group to the N-atom in a concerted way possesses a high order of steric hindrance [48]. However, at higher temperatures dialkylation may occur provided the desorption of NMA is not fast.

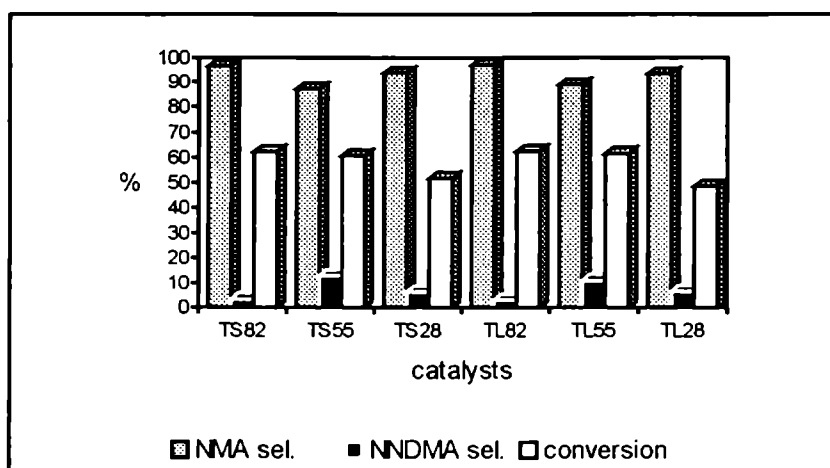


Figure 3.33 Effect of catalyst composition on the selectivity of products and aniline conversion

Calcination temp. 500 °C, Reaction temp. 350 °C, Molar ratio (Aniline methanol) 1:7, Feed rate 4 ml/h, TOS 1 h, Catalyst TS82. 3 g.

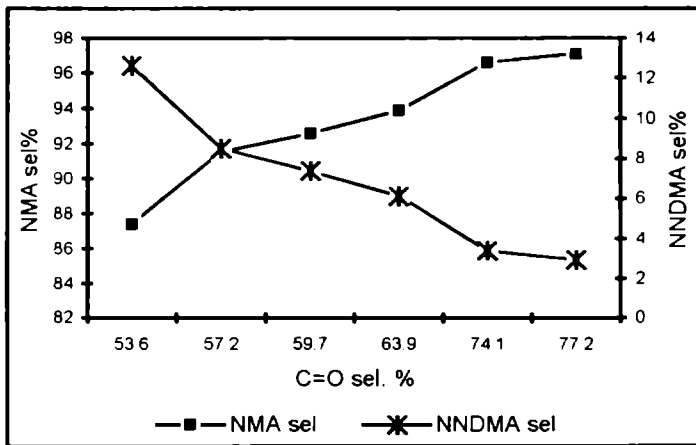


Figure 3.36 (a) Correlation between C=O selectivity in cyclohexanol decomposition and selectivity of NMA and NNDMA

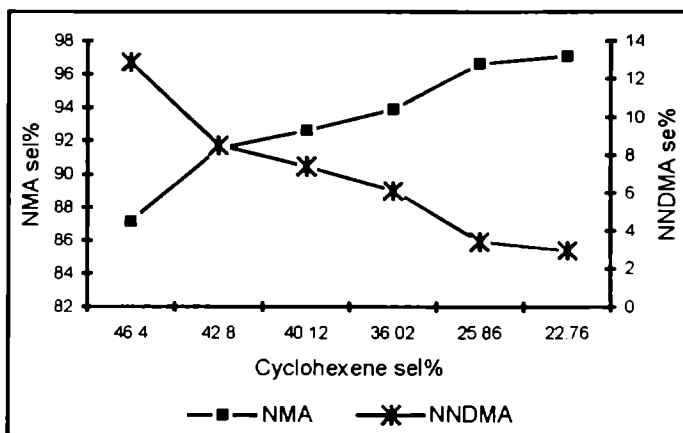


Figure 3.36 (b). Correlation between C=C selectivity in cyclohexanol decomposition and selectivity of NMA and NNDMA.

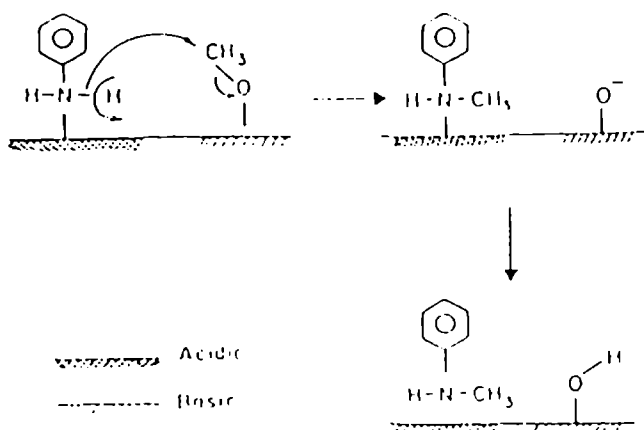


Fig. 3.37 Mechanism of aniline alkylation.

3.4.3 (e) Time on stream study of the catalysts

The activity of the catalyst for a 5 hours period is tested to see whether any deactivation is taking place. The catalysts TL82 and TS82 deactivate very slowly however faster deactivation is observed in the case of TS55 and TL28.

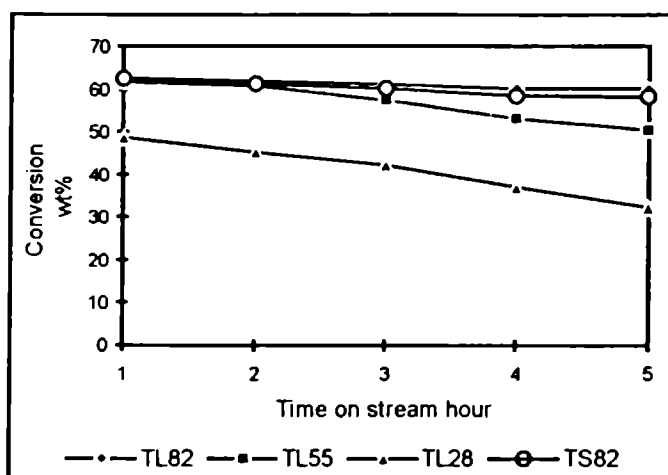


Figure 3.38 Time on stream study of the catalysts in the methylation of aniline

3.4.5 TRANSFER HYDROGENATION OF NITROBENZENE USING ISOPROPANOL AS A HYDROGEN DONOR

A wide variety of homogenous as well as heterogeneous catalyst systems in combination with different hydrogen donors have been employed for selective functional group reductions [49]. Reduction of nitrobenzene can afford nitrobenzene[50], phenyl hydroxylamine [51], p-aminophenol [52], azobenzene [53], azoxybenzene [54], hydrazobenzene [55] or aniline [56] depending on the reaction conditions.

Aniline and azoxybenzene are the major products of this reaction. The selectivity of these products is greatly influenced by different reaction parameters. Aniline is the end hydrogenation product of this reaction whereas azoxybenzene is resulted from the partial reduction of nitro group. In the reduction of nitro group the oxygen is progressively being replaced by hydrogen. The reaction is highly exothermic, the heat of reaction being estimated to be 130 kcal/mol [57]. The mechanism of formation of different products is shown in Figure 3.39. The reaction proceeds via the intermediates as proposed by Haber from his work on the electrochemical reduction of nitrobenzene [58]. The final product aniline can be formed either from the partially hydrogenated product, N-phenylhydroxylamine, or from azobenzene or hydrazobenzene by reductive cleavage of these molecules. However when separately tested, they failed to undergo reductive cleavage to aniline under identical conditions over these catalysts. Hence formation of aniline via azobenzene is excluded. Azoxybenzene found in the reaction mixture, which might result from nitrosobenzene and N-phenylhydroxylamine further confirm the formation of this intermediates. Moreover N-phenylhydroxylamine is completely converted to aniline over these catalysts.

Taking into account the above conclusions a plausible reaction pathway is depicted in Figure 3 40, for the formation of aniline and azoxybenzene.

The activity of these catalyst towards transfer hydrogenation is evidently due to their bifunctional behaviour. Isopropanol is adsorbed on the basic site and the substrate on the adjacent acid site and finally the hydrogen is transferred as hydride on to the substrate to be reduced [59].

The product distribution is greatly affected by the catalyst concentration (Figure 3 41). At lower catalyst concentration (4%) nitrobenzene conversion is complete. Selectivity of azoxybenzene is maximum at lower catalyst concentrations whereas aniline selectivity is maximum at higher catalyst concentrations (>10%). When the catalyst concentration in the reaction medium decreases the complete reduction of nitro group become less probable leading to more partial reduction products like nitrosobenzene and N-phenylhydroxylamine which condense together to form azoxybenzene. However, at higher catalyst concentration transfer of hydrogen becomes more probable resulting in the formation of aniline selectively. The catalyst concentration is varied between 4 to 20 % by weight of the substrate. The catalytic activity of different catalysts follows the order TS82 >TS28>TS55 and TL82 > TL28 > TL55 (Fig 3 42). The observed order of catalytic activity can be correlated with the dehydrogenation activity of different catalysts in alcohol decomposition reactions which in turn is directly related to their basicity

In the beginning of the reaction a small amount of nitrosobenzene is detected. Maximum aniline selectivity is found during the first hour of the reaction. Then it decreased steadily giving more partial reduction products as indicated by the increase in amount of azoxybenzene. Other products like azobenzene, hydrazobenzene etc., are absent in the final stages of the reaction.

An optimum catalyst concentration (10%) is chosen for observing changes in the selectivity and conversion during five hour reaction period. At lower catalyst concentrations products resulting from the partial reduction predominates. However when sufficient amount of catalyst is used these side products are minimised even after five hour reaction time. Even at low catalyst concentrations about 80% of the reaction is complete in just one hour. There after the nitrobenzene conversion increases slowly taking about three more hours for the complete conversion. This is evidently due to other competitive reactions following the partial reduction of nitrobenzene. Use of other hydrogen donors like hydrazine and ammonium formate instead of isopropanol revealed that they are less effective as compared to the latter (Table 3.22). Conversion as well as the selectivity of the products are notably influenced by the use of different hydrogen donors. Employing ammonium formate as hydrogen donor enhanced the selectivity of azobenzene at about 15% nitrobenzene conversion; only traces of aniline being detected. When hydrazine is used a mixture of all the products are obtained, showing good selectivity towards azobenzene (62%). So in the case of mild hydrogen donors partial reductions are prominent than the complete reduction to aniline.

The addition of varying quantities of DMSO affected the conversion as well as the product selectivity (Table 3.23). DMSO concentration varied between 20 to 60% by the weight of nitrobenzene. Nitrobenzene conversion is unaffected even after the addition of, 40% by weight of DMSO. However, further increase in its concentration reduced the nitrobenzene to about 12%. Selectivity of aniline is decreased by the addition of increasing amount of inhibitor however a slight increase in aniline selectivity is observed at higher (60%) DMSO concentration. Decrease in aniline selectivity is accompanied by an increase in selectivity of azoxybenzene. An examination of effect of reaction time indicate that at lower nitrobenzene conversion (5%) azobenzene is the main product followed by azoxybenzene and small quantities of nitrobenzene

Table. 3.22.

Effect of different hydrogen donors

Hydrogen donors	Conversion (%)	Selectivity (%)		
		Aniline	Azobenzene	Azoxybenzene
IPA	100	93.63		5.80
Hydrazine hydrate *	11.49	10.69	61.59	27.56
Ammonium formate *	14.87	0.200	78.36	27.31

* Traces of phenylhydroxylamine detected

Reaction conditions: catalyst = TL 82 (100 mg). temperature = 353 K. Reaction time = 5h solvent = IPA. reactant = Nitrobenzene (500 mg)

Table. 3.33.

Effect of dimethylsulphoxide as an inhibitor

Amount of DMSO added (gm)	Conversion (%)	Selectivity (%)		
		Aniline	Azobenzene	Azoxybenzene
0.1	100	52.75		47.24
0.2	100	40.56	3.21	56.20
0.3	87.42	44.30	3.30	49.04
No inhibitor	100	93.63		5.80

Reaction conditions ; catalyst = TL 82 (100 mg). temperature = 353 K , reaction time = 5h. Solvent = IPA, reactant = Nitrobenzene (500 mg)

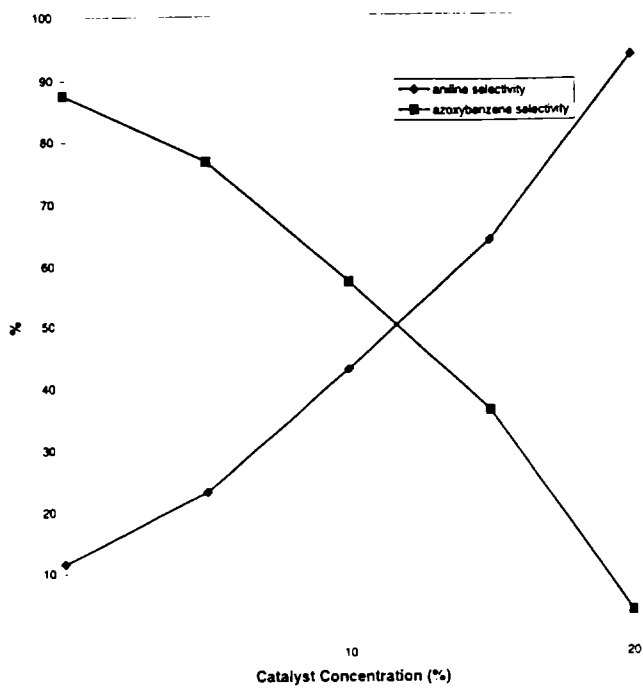


Fig. 3 41 Effect of catalyst concentration on the product selectivity

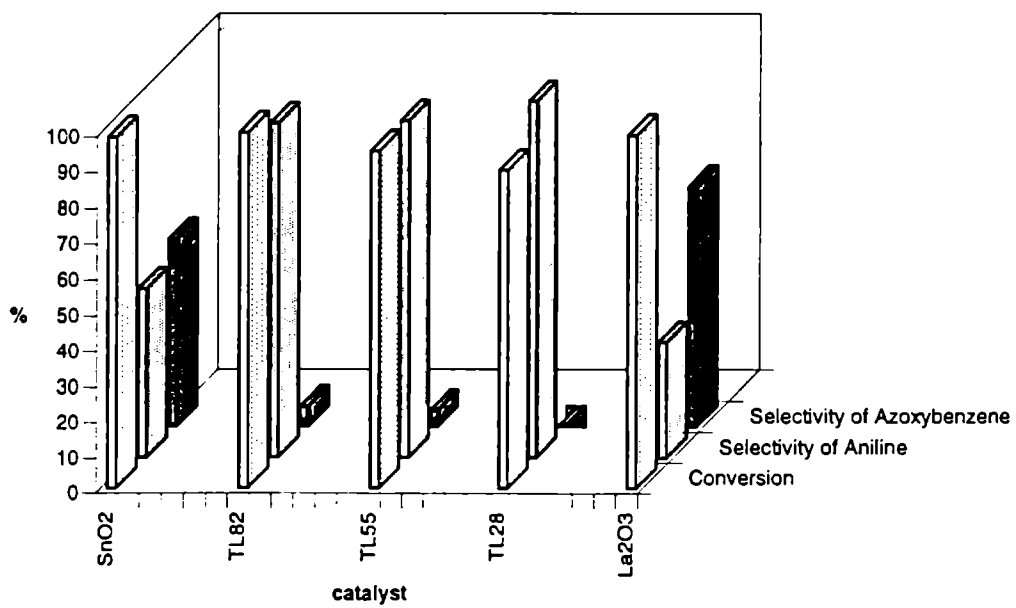


Fig. 3 42 Effect of catalyst composition on the product selectivity

Since these catalysts show activity in the reduction of nitrobenzene, they were tested in the reduction of aromatics containing various reducible groups. Recently Ni stabilised zirconia has been reported to show chemoselectivity in transfer hydrogenation using propan-2-ol as a hydrogen donor. The results of the reduction of various substrates is summarised in table1. It can be seen that the present catalyst system efficiently reduces both nitrobenzene and acetophenone. Remarkably p-nitrobenzophenone and cinnamaldehyde are chemoselectively reduced to p-aminobenzophenone and cinnamyl alcohol respectively. Moreover C-Cl bond, C-CH₃ and C-OCH₃ are not affected by reduction. Interestingly m-dinitrobenzene is regioselectively reduced to m-nitroaniline.

Table 3.24: Transfer hydrogenation of various aromatic substrates using propan-2-ol over TL82^a

Substrate	Time (h)	Product	Yield(%) ^b
nitrobenzene	3	aniline	95
p-chloronitrobenzene	3	p-chloroaniline	92
p-nitroanisole	3	p-anisidine	93
o-nitrotoluene	3.5	o-toludine	89
m-dinitrobenzene	4	m-nitroaniline	65
		m-phenylenediamine	22
acetophenone	3	1-phenethylalcohol	93
benzophenone	4	benzhydrol	90
p-nitrobenzophenone	3	p-aminobenzophenone	80
cinnamaldehyde	3	cinnamylalcohol	72

^aReaction conditions substrate 10 mmol, KOH 10 mmol, catalyst 10 wt% of substrate, propan-2-ol 15 ml, reflux. ^bIsolated by column chromatography

REFERENCES

- 1 F Lonyi, J Valyon, J Engelhardt, F Mizukami., J. Catal. 160 (1996) 279
- 2 M. M. Dubinin, Chem. Rev., 60 (1960) 235.
- 3 S. Caillere, S. Henin, in "*The Differential Thermal Investigation of Clays*" (Eds.) R. C. Mackenzie, The Central Press, Abardeen, (1956) p. 240.
- 4 M. P Rosynek, P T Magnuson, J. Catal., 46 (1977) 402.
- 5 M. N. Ambrozhi, L. M. Dvornikova, Zh. Neorg. Khim., 11 (1966) 86.
- 6 M. P Rosynek, D. T Magnusun, J. Catal., 48 (1977) 417; M. L. Hair, "*Infrared spectroscopy in surface chemistry*", Dekker, New York, 1967
- 7 K. A. Wickersheim, R. A. Lefever, J. Am. Chem. Soc., 83 (1961) 1147
- 8 R. A. Nyquist, R. O. Kagel, "*Infrared Spectra of Inorganic Compounds*", Academic press, 1971
- 9 N. T McDevitt, W L Baun., Spectrochim. Acta., 20 (1964) 799
- 10 G. C. Bond, A. J. Sarkani,, G. D. Parfitt, J. Catal., 57 (1979) 476.
- 11 K. Tanabe, M. Misono, Y Ono, H. Hattori, "*New solid acids, bases, their catalytic properties*", Stud. Suf. Sci. Catal., (Eds.) B. Delmon, J. T Yates, Elsevier, 51 (1989) 15.
- 12 T Yamanaka, K. Tanabe, J. Phys. Chem., 80 (1976) 1723.
- 13 H. Pines, C. N Pillai, J. Am. Chem. Soc., 82 (1960) 2401
- 14 C. P Bezouhna, M. A. Al-Zihari, Catal. Lett., 11 (1991) 245.
- 15 C. N. Pillai, H. Pines, J. Am. Chem. Soc., 83 (1961) 3274.
- 16 S. Kotasarenku, L. V Malysheva, Kinetai Katal., 24 (1983) 877
- 17 J. Take, T Matsumoto, Y Yoneda, Bull. Chem. Soc. Jpn., 47 (1974) 424.
- 18 A. Gervasini, A. Auroux, J. Catal., 131 (1991) 190.
- 19 K. Tanabe, M. Misono, Y Ono, H. Hattori, "*New solid acids and bases, their catalytic properties*", Stud. Suf. Sci. Catal., (Eds.) B. Delmon, J. T Yates, Elsevier, 51 (1989) 316.
- 20 I. Halasz, H. Vinek, K. Thomke, H. Noller, Z. Phys. Chem. Neue. Folge., 144 (1985) 157

- 21 K. Tanabe, M. Misono, Y. Ono, H. Hattori, "New solid acids and bases, their catalytic properties", Stud. Surf. Sci. Catal., (Eds.) B. Delmon, J. T. Yates, Elsevier, 51 (1989) 261.
- 22 A. J. Lindeen, R. Van Hoozer, J. Org. Chem., 32 (1979) 3387
- 23 T. Yamaguchi, K. Tanabe, Bull. Chem. Soc. Jpn., 47 (1974) 424
- 24 H. Pines, C. N. Pillai, J. Am. Chem. Soc., 83 (1961) 3270
- 25 H. Noller, K. Thombke, J. Mol. Catal., 6 (1979) 376
- 26 K. Thombke, Z. Phys. Chem. Neue Folge., 106 (1977) 302
- 27 M. J. Fuller, M. E. Warwick, J. Catal., 29 (1973) 441
- 28 J. D. Butler, T. C. Poles, B. T. Wood, J. Catal., 16 (1970) 239
- 29 L. Yue, O. Olaofe, Chem. Eng. Res. Des., 62 (1984) 81
- 30 H. Noller, W. Klading, Catal. Rev., 13 (1976) 149
- 31 D. E. Bryant, W. L. Kranich, J. Catal., 8 (1969) 8.
- 32 A. J. Lundeen, R. Van Hoozer, J. Org. Chem., 32 (1979) 3386.
- 33 L. T. Weng, P. Patrono, E. Sham, P. Ruiz, P. Delmon, J. Catal., 132 (1991) 360
M. Ai, S. Suzuki, J. Catal., 30 (1973) 362; L. T. Weng, B. Yasse, J. Ladriere.
P. Ruiz, B. Delmon, J. Catal., 132 (1991) 343
- 34 M. P. Rosynek, Catal. Rev. Sci. Eng., 16 (1) (1977) 111
- 35 T. Tagawa, T. Hattori, Y. Murakami, J. Catal., 75 (1982) 66.
- 36 C. Bezouhanova, M. A. Al-Zihari, Appl. Catal. A General, 83 (1992) 45
- 37 V. V. Rao, V. Durgakumari, S. Narayanan, Appl. Catal., 49 (1989) 165
- 38 E. Santacesaria, M. Diserio, P. Ciambelli, Appl. Catal., 64 (1990) 101
- 39 S. Balsama, P. Beltrame, P. L. Beltrame, L. Forni, G. Zuretti, Appl. Catal., 13 (1984) 161.
- 40 F. Nozaki, I. Kimura, Bull. Chem. Soc. Jpn., 50 (3) (1977) 614.
- 41 K. Tanabe, T. Nishizaki, Proc. 6th Intern. Congr. Catal., 2 (1977) 863; B. Xu, T. Yamaguchi, K. Tanabe, Materials Chem. and Phys., 19 (1988) 291
- 42 C. Benzouhanava, M. A. Al-Zihari, Appl. Catal., 8 (1992) 45; R. T. Tilemat-Manzalji, D. B. Bianchi, G. M. Pajonk, Appl. Catal., 101 (1993) 339
- 43 C. Benzouhanava, M. A. Al-Zihari, Appl. Catal., 8 (1992) 45.

- 44 R. T Tilemat-Manzalji, D. B. Bianchi, G M. Pajonk, Appl. Catal., 101 (1993) 339
- 45 M. Marczewski, J. P Bodibo, G. Perof, M. Guisnel, J Mol. Catal., 50 (1989) 211
- 46 S. Velu, C S. Swamy, Appl. Catal. A General 119 (1994) 241
- 47 J. M. Parera, A. Gonzalez, M. A. Burrel, Ind. Eng. Chem., 7 (1968) 259; K T Li, I Wang, K R. Chang, Ind. Eng. Chem. Res., 32 (1993) 1007, E. Santacesaria, D Grassu, D. Gelosa, S. Carra, Appl. Catal., 64 (1990) 83
- 48 J Santhanalakshmi, T Raja, Appl. Catal. A General, 147 (1996) 69
- 49 J. R. Kosak, "*Catalysis of Organic Reactions*", Marcel Dekker, Inc. New York, 1984 R. L. Augustine, "*Heterogeneous Catalysis for the Synthetic Chemist*" Marcel Dekker, Inc. New York, 1996.
- 50 J M. Schkeryantz, S. J. Danishefsky, J. Am. Chem. Soc., 117 (1995) 4722.
- 51 P E. Fanta, J Am. Chem. Soc., 75 (1953) 737
- 52 E. L. Derrenbacker, U.S. Patent, 4, 264, 529 (1991).
- 53 P N. Rylander, I. M. Karpenko, G. R. Pond, N. Y Ann, Acad. Sci., 172 (1970) 266.
- 54 Osuka, Shimizu, Suzuki, Chem. Lett., (1983) 1373.
- 55 S. L. Karwa, R. A. Rajadhyaksha, Ind. Eng. Chem. Res., 27 (1988) 21
- 56 S. A. Moya, R. Pastene, R. Sario, R. Sartori, P Aguirre, H. Lebozec, Polyhedron, 15 (1996) 1823
- 57 J I. Mcnah, Inst. Chem. Eng. Symp. Ser 15 (1981) 68.
- 58 F Haber, Electrochem., 4 (1898) 1506; F Haber, C. Z. Schmidt, Physik. Chem., 32 (1900) 279.
- 59 T T Upadhya, S. P Katdare, D. P. Sabde, V Ramaswamy, A. Sudalai, J Chem Soc. Chem. Commun., (1977) 1119.
- 60 Engelhard Minerals and Chemicals Corp., U.S. Patent, 3, 715, 397

CHAPTER IV

ACID-BASE PROPERTIES AND CATALYTIC ACTIVITY OF
SULFATE MODIFIED MIXED OXIDES OF TIN WITH
LANTHANUM AND SAMARIUM

4.1 PHYSICO-CHEMICAL CHARACTERISTICS

For simplicity the sulfate modified oxides prepared by different methods are denoted as,

STS82 (I) \Rightarrow sulfated TS82 prepared from the mixed hydroxide heat treated to 300 °C, by ammonium sulfate method (Method I).

STS82 (II) \Rightarrow sulfated TS82 prepared from the mixed hydroxide dried carefully at 110 °C, by ammonium sulfate method (Method II).

STS82 (III) \Rightarrow sulfated TS82 prepared from $\text{SO}_4^{2-}/\text{SnO}_2$ followed by impregnation with samarium nitrate solution (Method III).

The other sulfated analogues denoted as STS55 (sulfated TS55), STS28 (sulfated TS28) and STL82 (sulfated TL82) were prepared by method II.

The surface molar composition of the mixed oxides treated with sulfate anion was determined by EDX. The metal oxide percentage and sulfur percentage (as SO_3) are given in Table 4.1. The sulfur content obtained from EDX of STS82 and STS55 matches well with those calculated from the weight loss in thermogravimetric analysis. However a large variation is observed in the case of STS28. EDX of all the samples were taken after calcination at 500 °C. The large variation in the sulfate content of STS28 is due to the fact that a large amount of sulfate is retained on the sample even after heating to 1100 °C in air. To confirm this the sample treated to 1100 °C was subjected to EDX analysis and it was found that a considerable amount of sulfate was still retained in the sample (see Table 4 1)

Table 4.1 EDX analysis of sulfated oxides

Catalysts	Chemical composition %				
	Calcination temperature °C	SnO ₂	Sm ₂ O ₃	SO ₃	SO ₃ ^b
STS82 (I)	500	72.59	25.11	2.30	
STS82 (II)	500	72.63	25.03	2.34	2.24
STS82 (III)	500	70.62	24.58	4.80	
STS55 (II)	500	45.16	50.88	3.96	3.60
STS28 (II)	500	14.93	78.93	6.14	3.42
STS82 (II)	1100	75.93	23.94	0.13	
STS55 (II)	1100	44.10	55.62	0.28	
STS28 (II)	1100	13.80	83.62	2.58	

^b Calculated from TG weight loss.

The EDX analysis of other samples STS82 and STS55, heat treated at the same temperature, showed very small amount of sulfate. These observations suggest that the sulfate treatment of the system TS28, which contain more amount of samarium oxide, probably lead to the formation of bulk like sulfate species, which is retained on the sample even after heat treatment at high temperature. The sulfate content of different sulfated oxides prepared by different methods is also given in Table 4 1

The XRD patterns of TS82 and its sulfated analogue is shown in Figure 4 1. The intensity of diffraction peaks decreased after sulfate treatment [1]. We have noticed that addition of a second oxide viz. La_2O_3 or Sm_2O_3 to tin oxide decreases the XRD peak intensity. So the addition of sulfate and a second oxide to SnO_2 hinders the crystallisation of the originally amorphous material. It has been reported that the degree of crystallisation of the sulfated oxides is much lower than that of the oxides without the sulfate treatment [2]. Lonyi *et al* found that addition of sulfate and titania as a second oxide to zirconia hinder the crystallisation of the amorphous ZrO_2 [3]. No structural deterioration is observed in the case of sulfate treated samples. However from the present study it is not clear whether any metal sulfates are formed, particularly in the case of samples containing more amount of rare earth oxide, TS28. The SEM pictures of TS82 and STS82 are shown in Figure 4.2. Bigger crystallites are seen in the case of TS82 whereas in the case of STS82, smaller particles with almost uniform size are seen. This is expected as the addition of sulfate prevent the agglomeration of smaller particles [4].

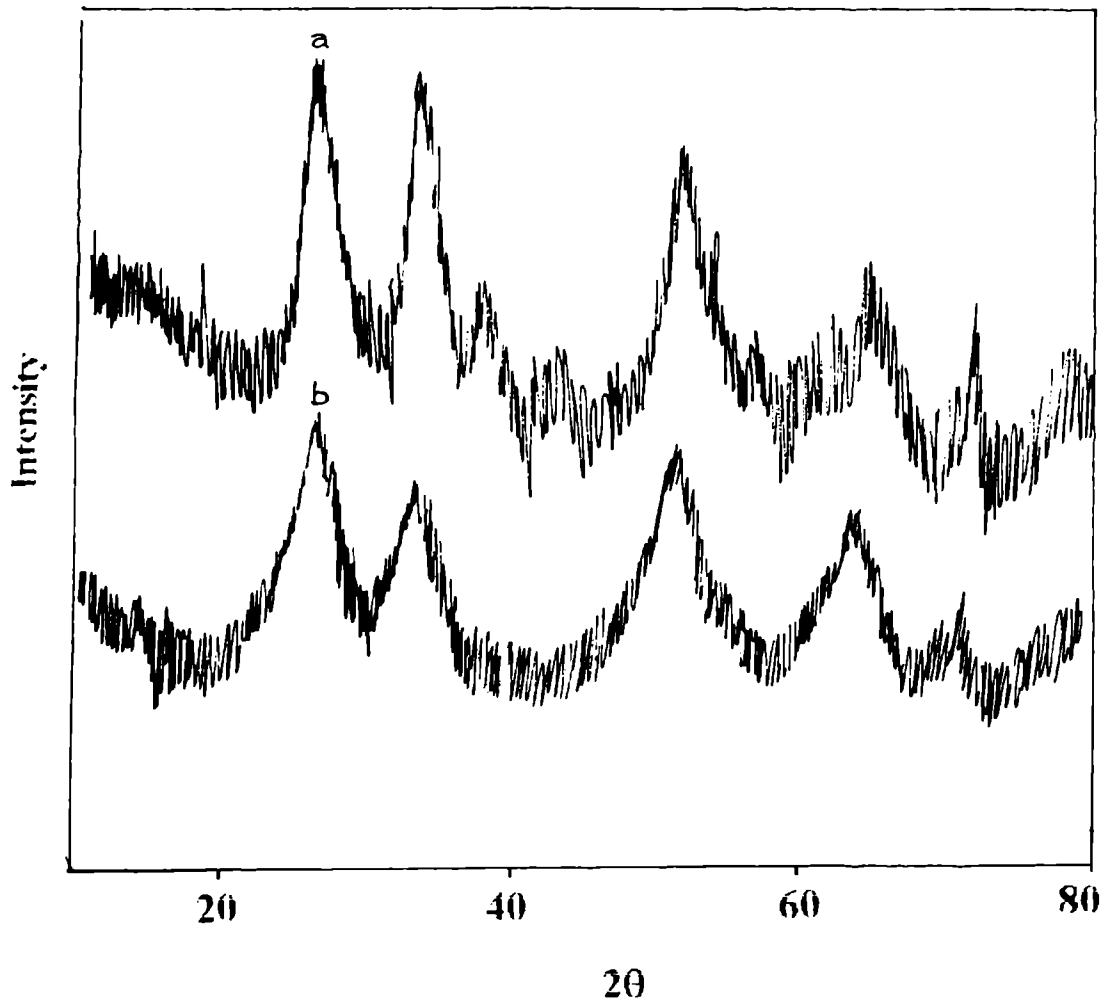
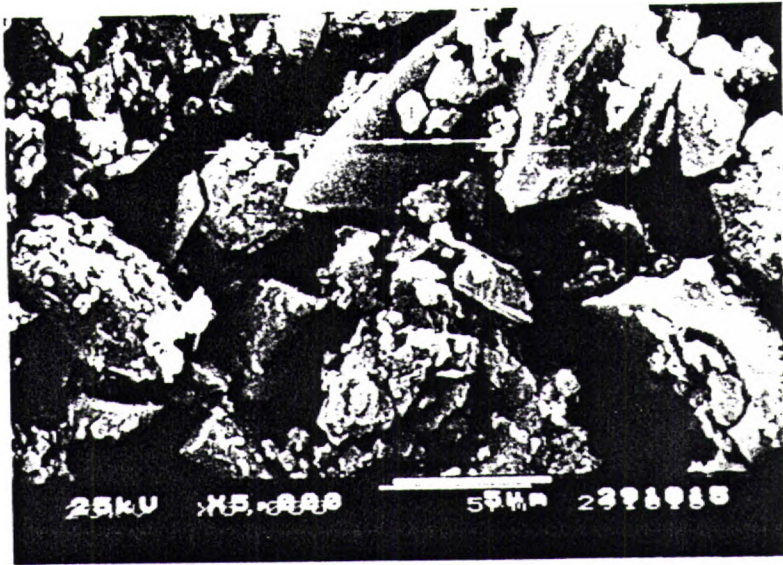
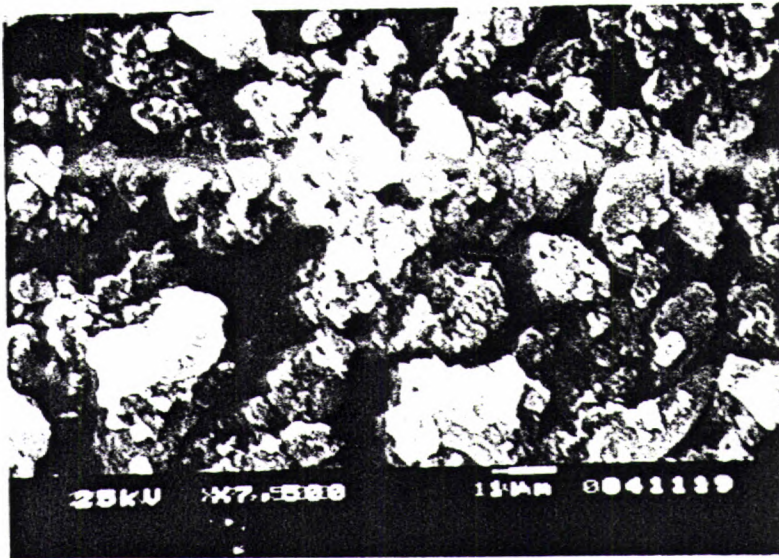


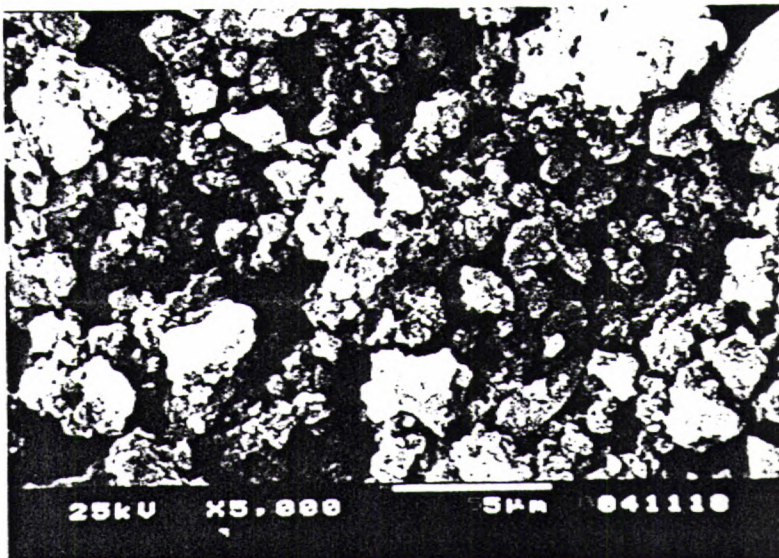
Figure 4 1 X-ray diffraction patterns of TS82^a and sulfate modified analogue (STS82)^b calcined at 550°C in air



a



b



c

Figure 4.2 SEM pictures of TS82^a and STS82 (II)^b and STS82 (III)^c calcined at 550°C

The specific surface areas of these catalysts are much higher than those of the unmodified oxides [4]. The reason for area increment is the retardation of crystallisation due to sulfate treatment. A large variation in surface area is observed as the method of preparation of catalyst is changed. Results are summarised in Table 4.2. The calcination of the sulfated material to high temperature produces a decrease in surface area but the fraction of decrease in surface area is smaller than that of the unmodified oxide [5]

Table 4.2 BET surface area of sulfated oxides

Catalyst	Calcination temp. °C	Surface area m ² /g
STS82 (I)	500	124.9 (102.7) ^a
STS82 (I)	550	130.6 (92.60)
STS82 (II)	550	152.1
STS82 (III)	550	195.6
STS82 (II)	600	148.1 (79.1)
STS82 (II)	650	131.1 (60.80)
STS82 (II)	750	91.1 (42.10)
STL82 (I)	500	110.5 (105.7) ^a

^a Values given in parenthesis are the surface area of unmodified analogue at the same temperature.

The pore volumes of the sulfated oxides are shown in Table 4.3. Pore volume decreased after sulfate treatment [5]. The pore volume of the unmodified

sample decreased from 0.30 to 0.18 m³/g by calcination, while that of the sulfated sample dropped from 0.28 to 0.23 m³/g by calcination.

Table 4.2 Pore volume of sulfated oxides:-- effect of method of preparation and calcination temperature

Catalyst	Heat treatment °C	Pore volume m ³ /g
STS82 (I)	500	0.287 (0.315)
STS82 (I)	550	0.285 (0.300) ^a
STS82 (II)	550	0.279 (0.300)
STS82 (III)	550	0.278 (0.300)
STS82 (II)	600	0.241 (0.271)
STS82 (II)	650	0.238 (0.221)
STS82 (II)	750	0.230 (0.181)
STL82 (I)	500	0.273

^a Values given in parenthesis are the pore volume of unmodified analogues at the same temperature.

The decomposition of sulfate takes place at higher temperature than in the case of sulfated tin oxide or zirconium oxide [6]. In SO₄²⁻/SnO₂ sulfur oxide evolution takes place in the temperature range 700-750 °C and in the case of SO₄²⁻/ZrO₂ the temperature of sulfate evolution is 700-740 °C. In the case of STS82 decomposition of sulfate takes place at very high temperature (> 920 °C) and the process is completed above 1000 °C (Figure 4.3b). Removal of sulfate in STS55 started around 900 °C and is completed near 1000 °C (Figure 4.3a and 4.3c). A

continuous weight loss above 500 °C is observed in STS28 including two distinct weight losses at 700 °C and 850 °C. Moreover as explained earlier weight loss doesn't correspond to the sulfur content obtained by EDX analysis. So the decomposition of bulk sulfate must be taking place well above 1000 °C. The higher thermal resistance of these catalysts is advantageous since it allows the regeneration of deactivated catalysts by high temperature calcination. In the DTA of TS55 an exothermic peak is noticed around 850 °C, which is ascribed to the formation of a new compound or a phase change. Same type of exotherm is obtained in the case of TS28 also but not very distinct as in the case of TS55. A shift in the DTA exothermic peak to higher temperature is observed in sulfate treated TS55 [7]. The DTA peak is shifted from 850 to 900 °C (Figure 4.4). The endothermal decomposition of sulfate and the exothermal crystallisation of oxide occurs at about the same temperature range. The rapid evolution of the heat of crystallisation results in the appearance of the sharp DTA peak superimposed on the broad peak of the exothermic sulfate decomposition. Due to the heat effect, the corresponding DTA peak of sulfate decomposition takes a complex peak profile.

The sulfated samples showed absorption bands at 960-980, 1060-1070, 1130-1150, and 1210 cm^{-1} which are assigned to the bidentate sulfate coordinated to the metal (Figure 4.5) [8]. The difference between chelate and bridged bidentate can be found by the location of the highest vibrational absorbing peak of SO_4^{2-} on the surface [9]. Peak at 1210 cm^{-1} corresponds to the nonsymmetrical vibration of chelate bidentate. A peak near 1400 cm^{-1} is due to the vibration of S=O group. [10]. According to Ward and Ko the chemical state of sulfate groups depends on the conditions of pretreatment of the catalyst [11]. After activation at low temperatures it has partial ionic character with the S=O bond order less than two, whereas upon treatment at higher temperatures the sulfate is converted into a

strongly covalent species with S=O bond order close to two. The existence of these covalent S=O bonds in sulfur complexes formed are necessary for superacidity generation.

By comparison with the XPS results it is clear that a strong absorption around 1380 cm^{-1} is typical of the highest oxidation state of sulfur (+6) in S=O bonds. It is concluded that the acidity generation is independent of the sulfating agents used and is brought about by the oxidation of sulfur to its highest oxidation state, +6.

The acid strength of the catalysts measured qualitatively after the pretreatment, ($550\text{ }^{\circ}\text{C}$ in air) using a series of Hammett indicators is given in Table 4.3. The acid strength of sulfated oxides prepared by different methods are in the order STS (III) > STS (II) > STS (I). Only weak acid sites are created by sulfate treatment employing method I, whereas the method III resulted in the creation of superacid sites with $H_0 \leq 13.75$. Super acidic character of the catalyst is retained even at very high temperature ($800\text{ }^{\circ}\text{C}$).

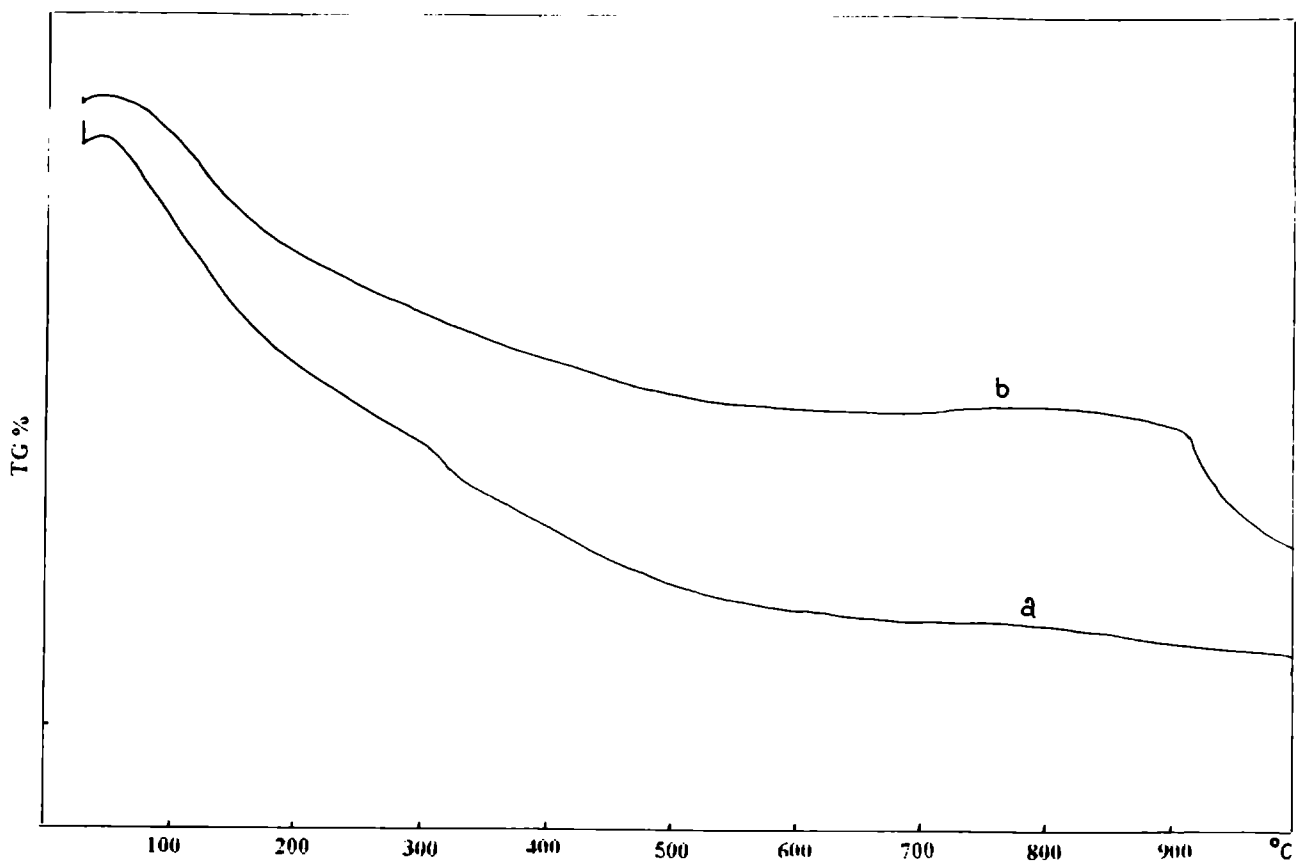


Figure 4.3a TG curves of TS55^a and its sulfate modified analogue, STS55^b

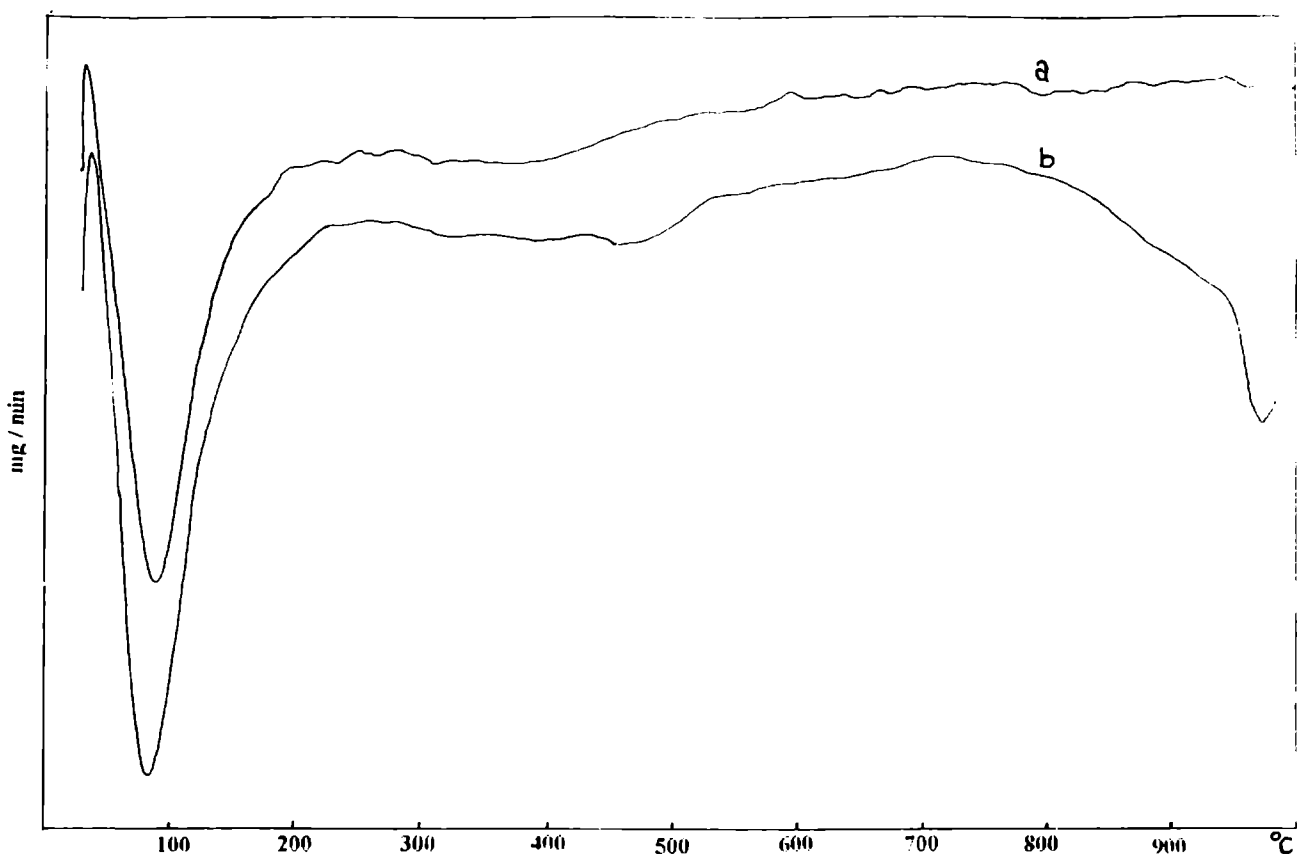


Figure 4.3b DTG curves of TS82^a and STS82^b

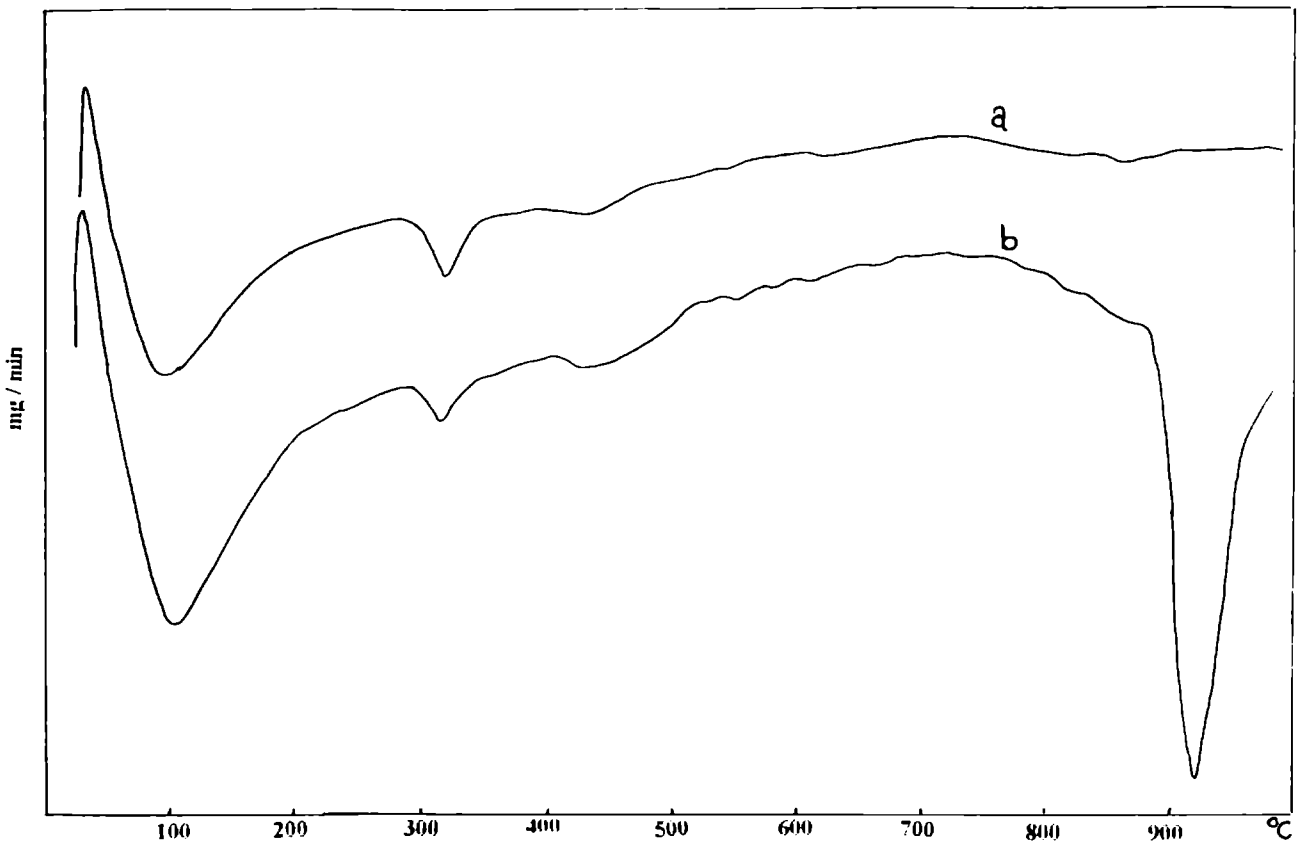


Figure 4.3c DTG curves of TS55^a and STS55^b

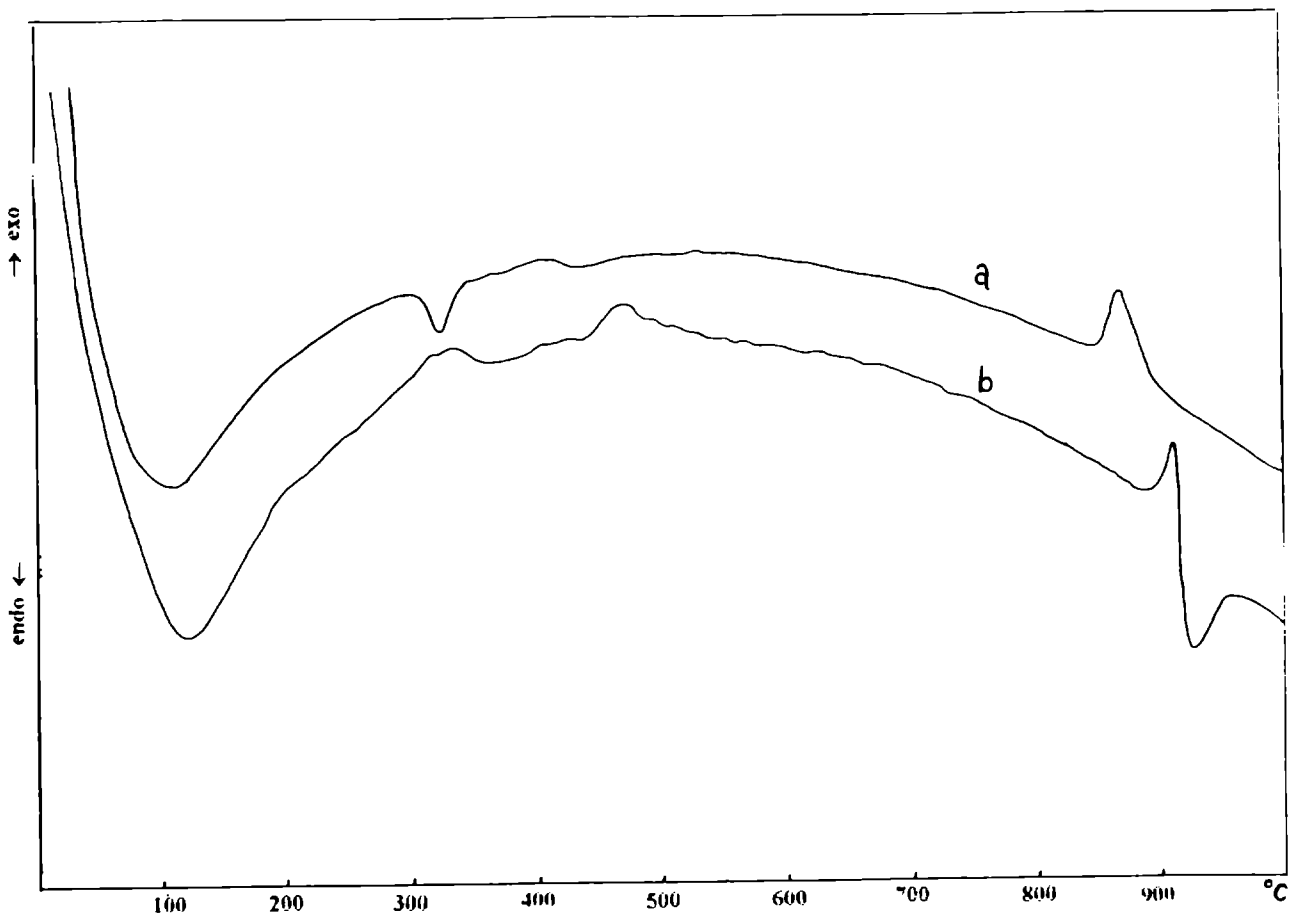


Figure 4 4 DTA curves of TS55^a and STS55^b



Figure 4.5 IR spectrum of sulfate modified TS82.

Table 4.3 Acid strength of sulfated oxides

Catalysts	pKa values of the indicators				
	-0.8	-3.0	-8.2	-11.35	-13.75
STS82 (I)	+ *	-	-	-	-
STS82 (II)	+	+	+	-	-
STS82 (III)	+	+	+	+	+ *
STS55 (II)	+	+	+ *	-	-
STS28 (II)	+	+ *	-	-	-
STS82 (II) ¹	+	+	+	-	-
STS82 (II) ²	+	+	+	-	-
STS82 (III) ²	+	+	+	+	+ *

¹ calcined at 700 °C, ² calcined at 800 °C, * colour not very distinct.

4.2 DECOMPOSITION OF ALCOHOLS

A comparative study of the various sulfated oxides under study are presented in Table 4.4. Sulfated oxides prepared by different methods show difference in catalytic activity. Catalyst prepared by method III gave maximum activity, however catalyst prepared from the oxide heated to 300 °C (method I) showed lesser activity. Catalytic activity decreases in the Sn-Sm and Sn-La series in the order STS82 > STS55 > STS28 and STL82 > STL55 > STL28. STS82 (I) produced a large amount of aldehyde via dehydrogenation. Only weak acid sites are detected in this case. Isobutanol decomposition is feasible at lower temperature over sulfated oxides compared to their unmodified analogues. The alcohol conversion is completed at 325 °C over STS82. At lower temperatures a large amount of dehydrogenation product, aldehyde is formed. However, the activity of unmodified oxide is very poor at this temperature (250 °C). Conversion to aldehyde is about 15.62 % at 250 °C, employing sulfated oxide as the catalyst whereas in the case of unmodified analogue it is about 18.59 % at 350 °C and only 5.25 % at 250 °C. This indicates that there is an enhancement in the dehydrogenation activity after sulfate treatment. But at higher temperature and low contact time dehydration predominates. When the feed rate is increased from 4 ml/h to 8 ml/h STS82 displayed an enhancement in the selectivity of dehydrogenation product, aldehyde. We have already noticed that the isobutanol dehydration over unmodified oxide systems afforded mainly isobutene alongwith small amounts of other butenes. From the results it is clear that sulfate addition resulted in the creation of strong acid sites capable of initiating isomerisation reactions. Alcohol dehydration usually require weak acid sites whereas isomerisation reactions requires stronger sites. A secondary carbenium ion formed

by the methyl migration of initially formed primary carbenium ion, undergoes further rearrangement to form 1-butene and 2-butene (Figure 4.6). A comparative study of the sulfate modified oxide and unmodified oxide is presented in Table 4.5

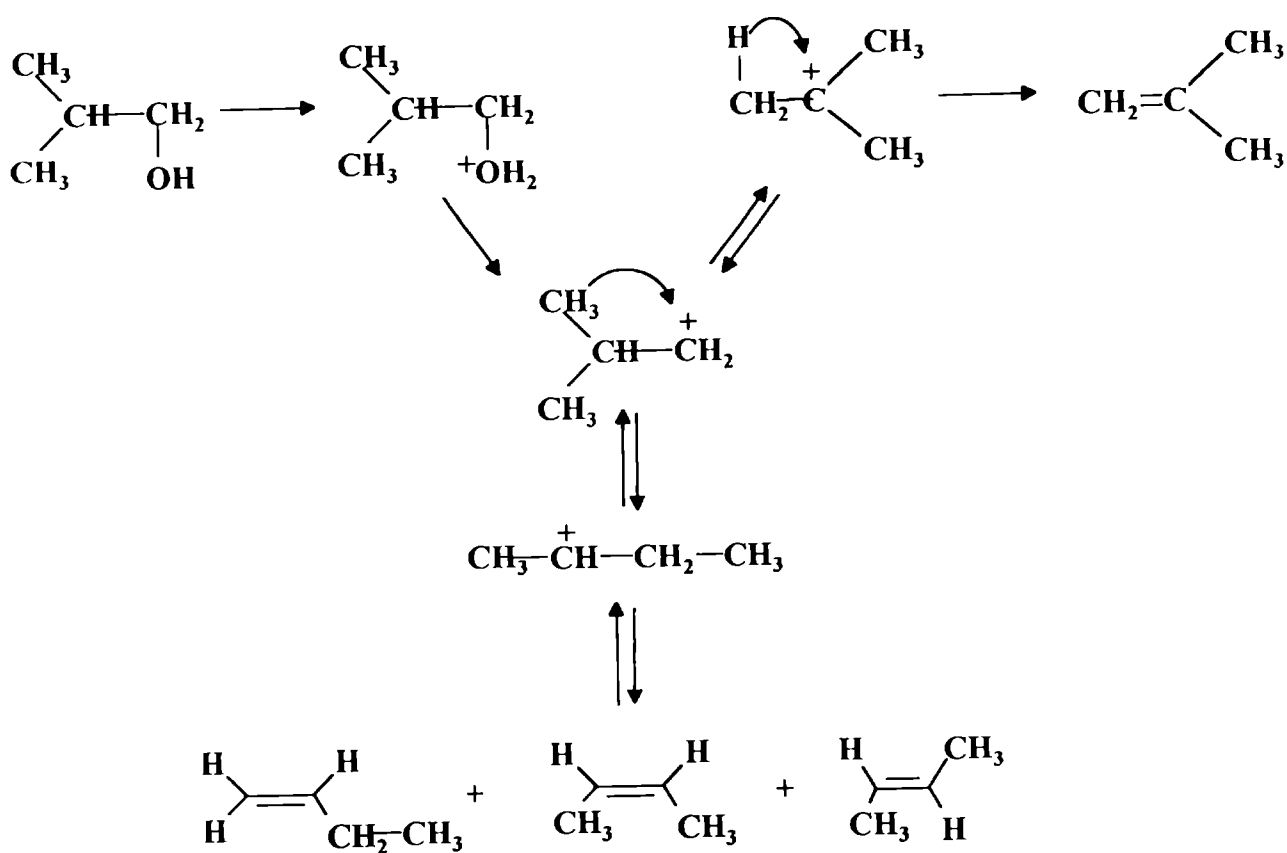


Fig. 4.6. Dehydration of isobutanol over acidic catalysts.

Table 4.4 Decomposition of isobutanol over different catalysts

Catalyst	Selectivity %				Conversion
	isobutene	1-butene	2-butene	ketone	%
STS82 ^a	34.80	38.10	20.80	4.30	88.00
STS82 ^b	37.80	37.10	18.43	4.50	87.20
STS82 ^c	66.16	5.60	4.12	30.12	63.80
STS55 ^b	43.90	32.18	20.72	3.20	86.10
STS28 ^b	68.18	15.60	14.80	1.42	71.20
STL82 ^b	40.16	34.81	19.55	5.08	87.80
STL55 ^b	42.60	35.18	22.22	4.90	86.90
STL28 ^b	71.80	13.10	12.60	2.50	72.80

Reaction conditions: Temperature 250 °C, feed rate 4 ml/h, TOS 3 h, ^{a,b,c} catalysts prepared by method 1, 2 and 3 respectively.

Generally the formation of 2-butene from 1-butanol is indicative of the E₁ mechanism. This mechanism occurs with strongly acidic catalysts such as aluminosilicates [12, 13].

The product distribution of *t*-butanol, isobutanol, 1-butanol and 2-butanol decomposition over sulfated oxide are also given in Table 4.6. *t*-Butanol is dehydrated mainly to isobutene alongwith a large amount of 1-butene and 2-butene. The initially formed isobutene can undergo isomerisation reactions to form 1-butene and 2-butene.

Table 4.6 Decomposition of different butanols over STS82

Product	<i>t</i> -Butanol	Isobutanol	1-Butanol	2-Butanol
selectivity				
Isobutene	48.92	34.60	3.18	9.80
1-Butene	24.34	38.10	26.30	20.10
2-Butene	21.94	20.10	62.46	60.45
Others	4.80	3.90	3.70	6.24
Ketone	nil	4.90	4.20	3.40
/Aldehyde				
Conv %	100.00	88.00	83.00	84.00

Reaction conditions: Temperature 250 °C, feed rate 4 ml/h, TOS 3 h, Catalyst weight 2.7 g.

Dehydration of 2-butanol produced a mixture of 2-butene, 1-butene and isobutene. The formation of Saytzeff elimination products suggest that the mechanism of dehydration can be either E₁ or E₂ type [13]. Here dehydration

products initially formed isomerises to produce other alkene isomers in presence of strong acid sites created by sulfate treatment. Hence the mechanism must be E₁ type. As discussed earlier the type of mechanism is influenced mainly by the strength of acid sites present on the catalyst surface.

From the above results we observed a possible change in the mechanism of alcohol dehydration after the sulfate treatment of a series of Sn-La and Sn-Sm binary oxide systems, which is ascribed to the generation of strong acid sites on the catalyst surface by sulfate treatment.

4.3 OXIDATIVE DEHYDROGENATION REACTIONS

4.3.1 Oxidative dehydrogenation of ethanol

Acetaldehyde and ethene were formed as the main products alongwith small amounts of acetic acid and carbon oxides. The effect of temperature on the product selectivity and conversion is presented in the Table 4.7. The selectivity of aldehyde is maximum at 400 °C (74.11%). But at higher temperatures aldehyde selectivity is decreased considerably. Alcohol is completely converted at 450 °C. But in the case of non-sulfated analogues, at lower temperature acetaldehyde selectivity is less, which increases with increase in temperature. At 450 °C it gave an aldehyde selectivity of only 36.78 % and at 400 °C aldehyde selectivity is only 19.80 %. The effect of feed rate on the selectivity is studied at 400 °C, and a small increase in acetaldehyde selectivity is observed when the feed rate is increased from 4 ml/h to 10 ml/h (Table 4.8). Conversion of alcohol decreases as expected. When aqueous ethanol (75 %) is used as the feed, a tremendous

increase in the selectivity of aldehyde is observed (96.37%) at a conversion of 80.93% (Table 4.9) [14].

Table 4.7 Effect of temperature on the product selectivity and conversion of ethanol

Selectivity %	Temperature °C					
	350		400		450	
	a	b	a	b	a	b
Ethene	74.80	35.15	76.10	20.18	50.70	45.00
Acetaldehyde	18.90	63.84	19.80	74.11	36.78	52.80
Carbon oxides	7.10	0.98	3.80	1.50	5.57	3.15
Conversion %	64.80	75.70	76.10	85.73	85.20	99.3

nonsulfated oxide, ^b sulfated analogue Reaction conditions: Reaction temperature 400 °C, feed rate 4 ml/h, TOS 2 h, Catalyst weight 2.7 g, Calcination temperature 500 and 550 °C, for TL82 and STL82 respectively

Table 4.8 Effect of feed rate on the product selectivity and conversion of ethanol

Selectivity %	Feed rate ml/h		
	4	6	10
Ethene	20.18	17.86	19.16
Aldehyde	74.11	79.98	80.12
Carbon oxides	1.50	0.81	0.71
Conversion %	85.73	73.80	59.10

Reaction conditions: Reaction temperature 400 °C, TOS 2 h, Catalyst weight 2.7 g, Calcination temperature 550 °C.

Table 4.6 Effect of water on the product selectivity and conversion of ethanol

Selectivity %	Water wt%		
	20 %	25 %	30 %
Ethene	10.80	3.63	3.20
Aldehyde	88.70	96.37	96.80
Conversion %	82.10	80.93	69.13

Reaction conditions: See foot notes in Table 4.8

A comparative study of the stability of sulfated oxide and the corresponding nonsulfated analogue is shown in Figure 4.8. Reaction is continued for 8 hours and it is found that sulfated oxide deactivated slowly compared to its nonsulfated analogue. Deactivation may be due to the reduction of active sites during the oxidation of ethanol.

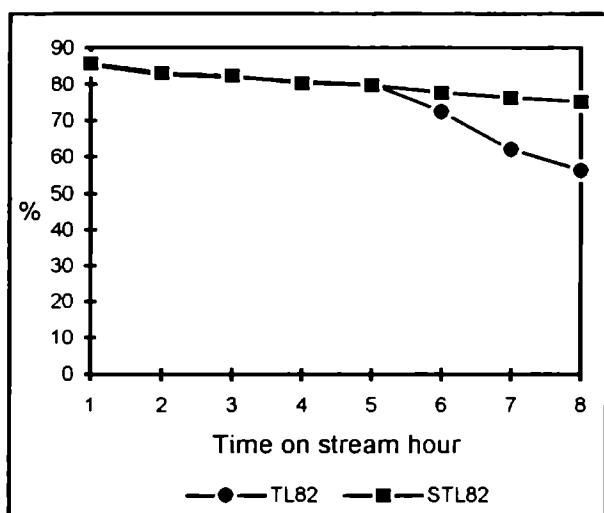


Fig. 4.8. Time on stream study of TL82 and STL82.

Reaction conditions: See foot notes in Table 4.8

4.3.2 Oxidative dehydrogenation of ethylbenzene and cyclohexane

A comparative study of ethylbenzene dehydrogenation over TS82 and STS82 at 425⁰C is presented in Table 4.10. The conversion of ethylbenzene to styrene is increased after sulfate treatment. Similar results are obtained in the case of sulfated TS55 also.

Table 4.10 Comparison of non-sulfated and sulfated oxides in the oxidative dehydrogenation of ethyl benzene

Product	TS82 ^a	STS82 ^a	STS82 ^b	TS55 ^a	STS55 ^a
distribution					
%					
Benzene	4.49	5.80	3.10	5.40	3.54
Ethylbenzene	70.41	50.60	66.20	81.95	71.81
Styrene	23.68	39.80	28.78	9.42	22.85
Carbon	1.42	3.80	1.92	3.23	1.80
oxides					
Conversion	29.49	49.40	33.80	18.05	28.19
%					

^a Reaction temperature 425 °C and ^b 400 °C

Reaction conditions: Feed rate 4 ml/h, TOS 2 h, Calcination temperature 550 °C

Carbon oxides selectivity is not much influenced by sulfation. According to Tagawa *et al* the acid sites of H₀ between 1.5 and -5.6 are proven to be the active sites to adsorb ethylbenzene reversibly, whose oxidation on the otherhand occurs on the basic sites of pK_a between 17.2 and 26.5 [15]. In the oxidative dehydrogenation of cyclohexane; the main products were benzene and cyclohexene (Table 4.11). As in the case of ethylbenzene reaction, the sulfate treatment lead to an enhancement in oxidation activity [16].

Table 4.11 Comparison of sulfate modified and unmodified oxides in the oxidative dehydrogenation of cyclohexane

Product distribution %	TS82	STS82
Benzene	4.80	6.80
Cyclohexene	14.20	24.48
Cyclohexane	78.56	66.90
Others	2.56	1.82
Conversion %	21.50	33.10

Reaction conditions: Reaction temperature 425 °C, Feed rate 4 ml/h, TOS 2 h, Calcination temperature 550 °C.

4.3.3 Oxidative dehydrogenation of cyclohexanol

The effect of temperature on the conversion and product selectivity is depicted in Table 4.12. Compared to unmodified oxide reaction takes place at lower temperature and cyclohexanol conversion is completed at 400 °C. The cyclohexanone selectivity is maximum at 250 °C. As the temperature increases cyclohexanone selectivity decreases. But in the case of unmodified oxide, cyclohexanone selectivity is not much influenced by increase in temperature. The unmodified oxide, TS82 at 400 °C showed 93.1 % selectivity towards cyclohexanone at a total cyclohexanol conversion of 53.61%. The corresponding sulfated analogue showed 74.9 % selectivity at 350 °C at a cyclohexanol conversion of 75.89 %. Thus the cyclohexanone yield (conversion × selectivity/100) is 56.84 % at 350 °C using STS82 as catalyst, whereas it is 49.9 % at 400°C employing TS82 as catalyst. At 300 °C cyclohexanone yield is 46 % for

STS82, while that of TS82 at the same temperature is only 29.24 % (Table 4 13). These results indicate that oxidation activity of the mixed oxide is increased after sulfate treatment. Due to the higher catalytic activity of sulfated oxides, dehydrogenation will be feasible at comparatively lower temperature. The effect of feed rate of cyclohexanol on the selectivity of cyclohexanone is shown in the Table 4 14 The cyclohexanone selectivity increased with increase in feed rate as expected.

Table 4.12 Effect of temperature on the product selectivity and conversion of cyclohexanol

Selectivity %	Temperature °C				
	250	275	300	350	400
Cyclohexene	3.10	3.70	4.90	22.80	59.71
Cyclohexanone	96.90	96.30	94.10	74.90	37.20
Conversion %	34.56	39.50	48.89	75.89	100.00

Reaction conditions: Catalyst STS82, Feed rate 4 ml/h Calcination temperature 550 °C.

Table 4.13 Comparative study of sulfate modified and unmodified oxides at different temperatures

Catalyst	250 °C		300 °C		350 °C		400 °C	
	a	b	a	b	a	b	a	b
TS82	15.89	97.20	31.86	91.80	42.03	90.10	52.81	93.60
STS82	34.56	96.90	48.89	94.10	75.89	74.90	100.00	37.20

a: conversion of cyclohexanol, b: selectivity of cyclohexanone Reaction conditions: See foot notes to Table 4.12

Table 4.14 Comparative study of sulfate modified and unmodified oxides at different feed rates

Catalyst	4 ml/h		6 ml/h		10 ml/h		12 ml/h	
	a	b	a	b	a	b	a	b
TS82	42.03	90.10	37.18	92.02	32.00	94.40	21.89	94.60
STS82	100.00	37.20	81.19	46.90	69.90	59.20	41.00	62.20

a: conversion of cyclohexanol, b: selectivity of cyclohexanone Reaction conditions: See foot notes to Table 4.8

4.3.4 Comparative study of the catalytic activity of $\text{SO}_4^{2-} / \text{SnO}_2$ and STS82 in the oxidative dehydrogenation of cyclohexanol

The oxidative dehydrogenation of cyclohexanol over $\text{SO}_4^{2-} / \text{SnO}_2$ and STS82 (both catalysts prepared by method II) is presented in Table 4.15 for comparison.

The activity of $\text{SO}_4^{2-}/\text{SnO}_2$ is less than that of STS82 at different temperatures. However there is not much difference in the selectivity of cyclohexanone at different temperatures. The activity of pure SnO_2 is very low compared to other systems. The sulfate content of the samples after the reaction is analysed (Table 4.18). It is clear that a small amount of sulfate is lost during the course of reaction. The loss is more in the case of $\text{SO}_4^{2-}/\text{SnO}_2$ compared to STS82. The stability of four catalysts viz. SnO_2 , TS82, $\text{SO}_4^{2-}/\text{SnO}_2$ and STS82 were examined by continuing the oxidation reaction for 6 hours (Fig. 4.9). The SnO_2 catalyst deactivated very fast compared to other catalysts [17]. TS82 and $\text{SO}_4^{2-}/\text{SnO}_2$ deactivated slowly with time and conversion dropped from 31.8 to 19 % in the case of TS82 and from 34.6 to 28 % in the case of $\text{SO}_4^{2-}/\text{SnO}_2$. The deactivation rate of STS82 is the slowest compared to other systems. The lesser deactivation must be due to the combined effect of SO_4^{2-} anion and rare earth oxide promoter

Table 4.15 Comparison of sulfated tin oxide and STS82 at different temperatures

Catalyst	250 °C		300 °C		350 °C		400 °C	
	a	b	a	b	a	b	a	b
$\text{SO}_4^{2-}/\text{SnO}_2$	21.22	97.10	34.67	93.70	59.45	76.90	78.90	40.12
STS82	34.56	96.90	48.89	94.10	75.89	74.90	100.00	37.20
TS82	15.89	97.20	31.86	91.80	42.03	90.10	52.81	93.60
SnO_2	3.40	98.60	8.79	98.10	17.80	97.10	22.89	96.30

a: conversion of cyclohexanol, b: selectivity of cyclohexanone

Reaction conditions: See foot notes to Table 4.12

Table 4.13 EDX analysis of samples after reaction

Sample	Sulfate ^a %	Sulfate ^b %
STS82	3.40	3.25
SO ₄ ²⁻ / SnO ₂	3.20	2.91

^a Sulfate content before the reaction, ^b sulfate content after the reaction

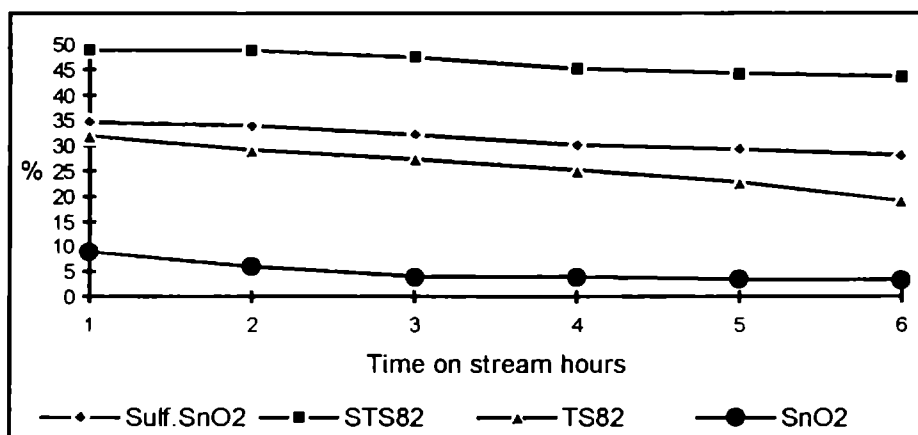


Fig.4.9 Time on stream study of SO₄²⁻ / SnO₂, STS82, TS82 and SnO₂ Reaction conditions: See foot notes to Table 4 12

4.3.4 Mechanism of oxidative dehydrogenation reactions

It is well known that dehydration prevails over metal oxides which are acidic and dehydration become dominant over basic oxides. In the case of oxidative dehydrogenation reactions since the rate determining step is probably the elimination of a proton, the basicity of a catalyst plays an important role, besides the redox properties of catalysts. The reaction proceeds via the abstraction of a proton by basic site (O_2^-), which is generally rate determining [18,19,20]. The mechanism of the simple dehydrogenation is shown below (Fig. 4.10) [21]. The alcoholic proton is discharged to the basic site and the hydrogen atom at the α -carbon atom is discharged to the acid site.

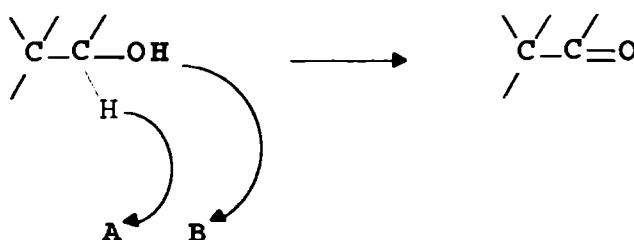


Fig. 4.10 Mechanism of dehydrogenation of alcohol, A and B denote an acid site and a basic site respectively

Ai and Co-workers reported that for several oxidation reactions catalysed by binary and ternary metal oxide catalysts, the catalytic activity and selectivity are correlated with the acid-base properties of the catalysts [22,23]. The correlation was explained by the strength of acid base interactions between reacting molecules and the catalyst surface [24]. According to the investigators more acidic catalysts interact more strongly with basic reactants and activate it more easily. It is further

claimed that the selectivity of the oxidation is classified to various types according to the acid base strength of reactants and products. Acid catalysts readily activate the reactants but not the products. In the oxidation of basic molecules to acidic products acid catalysts are more effective [25].

In the oxidative dehydrogenation of ethanol over nonsulfated oxides the selectivity of dehydrogenation product followed the order $TS_{82} > TS_{55} > TS_{28}$. However the basicity of the oxides as determined by alcohol decomposition reaction follows the order $TS_{82} > TS_{28} > TS_{55}$. We have already noticed that two factors are to be considered to explain the oxidation activity of metal oxide catalysts. First one is the acid-base properties of the catalysts and second one is their redox properties. The conversion of ethanol to acetaldehyde can be regarded as a process in which a basic substrate is converted into an acidic product. So it is expected that acidic catalysts can activate ethanol more easily and bring about oxidation. However, it is not clear whether strength of the acid sites present in the catalyst is higher than the acidity of ethanol. If so the order of catalytic activity should have been different. This suggests that in the present case the redox properties of the catalyst systems are important. The reaction takes place by the adsorption of ethanol on the catalyst surface followed by interaction with acid-base centres. But the total number of such sites also influence the rate of the reaction. It can be seen that as the SnO_2 percentage decreases the catalytic activity decreases. From this it can be concluded that Sn^{4+} sites could be the active sites for the reaction. The interaction of ethanol and Sn^{4+} sites lead to the reduction of these sites since oxidation is a process in which reactant losses electron [26]. The colour of the catalyst turned gray after continuous use due to reduction and consequently catalyst deactivation is observed. However SnO_2 deactivated very fast as a result of deep reduction. In metal oxides two possible states of activated oxygen can be recognized; highly reactive surface states of adsorbed oxygen and

less active, lattice incorporated oxygen species. Obviously the former species are usually considered to be important ones involved in complete oxidation and latter are believed to participate in selective partial oxidation [27]. In the present systems, rare earth oxide can produce mobile oxygen species which can migrate to the surface of SnO_2 and can regenerate the active sites by reoxidation of reduced sites (remote control mechanism). This may be the reason for slower deactivation of tin-samarium and tin-lanthanum binary oxides compared to pure SnO_2 . It has been experimentally evidenced by ^{18}O isotopic study that migration of oxygen species takes place from Sb_2O_4 to SnO_2 [28].

After sulfate treatment of the mixed oxides strong acid sites are created so that they can strongly activate alcohol molecule to bring about oxidation. The electron withdrawing effect of adsorbed sulfate species increases the electron deficiency of Sn^{4+} sites greatly. So these sites will have a greater tendency to accept electrons from the reacting species, which lead to the oxidation of the adsorbed species. This explains the enhancement in oxidation activity after sulfate treatment. Basic reactants like ethylbenzene can interact very strongly with acid sites. According to Tagawa *et al* the acid sites of H_0 between 1.5 and -5.6 are proven to be the active sites to adsorb ethylbenzene [29].

4.4 ALKYLATION OF PHENOL, ANISOLE AND ANILINE

4.4.1 Alkylation of phenol

A comparative account of TS82 and its sulfated analogue, STS82 at different temperatures is given in Table 4.17. Compared to TS82, sulfated catalyst produced an appreciable amount of O-alkylated product, anisole. Moreover large amounts of polyalkylated products are also formed when sulfated oxide is

employed as the catalyst. At 350 °C it afforded a mixture of different products including anisole, cresols, xylenols and polyalkylated phenols. This is expected as sulfate treatment lead to the creation of strong acid sites. It is reported that acidic catalysts such as silica-alumina and zeolites promote O-alkylation reactions giving anisole [30,31,32]. We have already discussed in section 3 4 1 how the acid base properties of catalysts affect product selectivity. The electron current the around benzene ring is influenced by strong acid sites and hence the aromatic ring lie parallel to the catalyst surface [33,34]. Since the alignment of phenol is parallel to the catalyst surface methylation is possible at all the positions, which lead to a mixture of various C-alkylated products.

The effect of feed rate on the product selectivity and conversion is studied to get an idea about the mechanism of the reaction (Table 4 18). The selectivity of anisole increases with increase in feed rate. This indicates that at low feed rates anisole is undergoing secondary reactions but as the feed rate is increased secondary reactions are suppressed, which results in increase in the anisole selectivity. The selectivity of o-cresol is almost constant whereas the selectivity of xylenol and polyalkylated products is decreased as the feed rate is increased. Xylenol may be formed by the direct C-alkylation of phenol via, o-cresol or from anisole. Anisole can undergo an intramolecular rearrangement to give o-cresol or it can undergo further methylation to give xylenol. The selectivity of o-cresol remained almost constant as the feed rate is changed, which suggests that the formation of o-cresol takes place by direct C-alkylation. Moreover the anisole formed initially must be undergoing further methylation to give xylenol. From the above discussion phenol methylation over the sulfated oxide is possible via, both pathways, (I) direct C-alkylation and (ii) involving anisole as the intermediate.

Table 4.14 Comparison of TS82^a and STS82^b catalysts in the alkylation of phenol at different temperatures

Product selectivity %	Temperature °C									
	250		300		350		400		425	
	a	b	a	b	a	b	a	b	a	b
Anisole	85.6	100	5.8	10.8	0.1	6.5	0.1	2.0	0.13	8
^a o-Cresol	14.3	0	74.7	21.2	59.9	18.7	31.9	23.8	23.6	27.8
^a 2,6-Xylenol	0	0	19.4	25.8	36.3	30.7	52.1	29.8	54.1	22.7
TMP	0	0		35.6		44.9*		42.7		45.9
Conv %	2.6	3.4	32.6	30.4	76.1	79.1	83.9	67.8	75.2	61.3

* Other products include polyalkylated phenols and condensation products.

^aIndicate a mixture of all the isomers in the case of sulfated oxide. Reaction conditions: Calcination temp. 550 °C, Molar ratio (Phenol / methanol) 1:6, Feed rate. 4 ml/h, Catalyst STS82 3 g

Table 4.18 Effect of feed rate on the selectivity of products in the alkylation of phenol with methanol.

Product selectivity %	Feed rate ml/h							
	4		6		8		10	
	a [*]	b [*]	a	b	a	b	a	b
Anisole	0.1	6.5	0.3	7.9	0.4	13.8	0.6	21.1
o-Cresol	59.9	18.7	70.8	24.1	79.5	23.9	80.3	21.3
2,6-Xylenol	36.3	30.7	27.3	28.9	22.1	22.1	18.9	
TMP	3.5	44.9*	1.4	39.9	0.4	32.1	nil	
C-Alkylation	99.8	91.8	99.7	87.6	99.6	72.5	99.3	64.3
Conversion %	76.1	79.1	61.3	63.9	49.2	50.3	30.1	32.8

* ^a TS82 ^b STS82 Reaction conditions Calcination temp. 550 °C, Molar ratio (Phenol methanol) 1:6, Feed rate. 4 ml/h, Catalyst STS82 3g

Self reactions of anisole and methylanisole were conducted for further study (Table 4 19). Anisole is converted into phenol alongwith only small amounts of o-cresol and xylenol. Phenol is formed by the dealkylation of phenol over strong acid site. Methylanisole is converted into xylenol alongwith small amounts of phenol, o-cresol and trimethylphenol. 2,6-xylenol must be formed by the intramolecular rearrangement of methylanisole. The reaction of anisole with methanol produced a mixture of products viz. phenol, 2,6-xylenol and small amounts of cresol, methylanisole and trimethylphenol. Compared to unmodified oxide, phenol formation is greater in the present case.

When a mixture of o-cresol and methanol is passed over the catalyst xylenol and trimethylphenol are formed as the major products alongwith other polyalkylated products.

The effect of time on stream on the conversion of phenol is shown in the Figure 4.11 Sulfated oxide deactivated very fast compared to its unmodified analogue. Faster deactivation may be due to the formation of coke.

Table 4.19: Self reactions of anisole, methyl anisole and alkylation of anisole and o-cresol with methanol

Product	Anisole		Anisole+ methanol		o-Cresol+ methanol		Methyl anisole	
	a	b	a	b	a	b	a	b
Anisole	90.61	82.90	72.79	51.60	nil	nil	nil	4.23
Phenol	6.50	12.30	1.02	6.24	nil	2.50	nil	nil
Methylanisole			1.50	8.80	2.70	1.10	42.5	49.80
Cresol	3.19	3.20	2.34	3.22	4.89	6.90	2.80	3.40
2,6-Xylenol	0.30	1.10	21.91	24.44	88.28	68.50	53.20	39.27
TMP			0.39	5.20	4.11	20.80	1.20	3.30
Conversion	9.39	17.10	27.21	48.40	95.20	93.10	57.50	50.20
wt%								
sel.phenol	67.07	71.92	9.2	12.90	nil	2.60	nil	nil
sel.cresol	33.97	18.71	8.59	6.67	nil	7.41	4.86	5.90
sel. 2,6-xylenol	3.19	6.43	80.52	50.50	92.93	73.57	92.52	78.22

Calcination temp. 550 °C, Reaction temp. 350 °C, Molar ratio (anisole/o-cresol methanol) 1:6 TOS. 1 h, Catalyst TS82. 3g

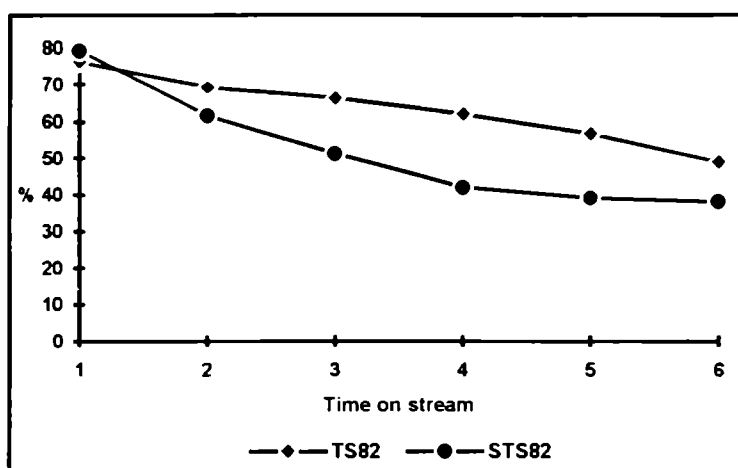


Fig4 11 Effect of time on stream-comparison of TS82 and STS82

Reaction conditions: See foot notes to the Table 4.18

4.4.2 Alkylation of anisole with methanol

A comparative study of STS82 and TS82 in the alkylation of anisole with methanol is depicted in Table 4.20. The sulfate treatment resulted in the formation of an appreciable quantity of phenol alongwith xylenol and trimethylphenol. The formation of phenol is expected as strong acid sites lead to dealkylation reactions. The xylenol formed must be undergoing further methylation to produce trimethylphenol and other polyalkylated phenols. The decrease in conversion of anisole in the case of STS82 above 400 °C must be due to the self decomposition of methanol. From the above discussion it is clear that sulfate treatment of the mixed metal oxide resulted in the nonselective formation of 2,6-xylenol from anisole.

Table 4.20: Alkylation of anisole with methanol- Effect of temperature on the product distribution

Product selectivity %	350 °C		380 °C		400 °C		420 °C	
	a	b	a	b	a	b	a	b
Phenol	0.40	12.90	2.20	17.90	3.98	20.10	3.12	18.80
Methyl anisole	22.68	18.20	4.06	2.23	nil	nil	nil	nil
Cresol	3.610	6.67	6.69	9.90	5.69	8.80	4.20	4.40
Xylenol	63.91	50.50	81.65	47.14	82.50	43.20	84.05	44.20
TMP	4.16	10.76	5.29	18.9	7.82	25.40	8.61	29.20
Conv wt%	43.20	48.40	56.80	62.10	65.20	69.40	83.62	65.8

a: TS82 b: STS82

Reaction conditions: Calcination temp. 550 °C, Reaction temp. 350 °C, Molar ratio (anisole: methanol) 1:6 TOS. 1 h.

4.4.3 Alkylation of aniline with methanol

The alkylation of aniline with methanol over STS82 lead to the formation of benzene, toluene, N-methylaniline, N,N-dimethylaniline and small amounts of toluidines and condensation products (4.21). Benzene is formed by the dealkylation of aniline. Toluene must be formed by the methylation of benzene. Sulfate treatment of TS82 lead to so many undesirable side reactions and selectivity of NMA is decreased alongwith total selectivity of N-alkylated

products. Since aniline is a base it can be easily adsorbed on strong acid sites created by sulfate treatment. This will alter the selectivity of products. Another disadvantage of the sulfated system is that it deactivates faster (Figure 4.12).

Table 4.21 Alkylation of aniline with methanol over STS82 and TS82 at different temperatures

Product sel. %	Temperature °C							
	300		350		375		400	
	a	b	a	b	a	b	a	b
Benzene	nil	3.40	nil	8.90	nil	11.70	nil	17.90
+ Toluene								
NMA	98.10	77.70	96.60	61.18	93.30	48.23	84.61	40.20
NNDMA	1.90	17.30	3.40	28.20	6.70	38.10	15.39	36.30*
Conversion %	32.80	29.10	62.30	56.98	68.10	72.30	73.18	74.12

a: TS82 b: STS82

* Other products include C-alkylated products and condensation products.

Reaction conditions: Reaction temp. 350 °C, Feed rate 4 ml/h TOS 1 h

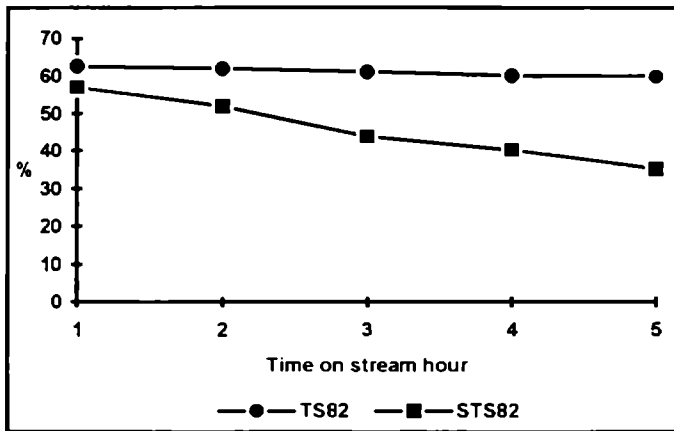


Fig.4.12 Effect of time on stream on the conversion of aniline over STS82
Reaction conditions: See foot notes to Table 4.21

REFERENCES

- 1 C. J. Norman, P. A. Goulding, I. McAlpine, *Catal. Today.*, 20 (1994) 313.
K. Arata, *Appl. Catal. A General*, 146 (1996) 3
- 2 H. Matsushashi, M. Hino, K. Arata, *Appl. Catal.*, 59 (1990) 205 M. Hino,
Ph. D. Thesis, Hokkaido Univ 1982.
- 3 F Lonyi, J Valyon, J Engelhardt, F Mizukami, *J Catal.*, 160 (1996) 279
- 4 A. Corma, *Chem. Rev* 95 (1995) 559
- 5 J. M. Parera, *Catal. Today*, 15 (1992) 481
- 6 R. Srinivasan, R. A. Keogh, D. R. Milburn, B. H. Davis, *J. Catal.*, 153
(1995) 123 R. A. Keogh, R. Srinivasan, B. H. Davis, *J. Catal.*, 151 (1995)
123.
- 7 F Lonyi, J. Valyon, *Therm. Anal.*, 46 (1996) 211
- 8 R.T Parfitt, R. S. C. Smart, *J. Chem. Soc., Faraday Trans. I*, 73(9)
(1977)796; T Xingyin, K. Fangming, Z. liqing, *Chemical Journal of Chinese
Universities*, 7(2) (1986) 161.
- 9 R. A. Nyquist, R. O. Kagel, "*Infrared spectra of inorganic compounds*"
Academic press (1971).
- 10 T Jin, *Inorg. Chem.*, 23 (1984) 4376
- 11 D. A. Ward, E. I. Ku, *J. Catal.*, 150 (1994) 18.
- 12 T Yamaguchi, K. Tanabe, *Bull. Chem. Soc. Jpn.*, 47 (1974) 424.
- 13 K. Tanabe, M. Misono, Y Ono, H. Hattori "*New solid acids and bases,
their catalytic properties*", *Stud. Surf. Sci. Catal.* (Eds.) B. Delmon, J. T
Yates, 51 (1989) 262.
- 14 H. Matsushashi, M. Hino, K. Arata, *Appl. Catal.*, 59 (1990) 205.
- 15 T Tagawa, T Hattori, Y Murakami, *J. Catal.*, 75 (1982) 66.
- 16 H. Matsushashi, M. Hino, K. Arata, *Chem. Lett.*, (1988) 1027
- 17 M. J Fuller, M. E. Warwick, *J. Catal.*, 29 (1973) 441.

18. H. Niyama, E. Echigoya, *Bull. Chem Soc. Jpn.*, 44 (1971) 1739
19. L. Nodek, J. Sedlacek, *J. Catal.*, 40 (1975) 34, N. Takezawa, C. Hanamaki, H. Kobayashi, *J. Catal.*, 34 (1974) 329
20. K. Thomko, *Z. Phys. Chem. NF*, 106 (1977) 225
21. C. L. Kibby, W. K. Hall, *J. Catal.*, 29 (1973) 144.
22. M. Ai, T. Ikawa, *J. Catal.*, 40 (1975) 203
23. M. Ai, *Shokubai*, 18 (1976) 17, M. Ai, T. Niikuni, S. Susuki, *Kogyo Kagaku Zasshi*, 73 (1979) 950; D. B. Dadyburjor, S. S. Jawur, E. Ruckenstein, *Catal. Rev. Sci. Eng.*, 19 (1979) 293
24. M. Ai, T. Niikuni, S. Susuki, *Kogyo Kagaku Zasshi*, 73 (1979) 950.
25. T. Seiyama, N. Yamazoe, M. Egashira, *Proc. 5th Intern. Congr. Catal. Palm Beach*, (1972) 997
26. M. J. Fuller, M. E. Warwick, *J. Catal.*, 29 (1973) 441
27. M. J. Fuller, M. E. Warwick, *J. Catal.*, 29 (1973) 441, E. W. Thorton, P. G. Harrison, *J. Chem. Soc., Faraday Trans. 1*, 71 (1975) 461
28. K. Wakabayashi, Y. Kamiya, N. Ohtu, *Bull. Chem. Soc. Jpn.*, 40 (1967) 2172; 41 (1968) 2776.
29. T. Tagawa, T. Hattori, Y. Musakami, *J. Catal.*, 75 (1982) 66.
30. M. Inoue, S. Enomoto, *Chem. Pharm. Bull. (Tokyo)*, 20 (1972) 232.
31. K. Tanabe, T. Nishizaki, *Proc. 6th Intern. Congr. Catal. London*, (1977) 863
32. Y. Fulcoda, T. Nishizaki, K. Tanabe, *Nippon Kagaku Zasshi*, (1972) 1754.
33. B. Xu, T. Yamaguchi, K. Tanabe, *Materials Chem. Phys.*, 19 (1988) 291
34. K. Tanabe, M. Misono, Y. Ono, H. Hattori "*New solid acids and bases, their catalytic properties*", *Stud. Surf. Sci. Catal. (Eds.) B. Delmon, J. T. Yates*, 51 (1989) 23

CHAPTER V

SUMMARY AND CONCLUSIONS

5.1 SUMMARY

A comparative study of acid-base properties and catalytic activity of Sn-La and Sn-Sm mixed oxides and their corresponding sulfate modified analogues are reported in this thesis. The catalytic activity and product selectivity in the decomposition of alcohols are correlated with the acid-base and redox properties of the catalyst systems under study. The effect of catalyst preparation, pretreatment and various reaction parameters on the catalytic activity of sulfate modified oxides is investigated in the oxidative dehydrogenation reactions. The experimental conditions are optimised to synthesise industrially important organic chemicals viz. 2,6 xyleneol, o-cresol, N-methylaniline and N,N-dimethylaniline employing the mixed oxide systems. The effect of sulfate treatment on the catalytic activity of these systems in the alkylation reactions of phenol, anisole and aniline is also investigated and the merits and demerits of sulfate treatment are highlighted.

CHAPTER I narrates a thorough review of the published literature on the acid-base properties and catalytic applications of oxide systems containing tin oxide and rare-earth oxides. The important physico-chemical aspects and catalytic reactions of sulfate modified metal oxides are also included in this chapter.

CHAPTER II discusses the preparation of catalyst and experimental techniques employed for the characterisation. The different methods for the preparation of sulfate modified mixed oxides are described. It is found that the generation of superacid sites depend on the method of preparation of the catalyst. The experimental set up used for the evaluation of catalytic activity is also incorporated.

CHAPTER III is devoted to the discussion of physico-chemical characteristics, acid-base properties and catalytic activity of the mixed oxide systems. The catalytic activity study comprises alcohol decomposition reactions, oxidation reactions, reduction of aromatics containing various reducible groups and alkylation reactions of phenol, anisole and aniline. From the results of *n*-butylamine and trichloroacetic acid titrations using Hammett indicators and alcohol decomposition reactions, it is found that basicity of the mixed oxides are in the order $\text{SnO}_2(80\%)\text{-La}_2\text{O}_3(20\%) > \text{SnO}_2(20\%)\text{-La}_2\text{O}_3(80\%) > \text{SnO}_2(50\%)\text{-La}_2\text{O}_3(50\%)$ and $\text{SnO}_2(80\%)\text{-Sm}_2\text{O}_3(20\%) > \text{SnO}_2(20\%)\text{-Sm}_2\text{O}_3(80\%) > \text{SnO}_2(50\%)\text{-Sm}_2\text{O}_3(50\%)$. The catalytic activity in the oxidative dehydrogenation reaction is found to depend on catalyst composition, acid-base properties, redox properties, catalyst pretreatment and various reaction parameters like, temperature, feed rate and presence of water. The product selectivity in the alkylation of phenol, anisole and aniline depends mainly on the acid-base properties of the catalysts. These oxides catalysed transfer hydrogenation of nitrobenzene efficiently with isopropanol and also resulted in the chemoselective reduction of aromatics containing different reducible functional groups.

CHAPTER IV of the thesis focuses on a comparative study of the physico-chemical characteristics and catalytic properties of the aforementioned mixed oxide systems and their sulfate modified analogues. An appreciable change in the physico-chemical properties of the catalyst is observed upon sulfate treatment followed by calcination in air. The sulfate treatment leads to the formation of stronger acid sites, though the strength of these sites varies with the method of preparation of the catalyst. The activity of sulfate modified systems in the alcohol decomposition reactions and oxidative dehydrogenation reactions is much greater than unmodified counterparts. The stronger acid sites lead to the faster

deactivation of the catalysts and to the formation of undesirable products in the alkylation of phenol, anisole and aniline.

CHAPTER V includes the summary and conclusions of the results which are obtained from the present study

5.2 CONCLUSIONS

The following conclusions are drawn from the experimental investigations carried out to elucidate the effect of sulfate modification of binary mixed oxides containing tin and rare earth elements (La and Sm) on their acid-base properties and catalytic activity.

- 1 The textural properties, acid-base properties and catalytic activity of the Sn-La and Sn-Sm binary oxide systems vary appreciably with their chemical composition
2. The decomposition of different alcohols can be used to gather very important informations about the surface acid-base properties of the catalysts.
- 3 The catalytic activity in the oxidative dehydrogenation reaction is found to depend on catalyst composition, acid-base properties, redox properties, catalyst pretreatment and various reaction parameters like, temperature, feed rate and presence of water.
4. The mixed oxides containing Sn and rare earth elements (La and Sm) are effective in the synthesis of industrially important chemicals like 2,6-xyleneol, o-cresol, N-methylaniline and N,N-dimethylaniline.

- 5 The Sn-La and Sn-Sm mixed oxides can be used for the chemoselective transfer hydrogenation of various aromatics containing different reducible groups, under optimised conditions.
6. The sulfate treatment leads to a remarkable increase in the surface area of the oxides because samples were cracked into fine particles, which is confirmed from SEM pictures and broadening of XRD peaks.
- 7 The decomposition of sulfate takes place at higher temperature compared to sulfated tin oxide and sulfated zirconia and decomposition temperature depend on the catalyst composition.
- 8 The strength of acid sites created as a result of sulfate treatment depend on the method of preparation, catalyst pretreatment, sulfating agent and chemical composition of catalyst precursor
9. The activity of sulfate modified systems in the alcohol decomposition reactions and oxidative dehydrogenation reactions is much greater than unmodified counterparts.
10. In the alkylation of phenol, anisole and aniline, the stronger acid sites lead to the faster deactivation of the catalysts and to the formation of undesirable products.
- 11 Sulfated mixed oxides are found to be more active than sulfated SnO₂.